THE STUDY OF TRACE METALS IN NATURAL WATER USING ANODIC STRIPPING VOLTAMMETRY

A THESIS SUBMITTED FOR THE DEGREE OF

MASTER OF PHILOSOPHY

OF THE COUNCIL FOR NATIONAL ACADEMIC AWARDS

BY

NIGEL DUNCAN BIRKS. B.Sc., M.Sc.

DEPARTMENT OF CHEMISTRY

SHEFFIELD CITY POLYTECHNIC

SEPTEMBER 1978

TABLE OF CONTENTS

LIST OF FIGURES.

LIST OF TABLES.

Acknowledgements

I would like to express my thanks to Dr. M.P. McDonald for his supervision and guidance throughout the research work. I would also like to thank my external supervisor Mr. Seddon for his help and co-operation in permitting me to sample the Ladybower reservoir and catchment area.

It is with sadness that I recall my gratitude to the late Dr. D. Hubbard for his supervision and encouragement with the initiation of the early stages of this work.

Thanks are also due to the respective Heads of the Sheffield Polytechnic Chemistry Department: Dr. A. Crawshaw and Dr. M. Goldstein for allowing me to use the facilities of their department.

Finally I would like to thank all the technicians of the Chemistry and Biology Departments for their assistance throughout this work.

CHAPTER 1.

INTRODUCTION

1.1. The analytical technique of anodic stripping voltammetry

Anodic stripping voltammetry (ASV) is an electroanalytical technique with the required sensitivity for the determination of trace metals in the 10^{-6}mol dm^{-3} to 10^{-11}mol dm^{-3} concentration range and is thus aptly suited to the analysis of aqueous environmental samples.

The sensitivity of ASV is achieved through a pre-concentration process in which certain trace metal ions in solution are reduced by a controlled potential more negative than their reduction potential. The reduced metals are electrodeposited on to an electrode and after a prescribed plating time the deposit is oxidised back into solution by scanning the potential in the anodic direction.

The metal is stripped from the electrode in an anodic scan and a peak is produced in the resultant current vs. potential trace, the height of the peak (i_p) being a quantitative measure of the metal ion concentration in solution, whilst the peak potential (E_p) is an indication of its identity.

The sensitivity of the technique may be controlled to some extent by the duration of the deposition step which can range from 2 to 70 minutes.

The technique of electrolytic stripping was first used by Zbinden 1931 (1). He was attempting to determine copper electro-gravimetrically by plating it onto a platinum electrode. The amount of plated material was too small to weigh accurately so he devised the technique of reversing the current and oxidising the copper back into solution. A quantitative measure of the copper plated was obtained by measuring the area under the copper peak on the i-E trace produced from an anodic scan.

Further development of ASV was not forthcoming until the 50's when Rogers et al (2), Barker and Jenkins (3) and De Mars and Shain (4) working with mercury drop electrodes demonstrated the sensitivity of the method for the analysis of dilute solutions in the concentration range 10^{-6} to 10^{-9}mol dm^{-3}. Further work by Kemula and Kublik (5) improved the apparatus and increased the accuracy and reproducibility of the technique.

The types of electrode used for ASV range from mercury electrodes either in the form of a hanging mercury drop electrode (HMDE), sessile mercury drop electrodes (SMDE) or dropping mercury electrodes (DME's) used with long drop times. Mercury may also be plated on to an inert substrate like Pt, Ni, graphite or carbon to produce mercury film electrodes (MFE). The composite mercury graphite electrode (CMGE) has been much used by Matson (6) in the examination of numerous environmental samples. The electrode is a graphite rod impregnated with wax, the electroactive surface is polished and plated with mercury to produce a MFE. Mercury pools were used by Nikelly and Cooke (7) as ASV electrodes which although, they showed excellent cathodic deposition suffered from broad stripping peaks owing to diffusion of the metal into the mercury.

Solid electrodes were either of solid metal or graphite, they were used for metals like silver and gold which have oxidation potentials more positive than that of mercury. Surface contamination and reproducibility posed problems; if more than one species was deposited difficulties were found to arise in the stripping process. The deposited metals are not interdiffusible and so their stripping peaks tend to overlap each other.

Eisner and Mark (8) used a wax impregnated pyrolytic graphite electrode polished to a very smooth surface on one end for the analysis of Ag in rain and snow samples. The ASV technique together with use of ion exchange to preconcentrate the metal allowed the analysis of concentrations as low as 10^{-11}mol dm^{-3} Ag to be performed for the first time. At the 4×10^{-9}mol dm^{-3} level the reproducibility of peak heights was ± 5%.

The use of carbon as a paste for an electrode material suitable for ASV was first reported by Jacobs (9). The paste was made with a nujol and graphite powder in a 4:10 mixture and compressed in a suitable bore tube allowing a known surface area in contact with the solution; electrical contact was made with the paste via a platinum wire. Jacobs cited seven variables that should be considered in an ASV analysis, these are: the type of supporting electrolyte, the deposition potential, deposition period, solution volume, electrode area, stirring rate and voltage scan rate.

The most widely used electrodes are the HMDE and the wax impregnated graphite which may be used as a solid electrode or a CMGE. More recently glassy carbon has been used as a substrate for plating mercury to form a MFE. Glassy carbon requires no wax impregnation and only polishing with fine abrasive to produce a suitable electrode for mercury deposition.

Where mercury electrodes are used the trace metals which can be determined are restricted to those capable of forming reversible amalgams.

The HMDE's have several disadvantages, a 30 second rest period is required after plating to allow the amalgam concentration to become more homogeneous and to allow convection in the solution to damp out. Diffusion of metal out of the drop during stripping causes peak broadening and thus loss of selectivity, diffusion may also occur up the column of mercury and lead to non quantitative results. Vibration caused by high stirring rates associated with increasing the sensitivity of an electrode has a deleterious effect on HMDE's owing to their fragility; their use in the field is thus limited.

MFE's are more robust and have been preferred by some workers developing electrodes for the analysis of 10^{-8}mol dm^{-3} to 10^{-11}mol dm^{-3} solutions. The peak current is dependent upon the electrode area for a MFE and to the radius of the drop in the HMDE. Since it is more easy to produce a film of greater area than a drop of increased radius the MFE has been favoured in development for determinations involving high sensitivity. Mercury films give superior selectivity since diffusion from the bulk of the film to its surface is very fast. Marple and Rogers (10) using platinum and silver wires as substrates on which to plate mercury found that both metals form intermetallic compounds which altered the property of the mercury film with use. The use of carbon electrodes however, removes the risk of intermetallic compound formation with the substrate material and provides an inert, mechanically strong support with good electrical conductivity and a high hydrogen overpotential. The MFE's increased sensitivity is coupled with an increased susceptibility to fail at more frequent intervals than HMDE's; the electrode may become overloaded with metal when long plating times are used, resulting in the formation of intermetallic compounds with the metal electrodeposited from solution.

Shorter plating times were practical with a rotating glassy carbon electrode (GCE) and simultaneous electrodeposition of mercury from mercuric nitrate added to the sample in the procedure adopted by T.M. Florence (11). The electrode was wiped with a tissue after each analysis to remove the mercury film; the risk of intermetallic compound formation is thus reduced. Rotation of the electrode throughout the plating and stripping step enhanced peak currents. Excellent resolution of neighbouring peaks was made possible owing to the highly polished surface of the GCE. A limit of detection of 7×10^{-10} mol dm^{-3} Pb was recorded. An electro-deposition period of five minutes was used in the trace metal determinations. ASV thus extends the range of classical polarography by three or four orders of magnitude making possible analyses in the 10^{-7} to 10^{-11} mol dm^{-3} concentration range.

1.2. Application of ASV to natural waters.

ASV has been used to examine trace metals in lakes, rivers and marine environments. Cu, Zn, Cd, Co, Cr, Ni and Mo are essential micronutrients involved in enzymatic transformations which govern the productivity and fertility of natural water bodies with respect to phytoplankton. In high concentrations these metals may become inhibitory or toxic to biological systems. The use of ASV has allowed much information to be gained about trace metals from both natural geochemical weathering and industrial pollution and their availability and effect on biological systems in natural waters.

The fact that natural waters are often supersaturated with respect to many inorganic compounds and that metal ion concentrations are higher than those calculated from solubility products tends to implicate the presence of soluble organo-metallic complexes; further evidence, in that the metal is non-extractable with suitable solvents, non-dialysible and non adsorbable but may be released as analytically detectable metal species upon acidification or oxidation, points to the existence of organo-metallic complexes.

Increase or decrease of biological activity as a result of addition of organic material or chelate formers signifies that organic complexation of metal ions is necessary before incorporation into a living system.

The metal species may be present as a colloid, or associated with lipids or adsorbed on colloids. Acidification could release these metals as well as causing protolysis reactions in metallo-organic complexes. Oxidation or destruction of organic material would similarly release metals associated with colloids and thus complicate any picture of organo-metallic complexes based on formation constants.

Biological activity may equally be associated with colloidal dispersions and ionic interactions in solution which probably involve organic complexation as well.

Allen et al (12) favoured the CMGE for the analysis of natural water samples and have shown that both qualitative and quantitative information on free and combined metal ions and their distribution could be gained by varying the sample pretreatment, total metal content being determined by perchloric acid digestion of a sub-sample prior to ASV. Filtration of the sample through 0.45μ filters separated dissolved from particulate fractions on the basis of variations in particle size and made it possible for these workers to investigate the trace metal association with each fraction of the water sample.

In the field of oceanography Ariel and Eisner (13) used ASV for the analysis of Zn and Cd in Dead Sea brine and favoured the technique because of its efficiency, sensitivity and comparative freedom from risks of contamination. Zn and Ni anodic peaks tended to overlap each other in sea water since their peak potentials were very similar. To overcome this problem, another medium was employed in the stripping process which would allow the peaks to be resolved owing to a different oxidation potential for the two metals in the new medium. Zn was analysed at 5.7×10^{-7} mol dm^{-3} with a standard deviation of ± 3% whilst Cd at the 10^{-8} mol dm^{-3} level gave a 2 to 4% standard deviation. These workers observed no interference between the metals under examination.

Whitnack and Sasselli (14) also used the HMDE for the analysis of seawater for Cu, Pb, Cd and Zn. The possible role of Ni as an interfering element in Zn analysis was postulated since their peak potentials differ by only 200 mV in seawater; by making standard additions of Ni (II) to seawater a double wave was produced at the previous Zn peak potential. Thus their data for Zn includes the Ni concentration as well. At the 10μg dm^{-3} level the data was accurate to within ± 5% and at the μg dm^{-3} level to ± 10%. The reproducibility of mercury drops from the DME had to be monitored carefully before being attached to the platinum wire to make a HMDE otherwise errors of as much as 100% were found in results and were directly attributable to the variation in the initial mercury drop volume.

Smith and Redmond (15) used a Kemula HMDE electrode in which the drops of mercury were exuded by the piston action of a micrometer syringe. These workers have confirmed a degree of interference of Ni with Zn and of V and Ni with Cu, these interferences are thought to take the form of inter-metallic compounds being formed in the mercury electrode.

The simultaneous determination of Cu, Cd, Pb and Zn ions in natural waters other than seawater was performed successfully by I. Sinko and J. Dolezal (16) by using 0.1 mol dm^{-3} acetate buffer as the supporting electrolyte. The buffer was required in order to displace the H_2 evolution potential below that of Zn.

The buffer also stabilised the slow drift in pH during the analysis time which would otherwise have led to inaccuracy. It was also shown by these workers that from pH 7 to pH 10 the oxidation peak currents decreased for all four metals and that a copper doublet peak appeared above pH 7.8.

The proportionality between the concentration of Zn in solution and the oxidation current peak was seen to deviate from linearity above pH 8; the same was found to be true for Cd and Pb; Cu peak currents deviated at pH values above 7. Deaeration of the sample solution with nitrogen was found to cause considerable change in the pH in the first 10 minutes and this only stabilised after 35 minutes but still showed a slow change owing to the removal of CO_2 from the water. A standard deviation of between 3 and 6% was obtained on the measurement of the anodic peaks at the 10^{-8}mol dm^{-3} level for Zn, Cd, Pb and Cu.

Matson (17) using a CMGE has investigated those amalgam forming trace metals: Zn, Cd, In, Pb, Cu and Bi in polluted and pollution free, fresh and saline waters and has shown the association of such metals with natural organic chelators like humic and fulvic acids. By adding Cu standards of 0.13μg Cu to a 10 cm^3 sample and observing the decay of the ASV signal with time, Matson has shown the capacity of Rouge River water to complex such a metal within half an hour. Double peak phenomena were observed and were attributed by Matson to oxidation of the free and organically complexed metals; by titration with free metal Matson was able to derive formation constants for the metal ligand complexes in natural water.

The interpretation of the data on natural organic chelators with trace metals as obtained by Matson has been shown by D.N. Hume (18) to be more complex since double peak phenomena referred to by Matson have been observed in solutions containing only trace metal ions in distilled water. Hume showed that in the preparation of the CMGE that the plating potential of mercury on to the electrode to produce a thin film is critical and that mercury was not deposited on all the sites of the exposed graphite surface unless a plating potential in excess of - 200 mV vs SCE was used. The metal deposited on to the CMGE may deposit both on the mercury and the bare graphite. The double peak may thus be caused by metal being stripped from these two sites at different peak potentials and not by the presence of free metal and metal ligand complexes.

Stulikova (20) studied the effect of plating potential on the size and distribution of mercury droplets in a mercury film plated on to glassy carbon and confirmed the physical existence of different sites for mercury deposition, by the use of electronmicroscopy. The mercury was deposited on sites of different activity according to the plating potential used. At potentials as low as 0.0V vs SCE mercury deposit was only on the most active sites on the glassy carbon surface and further deposition at this potential favoured the reduction of mercury on mercury so that the original droplets merely increased in size whilst their distribution remained the same.

The plating of a fresh glassy carbon surface at more negative potentials deposits mercury on less active sites and a more even distribution of droplets results. At plating potentials as great as - 0.5V and more, even the least active sites are covered and the energy differences among the various types of site become negligible with the result that a macro-layer of mercury is deposited on all the sites leading to a more uniform distribution of droplets. The nature of the mercury film on a carbon electrode and the possibility of mono-layer and macrolayer coverage on sites of differing activity at plating potentials lower than - 0.50V was found by Hume to account for double peak phenomena associated with the electrode structure itself.

The deposition of mercury at potentials at which simultaneous hydrogen evolution occurs is considered advantageous by Stulikova since the drop size and distribution is more even, producing a more uniform film for stripping analysis of less electro-positive metals.

Hume has shown that the CMGE behaviour may be easily disrupted by surface active organic materials present in the natural water, such as humic acid which appears to become adsorbed on the electrode surface.

ASV on standard solutions and natural waters which have been acidified or have had their organic contents oxidised by perchloric acid digestion or irradiation by U.V. light, show increased concentrations of metals. Fitzgerald (21) has claimed that the release of metal is attributable to the oxidation of organo-metallic complexes which thus allows the metal to be measured as the free ion. The information on acid release of metal from organic complexes has been substantiated by ligand exchange in the sample where the sample is made 10^{-4} to 10^{-5}mol dm^{-3} with Mn^{2+} or Fe^{3+} at 90°C and at pH 4. The ligands of the existing organo-metallic complexes in solution complex the added metal and release trace metals from their original complexes in the natural water sample. The trace metal can then be measured by ASV. Fitzgerald showed that as much as 70% of the total Cu found in nearshore water is complexed organically. Complexes which are not acid labile have been implicated when U.V. irradiation has yielded more metal than acidification. Model Pb - EDTA systems were found to release Pb in a reversible manner when the pH was adjusted to 8 from a lower value. Natural organic chelators may behave in a similar manner in water bodies of varying pH.

Zirino and Healy (21) have used two HMDE's in a differential ASV analysis where much of the residual current and some of the hydrogen reduction current is cancelled out by having a working electrode and a similar electrode in a blank solution, connected in opposition to each other. High amplification and slow voltage scans with the resultant improvement in resolution were thus possible.

The analysis was pH controlled by use of a mixture of CO_2 and N_2 as the purge gas. The ratio of the gases could be varied giving a range of 4 pH units from 4.3 to 8.7. The technique allowed the determination of ionic and pH labile Zn, Cd, Pb and Cu using a 5 minute plating cycle. In freshwater the dissolved carbonic acid acts as the supporting electrolyte making the addition of a salt unnecessary.

Zirino and Healy (1970) (22) have shown the presence of a Zn adsorption peak 0.1V anodic to the main diffusion peak for Zn at a pH of 8.8 in seawater. The peak disappears at lower pH values. These workers imply that a complex of Zn is formed above pH 8.8 which is nearly the natural pH of seawater and they consider that it may be of biological significance in controlling the availability of Zn to marine organisms.

Florence (23) using a glassy carbon electrode with a mercury film plated in situ from the sample has been able to look at free amalgam forming trace metal ions in Jervis Bay surface seawater and also in marine organisms by using perchloric acid digestion and dry ashing in a muffle furnace. The residue was dissolved in HNO_3 and buffered in citrate before an ASV analysis to determine Pb, Cd and Cu.

Gachter, Lum-Shue-Chan and Chau (24) investigated the complexing capacity of nutrient medium and its relationship to inhibition of algal photosynthesis by copper since this metal is added to lake water to restrict plankton blooms. The above workers have shown that a water's complexing capacity did not guarantee that an equivalent amount of copper would be tolerated by the plankton. NTA and EDTA can counteract this toxicity partially or completely as can extracellular polypeptides of Anabaena cylindrica, a protein digest and a zooplankton extract. The ability to mask the addition of aliquots of ionic copper was defined as the complexing capacity of the water. Filtered water from different lakes and locations and a culture medium showed different masking properties which they assumed to be mostly complexation, since it was not directly related to toxicity as measured by depression of photosynthesis.

Speciation of the ions being analysed is thus important in discussing the validity of ASV results. A cathodic shift with the formation of carbonato complexes of lead was observed by Stumm and Bilinski (25). Adsorbability of Pb^{2+} aq. is negligible on silica but carbonate complexes are strongly sorbed as shown by the above workers.

In the plating step in an ASV analysis there is a possibility of dissociating strong complexes by plating out the ionic metal in equilibrium with them. This will impose a limitation on the ASV technique with regard to the differentiation of the labile and strongly bound metal.

In waters where the metal is in excess, the deposition step would not affect the complex equilibria. A short plating step would minimise the problem; Chau and Lum-Shue-Chan (26) used three minute plating times to overcome this problem.

The rigid separation of free metal ion, organically complexed trace metal and trace metal associated with colloids and particulate material which may have formed authigenically after filtration can complicate the simple picture of free and bound metal in the aqueous environment and must therefore influence the individuals interpretation of such results.

1.3. Purpose of the present work

In this work the ASV technique is going to be used to analyse Cu, Pb, Cd and Zn in natural water samples taken from the Sheffield area.

The initial objective is to make an ASV system using a conventional polarograph capable of scanning potential in the reverse direction or anodically.

A mercury film electrode is to be developed since this type of electrode possesses the required sensitivity (10^{-7} to 10^{-11}mol dm^{-3}) for the analysis of trace metals in natural water samples. An inert substrate material like graphite or glassy carbon will be used to prepare the ASV electrode as these materials require the minimum of pre-treatment to convert them into an electrode. The inertness of the material will ensure no contamination of the film from the substrate. In order to achieve maximum sensitivity the electrode will be rotated to enhance both stripping and deposition currents.

The procedure for plating the electrode with mercury will be that pioneered by Florence where the mercury is plated simultaneously with those trace metals in the sample. A fresh mercury film will thus be produced in each sample so that complications associated with ageing electrodes will not arise. Instrument settings on the polarograph will be altered to investigate ASV parameters in order to verify that the electrode is behaving as a thin film electrode. Once the behaviour of the electrode has been characterised and it is seen to function normally in different solutions the electrode will be calibrated for the metals Zn, Cd, Pb and Cu. Prior to the analysis of natural waters maximum sensitivity for those trace metals under investigation will be achieved through instrument settings, electrode rotation rate and cell configuration.

Natural water samples will be collected and analysed by ASV such that the risk of contamination through sample pre-treatment or trace metal removal in the collection vessels will be minimal. An analysis procedure will be developed to give information about trace metal content in the sample. Ion complexation by pH labile ligands will be investigated by altering the pH in the sample and repeating the ASV analysis.

In this work it is hoped to gather information using the ASV techniques about trace metal concentrations and complexation in natural water over a period of months. Complexation of certain trace metals has been shown to be necessary to initiate algal growth. Trace metals and complexation thus have an influence on the productivity and fertility of natural waters. It is hoped to be able to discuss the findings of this work in terms of the possible effect of trace metals on fertility and productivity in the natural water sources studied.

CHAPTER 2.

THEORY OF ANODIC STRIPPING VOLTAMMETRY

2.1. Introduction

The main feature of the MFE is the high surface to volume ratio of the thin mercury film which approaches a hypothetical ideal mercury film as compared to the least efficient form of a sphere associated with SMDE's and HMDE's.

Roe and Toni (27) derived equations for mercury film electrodes on the assumption that diffusion in the mercury film may be ignored and that the solution is stirred. If the thickness of the mercury film (l) is sufficiently small, the concentration gradient in the mercury is negligible; in practice (l) is of the order of 10^{-4}cm.

Figure 1.

Model for anodic stripping from a mercury film electrode in a stirred solution.

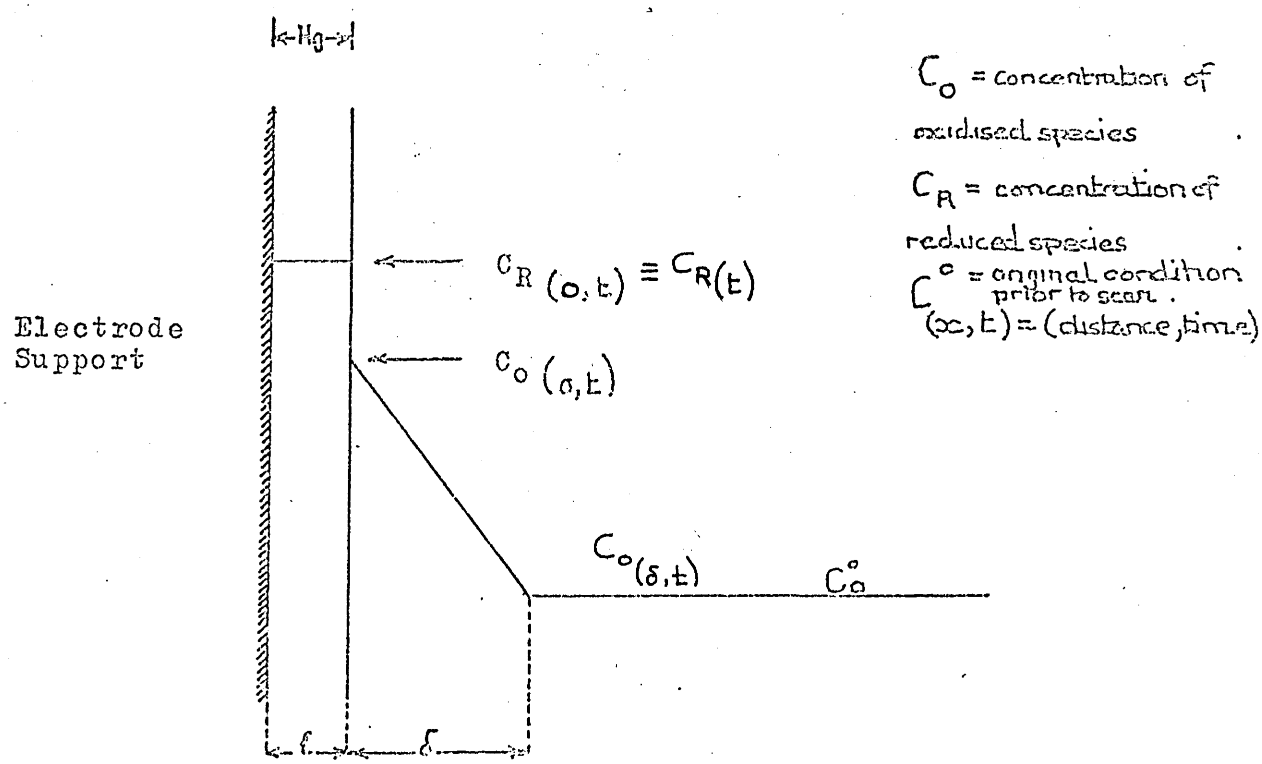

The procedure in an ASV analysis originally consisted of three distinct stages.

(i) The concentration step.

(ii) The rest period.

(iii) The stripping step.

2.1.1. <u>Concentration step</u>. In the initial electrodeposition period (t) the trace metal ions in solution capable of forming liquid amalgams are cathodically reduced at the mercury film/solution interface. If throughout the plating of the metal on to the electrode, the concentration of the metal ion in solution is not appreciably changed and providing the solution is stirred at a constant rate it is assumed that a constant current is maintained.

The concentration of the metal in the amalgam (C_R°) in a film of area A and thickness l is given by Faraday's Law.

$$C_R^\circ = \frac{i\ t}{nFlA} \quad \text{mol dm}^{-3} \qquad (1)$$

$$C_R^\circ = \frac{i\ t}{nFV} \quad \text{mol dm}^{-3}$$

i = reduction current (amperes)

t = duration of the plating step (minutes)

n = number of electrons involved in the reduction of the metal under consideration

F = Faraday's constant

V = volume of mercury in the film (l x A) or drop (dm^3)

The reduction current is analogous to the limiting current in a diffusion controlled process (Meites) (28).

$$i = \frac{nFADC_O^\circ}{\delta} \quad \text{ampere} \qquad (2)$$

D = diffusion coefficient ($m^2\ sec^{-1}$)

C_o° = concentration of the metal ion in the bulk of the solution (mol dm^{-3})

A = electrode area (m^2)

δ = thickness of the diffusion layer (m)

The value of δ will be affected by the stirring rate, cell geometry and electrode design.

Substitution of equation (2) into equation (1) gives the final equation for C_R.

$$C_R^\circ = \frac{D\ C_o^\circ\ t}{\delta \ell} \qquad (3)$$

The concentration C_R is a function of time only in any particular solution and it is assumed to be uniform through the mercury layer (ℓ).

2.1.2. Rest Period

HMDE's require a quiescent period after plating to allow convection and diffusion of the metal in the mercury drop to damp out; and the distribution of the metal to become homogeneous within the drop. The rest is necessary for this electrode to avoid distorted peaks being formed in the following anodic scan. The procedure has been followed by some workers using MFE's or rotating electrodes where rotation and degassing with N_2 is stopped to allow the solution to become quiet. Nitrogen or other inert gases have been used to flush the surface of the electrolyte within the cell.

Plating is still being performed in this period but the reduction current is reduced owing to an increase in δ, the thickness of the diffusion layer around the electrode. Calculations to allow for further plating at a reduced reduction current are therefore necessary but are usually avoided by standardising the procedure.

2.1.3. The stripping step. After the plating period the metals from the solution are concentrated in a thin mercury film. The application of a linear potential sweep in the anodic direction strips the metal from the amalgam.

The initial potential (E_i) of the MFE prior to the stripping step may be written in the form of a Nernst equation:

$$E_i = E_f + \frac{RT}{nF} \cdot \ln \frac{C_O^\circ}{C_R^\circ} \qquad (4)$$

Where E_f = formal electrode potential.*

or

$$\frac{C_O^\circ}{C_R^\circ} = \exp \phi \; (E_i - E_f) \qquad (5)$$

where $\phi = \frac{nF}{RT}$

The potential (E) at any point in time during the scan is governed by the scan rate:

$$E = E_i + \nu t \qquad (6)$$

ν = scan rate (mV min^{-1})

t = time after initiation of scan (minutes)

at the mercury film/solution interface

$$E = E_f + \frac{RT}{nF} \cdot \ln C_{O(o,t)} / C_{R(t)} \qquad (7a)$$

$$\nu t = E - E_i = RT/nF \; \ln \left[C_{O(o,t)} \; C_R^\circ / C_O^\circ \cdot C_{R(t)} \right]$$

or

$$\frac{C_O(o,t)}{C_{R(t)}} = \frac{C_O^\circ}{C_R^\circ} \; \exp. \phi \nu t \qquad (7b)$$

also $C_{O(\delta,t)} = C_O^\circ$

The application of Fick's first Law to the thin film electrode model in (fig.1) gives the diffusion flow of material per unit area of diffusion layer.

* E_f = The electrode potential in a solution of unit concentration rather than unit activity

The flux $= - D_o \frac{\delta c}{\delta x}$

i.e. for the thin film electrode model:

$$\ell \frac{[C_R^\circ - C_R(t)]}{dt} = \frac{D_o[C_o(o,t) - C_o^\circ]}{\delta} \text{ moles cm}^{-2}\text{ sec}^{-1} \quad (8)$$

by substitution of $C_o(o,t)$ from equation (7) into equation (8) and integrating the result, Roe and Toni produced the following expression for the current (i) by substituting into the Faraday expression: equation (1);

$i = nFA\ell\, \partial C_{R(t)} / \partial t$ and the peak current is given by

$$i_p = nFA\ell\, C_R^\circ \nu \ \phi \ e^{-1} \quad (9)$$

Substitution of C_R° from equation (3) into equation (9) results in a final equation (10).

$$i_p = \frac{n\ F\ \phi\ D\ e^{-1}\ A\ C_o^\circ \nu t}{\delta} \quad \text{(amperes)} \quad (10)$$

which shows the dependence of peak current on scan rate (ν); area of the electrode surface (A), time of electro-deposition (t) and concentration of the metal ion in solution (C_o°), providing cell geometry and stirring rate are maintained constant. The fixing of scan rate (ν), electrode area (A) and time of electro-deposition (t) results in the peak current (i_p) being proportional to the concentration of the metal ion in solution (C_o°).

$$i_p = K\ C_o^\circ$$

At the potential E_p where i is a maximum it is shown by Roe and Toni that:

$$\frac{C_o(o,t)}{C_{R(t)}} = \frac{\phi \delta \ell \nu}{D} \quad (11)$$

$$E_p = E_f + \frac{2.3}{\phi} \log \frac{\delta \ell \nu \phi}{D} \quad (12)$$

E_f is the formal electrode potential in the particular solution concerned. The potential of the stripping peak varies as the logarithm of the potential scan rate and it has been experimentally proven by Hume et al that plots of E_p vs logν were linear and they concluded that although the Roe and Toni equations were derived for a uniform thin film electrode such as mercury on a nickel support, the same equations are applicable to carbon and graphite electrodes plated with thin mercury films although, the nature of the film is one of microdroplets.

2.2. Rotated electrodes.

The above equations which describe the theoretical considerations behind the use of a stationary thin film electrode in a stirred solution are applicable to rotated electrodes but require modification to allow for rotation.

Florence has shown that both deposition and peak current are proportional to (electrode rotation rate)$^{\frac{1}{2}}$ and that the peak current (i_p) is further enhanced in the same manner if rotation is maintained throughout the stripping stage of the analysis; an observation disputed by F. Vydra (29) who claims that the electrochemical noise produced outweighs the enhancement effect on the signal.

The effect of electrode rotation is thought to decrease the thickness of the diffusion layer and therefore to increase stripping and plating currents since (i_p) and (i_d) are $\propto \delta^{-1}$.

The rotated disc electrode was thought by Nernst to have a diffusion layer of between 10^{-2} and 10^{-3} cm and he proposed that the diffusion current could be treated in the same manner as that in a quiet solution since the layer has zero velocity with respect to the electrode surface. For the diffusion current the equation is:

$$i = nFAD \frac{C_0}{\delta} \qquad (13)$$

but the thickness δ of the diffusion layer lacked clear definition since the thickness of the zero velocity layer as shown in (figure 2) is too large for the layer to adhere to the electrode by molecular forces and therefore it cannot be assumed to be perfectly stationary.

Figure 2.

Distribution of velocities (u) and concentrations (c) of the metal ion in the diffusion layer.

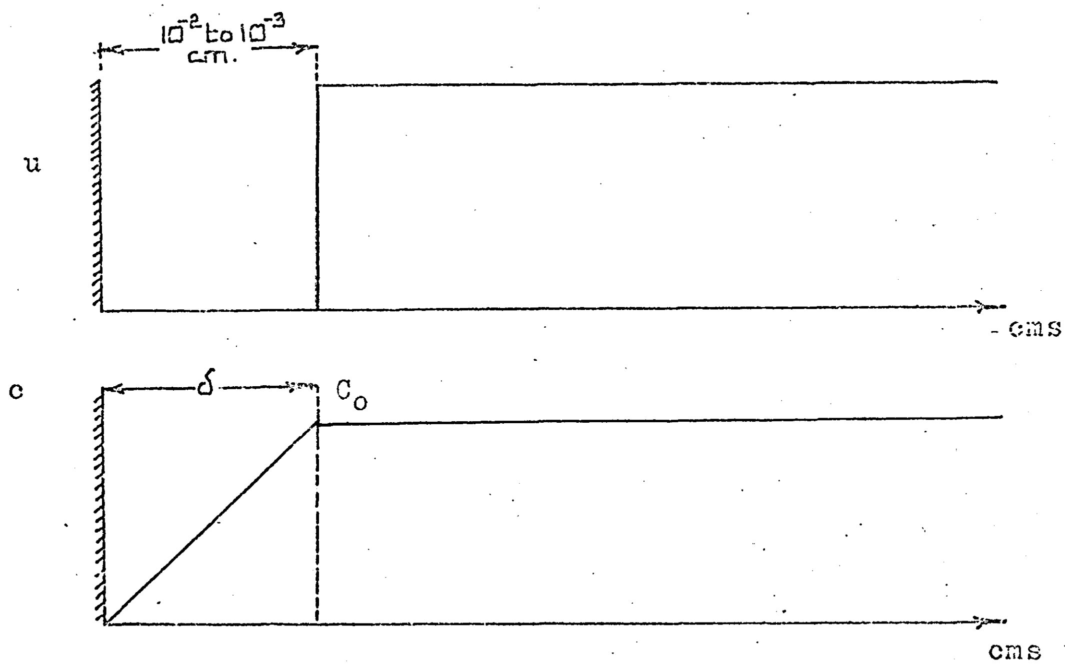

A more quantitative approach by Frumkin et al (30) considered the hydrodynamics of the electrode.

The velocity was considered to be zero at the electrode surface (Fig.3) and to increase until it becomes constant and equal to u_o. The layer in which the uniform motion of the liquid is disturbed is known as the Prandtl boundary layer (δ^*).

The thickness of the Prandtl layer (δ^*) depends on the speed of the liquid and the kinematic viscosity of the liquid (v) and is related to the length l of the electrode surface subjected to laminar flow in solution by equation (14).

Figure 3.

The Prandtl Boundary Layer.

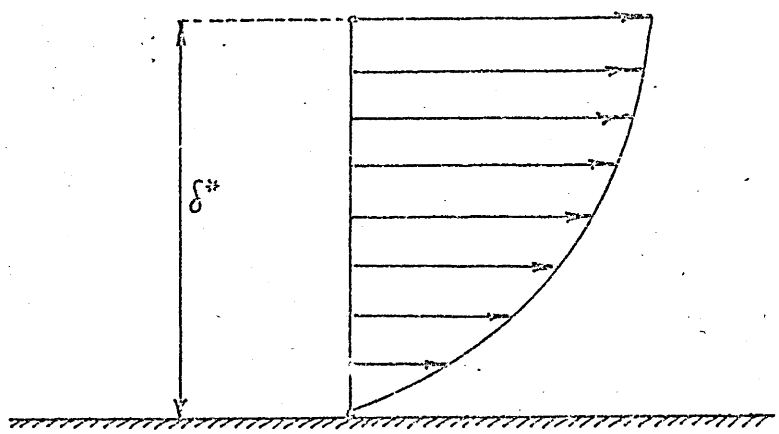

Figure 4.

Prandtl Layer relationship

to the electrode surface.

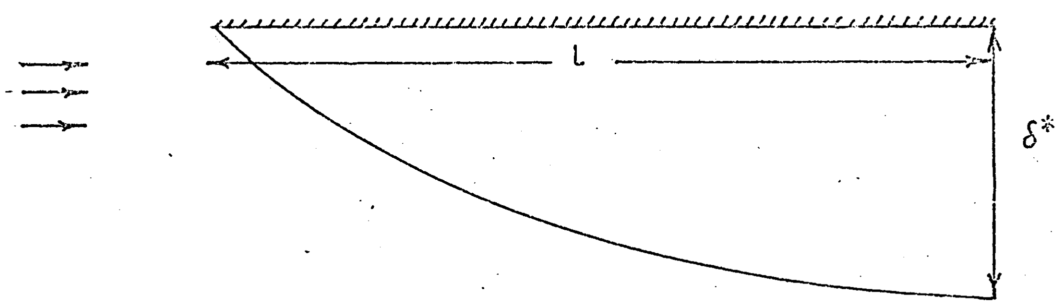

$$\delta^* \simeq \sqrt{\frac{\nu x}{u_0}} \qquad (14)$$

The Prandtl layer δ^* is formed under conditions of laminar flow only i.e. (low Reynolds numbers; $R = \frac{u_0 L}{\nu}$, where L = dimension of the body in the liquid stream) (Fig.4).

The diffusion layer thickness (δ) has been shown by Levich (31) to be related to the Prandtl layer by the ratio.

$$\frac{\delta}{\delta^*} = \left(\frac{D}{V}\right)^{1/3} \qquad (15)$$

in aqueous solution, the thickness of the diffusion layer represents about 1/10th of the Prandtl boundary layer.

Substituting for δ^* from equation (14) into equation (15)

$$\delta = D^{1/3} \; v^{1/6} \; x^{\frac{1}{2}} \; u_o^{-\frac{1}{2}} \qquad (16)$$

Equation (16) shows the dependence of the diffusion layer thickness on the diffusion coefficient (D) of the metal ion and the velocity of streaming (u_o).

Figure 5.

The motion of a liquid of a rotated disc electrode.

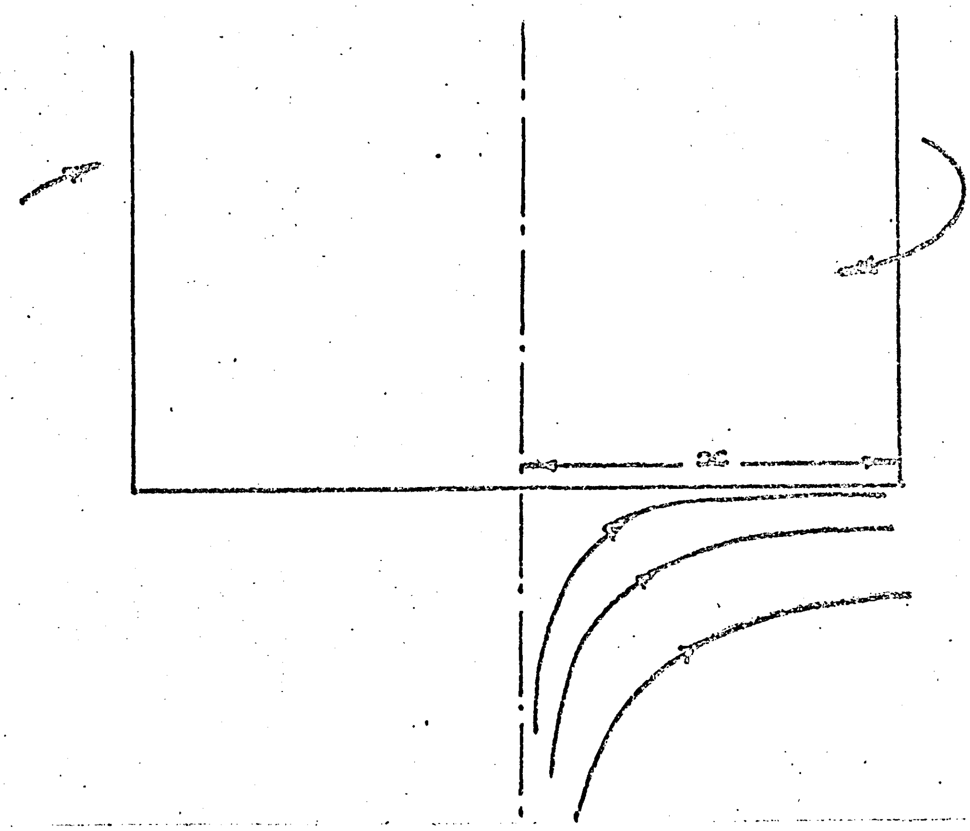

The motion of liquid at a rotated disc electrode is directed towards the centre of the disc after which laminar flow is apparent on the passage to the periphery of the disc. The Prandtl boundary layer thickness is a linear function of the (disc radius)$^{\frac{1}{2}}$ from equation (14) and thus increases towards the periphery. The linear velocity (u_o) of the point at the centre of the disc increases with the flow of liquid towards the periphery of the disc thus the thickness of the boundary layer decreases as can be seen from equation (14) (Fig.5).

The two effects compensate each other and the thickness is thus constant over the whole surface of the disc. The diffusion layer thickness (δ) is similarly constant at all points on the surface of the disc as is the current density.

A homogeneous layer of metal cations at a disc electrode therefore leads to a homogeneous metal layer being formed on the disc surface.

Figure 6.

Planar surface model

of a rotating disc electrode.

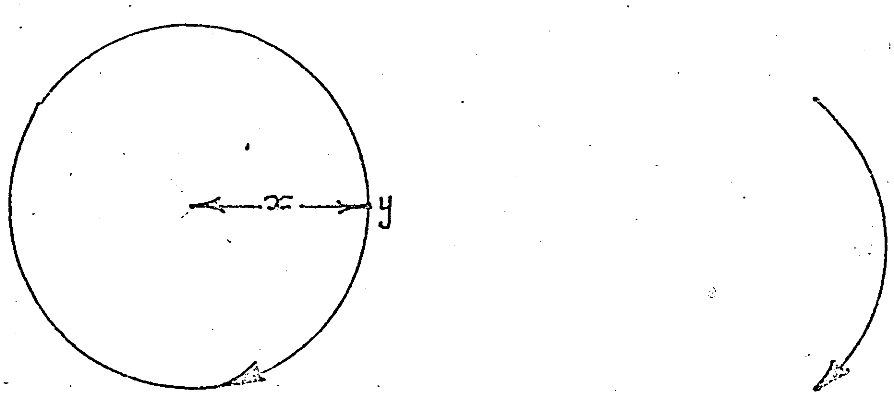

The linear velocity of streaming (u_o) at a point (y) on the disc electrode is required in order to modify equation (16) into an equation giving the diffusion layer thickness (δ) for a rotated disc electrode. The angular velocity (ω) of the point y is:

$$\omega = 2\pi v' \qquad \text{(Figure 6)}$$

Where v' = cycles per second (c.p.s)

$$v' = \frac{\omega}{2\pi}$$

in one second $2\pi r$ (m) are covered in one revolution; at v (c.p.s) the linear velocity (u_o) is:

$$u_o = 2\pi x v' \qquad (17)$$

Substitution of equation (17) into equation (16) gives the diffusion layer thickness at a rotating disc electrode.

$$\delta = K D^{1/3} V^{1/6} x^{\frac{1}{2}} (2\pi x \nu')^{-\frac{1}{2}}$$

cancelling x

$$\delta = K D^{1/3} V^{1/6} \omega^{-\frac{1}{2}} \qquad (18)$$

The thickness of the diffusion layer is therefore proportional to $\omega^{-\frac{1}{2}}$ and therefore to (rotation rate)$^{-\frac{1}{2}}$. Since the deposition and peak currents (i_d and i_p) are inversely proportional to the thickness of the diffusion layer (δ).

$$i_d \text{ or } i_p \propto (\text{rotation rate of the electrode})^{\frac{1}{2}} \qquad (19)$$

Increasing the sensitivity of an electrode by rotation has allowed total analysis times to be shortened since the plating time (t) can be reduced whilst still producing an analytically useful signal. The concentration of reduced metal C_R^c in the mercury film model (Fig.1) is now a function of time and electrode rotation rate.

2.3. <u>Electrochemical Noise</u>. The total current flowing through the system is:

$$i_t = i_{(f)} + i_{(c)} + i_{(b)} \qquad (20)$$

Where $i_{(f)}$= Faradaic current, $i_{(c)}$= Charging current and $i_{(b)}$= Background current.

The electrochemical noise in an ASV analysis is produced from the residual current which constitutes a charging current (i_c) owing to the charging of the electrode/solution interface. The background current (i_b) also contributes to noise and may be attributed to the oxidation of impurities or decomposition of electrolyte. The impurities may be organic and of comparatively low concentration, so no anodic peak is produced but an increased slope to the i - E trace is observed.

The base electrolyte chosen is usually a salt of the alkali metals so the electrolyte is unlikely to contribute to the noise even at high negative potentials providing it is not an acidic solution.

The charging current (i_c) is related to the area A of the electrode surface in contact with the solution by the expression:

$$i_c = A \nu (\partial q/\partial E) \qquad (20)$$

Where $(\partial q/\partial E)$ is the differential double layer capacity. Thus although the increase of scan rate (ν) or electrode area is beneficial to the signal as shown in equation (10) it also increases the contribution of the charging current (i_c) to the total current flowing.

The nature of the mercury film whilst being dependent on the deposition potential for size and distribution of mercury droplets (Stulikova) has a direct influence on the charging current (i_c) since the effective surface area of the electrode will also change as mentioned earlier.

A high background current may be the result of traces of oxygen remaining in solution or the re-entry of oxygen when the purge gas is removed from the solution to flush the surface in the rest period phase of certain procedures.

The base electrolyte to be used in the analysis together with the sample must be purged of oxygen since oxygen will be reduced at negative potentials with respect to the saturated calomel electrode. Purging the solution may be performed by bubbling an inert gas like nitrogen, helium or argon through the solution.

Oxygen gives two polarographic waves. The first is due to the reduction of oxygen to hydrogen peroxide or hydrogen peroxide and hydroxide (depending on the pH)

$$O_2 + 2H^+ + 2e \rightleftharpoons H_2O_2 \text{ (acid media)}$$

$$E_{\frac{1}{2}} = -0.05V \text{ vs. SCE}$$

$$O_2 + 2H_2O + 2e \rightleftharpoons H_2O_2 + 2OH^- \text{ (neutral or alkaline media)}$$

The second wave involves the reduction of hydrogen peroxide to hydroxide or water:

$$H_2O_2 + 2H^+ + 2e \rightleftharpoons 2H_2O \text{ (acid media)}$$

$$E_{\frac{1}{2}} = -0.5V \text{ to } -1.3V \text{ vs. SCE}$$

$$H_2O_2 + 2e \rightleftharpoons 2OH^- \text{ (neutral or alkaline media)}$$

Two types of complication can arise if oxygen is not removed in the ASV analysis procedure. The hydrogen peroxide produced can act both as an oxidising and a reducing agent and therefore can affect the other electro-active species in solution.

pH changes can occur in the vicinity of the MFE due to the electro-reduction of oxygen. The resultant increase in pH in the vicinity of the MFE can precipitate heavy metal ions and thus diminish their diffusion currents with a result that a decreased peak current is observed; the peak itself may also be distorted. Organic species in solution whose reduction involves hydrogen ions would be adversely affected owing to the localised increase in pH at the MFE.

The mercury film itself is particularly sensitive to traces of oxygen which may participate in the following non-electrochemical process:

$$O_2 + 2Hg + 2Cl^- + 2H_2O \rightleftharpoons H_2O_2 + Hg_2Cl_2 + 2OH^-$$

Such a reaction can occur in neutral, unbuffered salt solutions and would inactivate the MFE.

The reproducibility of the MFE has been criticised since there is an increased risk of intermetallic compound formation in the mercury layer with the trace metals deposited. The manipulation of ASV parameters like plating time (t) allows a flexibility to the system so that at relatively high concentrations (C_O^o) of metal in solution, (t) may be reduced with the result that the concentration of reduced metal (C_R^o) in the film does not reach the optimum value where intermetallic compound formation with mercury occurs. By using shorter plating times the electrode is protected from being overloaded with reduced metal and is thus less susceptible to failure.

CHAPTER 3.

EXPERIMENTAL

3.1. Apparatus and reagents.

3.1.1. Polarograph: The instrument used for anodic stripping voltammetry (ASV) was a conventional polarograph, the Polariter PO-4g manufactured by Radiometer of Copenhagen. A chart recorder is built in to the polarograph. Voltage scans can be made in both directions with this instrument and it is therefore usable for ASV work.

On the Polariter PO-4g the scan rates are selected from a combination of chart speeds (cm min^{-1}) and (volt cm^{-1}) selectors. The range of scan rates is set out in Table 1.

Table 1

Volt cm^{-1}	Chart Speed cm min^{-1}	Scan Rate mV min^{-1}
0.5	2	100
"	4	200
"	8	400
1.0	2	200
"	4	400
"	8	800

The voltage range of the instrument was from -3.0V to + 0.5V.

3.1.2. Cell The cell was a standard polarographic cell supplied by Radiometer and had a 20 cm^3 capacity. The lid of the cell was made of plastic and required provision for a stirrer, a bubbler for degassing the solution of oxygen and two further apertures; one for a saturated calomel reference electrode (SCE) and the other for the graphite or carbon electrode to be used for ASV. A Gallenkamp waterbath and pump was used to circulate water in the cell jacket to maintain the cell contents at 20°C.

Stirring of the solution and later electrode rotation was performed by using a Radiometer E.70, rotating platinum electrode assembly without the platinum electrode. The E.70 assembly possessed 3 pulleys on the drive motor which connected via a rubber belt to another 3 pulleys on the cell body. The range of rotation speeds possible are shown in Table 2.

Electrode rotation was measured by a light stroboscope type 3D, manufactured by E.M.I. Electronics Ltd.

Table 2

Motor pulley setting	Cell pulley setting	Revolutions of electrode (r.p.m.)
3	1	2,550
2	1	2,010
1	1	1,373
3	2	1,775
2	2	1,400
1	2	952
3	3	1,422
2	3	1,125
1	3	764

3.1.3. Electrode material for ASV Spectrographic carbon rods (2mm in diameter) and spectrographic graphite rods (6mm in diameter) were obtained from the Morganite Company and National Carbon Co. Ltd., respectively. Glassy carbon rods (3mm in diameter) were supplied by the Le Carbone Co. Ltd.

3.1.4. Reference Electrode Initial work was performed with a Radiometer calomel electrode, type K502.

Mercury pool internal reference electrodes were also used and prepared from triply distilled mercury supplied by Belgrave Mercury Ltd.. A small Beckmann SCE (Part No. 41239) was used in one experiment but found unsuitable due to the small current passed.

All saturated calomel electrodes were later made in the laboratory and placed in a jacket of saturated Analar potassium nitrate to reduce contamination from the SCE owing to the migration of Cl^- into the main cell compartment (Fig.11).

3.1.5. Counter Electrode A platinum wire (0.3mm in diameter) was used as a counter electrode so that minimal current passed through the SCE during the deposition stage of the analysis.

The counter electrode was jacketed so that any oxygen evolved during the electrodeposition period would not contaminate the whole cell contents.

3.1.6. Other Equipment Two Phillips electronic AVO meters (type PM.2403) were used as a high impedance voltmeter and an ammeter.

pH measurements were made with a Pye Unicam model 290 pH meter using a small cylindrical Pye Ingold glass electrode assembly (Pye 405 MS) which could be inserted into the ASV cell to take in situ pH measurements at various stages in the analysis.

The pH meter was calibrated daily with the use of buffer solutions of pH 4, 7 and 9. A buffer solution of pH 4 was prepared by dissolving one tablet of Soliol Brand (Burroughs & Wellcome & Co., London) in 100 cm^3 of cold distilled water. The same procedure was observed for BDH buffer tablets to give individual solutions of pH 7 and 9 at a temperature of 20°C.

The solutions were prepared at weekly intervals and kept in a refrigerator between successive calibrations.

A Gallenkamp (0-6000 r.p.m.) centrifuge was used to centrifuge some natural water samples to separate a clear supernatant layer from a layer containing the centrifugate. 200 cm^3 centrifuge tubes were used with the appropriate head fitting.

3.1.7. <u>Purge Gases</u> The solutions under examination were purged either with white spot nitrogen or carbon dioxide supplied by Air Products Ltd. Carbon dioxide also provided a supporting electrolyte of carbonic acid in solution. The flow rate of the gases used was maintained constant throughout the ASV analysis.

3.1.8. <u>Supporting Electrolytes</u> The supporting electrolytes used were prepared from Analar grade reagents. These salts were purified by cathodic reduction in a cleansing cell where trace metal ions are reduced in a mercury pool cathode (32). The anode is a platinum gauze of high surface area and is placed as near to the surface of the mercury pool as possible to reduce the resistance of the cell.

A high concentration of supporting electrolyte (1 to 3mol dm^{-3} is necessary to allow the passage of a 5mA current; if smaller currents are passed the time for electrolytically cleaning the salt becomes too lengthy.

Cathodic deposition over a mercury pool allowed trace metal levels of 10^{-7}mol dm^{-3} Pb, found in Analar reagents like KNO_3 and sodium acetate to be reduced to 10^{-9}mol dm^{-3} within five days by holding a potential of between -2.1 and -2.9V across the cell in order to maintain a constant current of 5mA.

The power pack used was a Vokam potentiostat SAE 2761 (supplied by the Shandon Co.) used in the constant current mode.

Recrystallisation was also used to purify Analar reagents for use as supporting electrolytes and in this way the concentration of lead in Analar potassium nitrate (0.1mol dm^{-3}) was reduced to 10^{-8}mol dm^{-3}.

3.1.9. Metal Ion Solutions A 1 x 10^{-2}mol dm^{-3} mercuric nitrate solution was prepared from triply distilled mercury and high purity nitric acid (Analar). The solution was adjusted to pH 2 with Analar nitric acid. A 10^{-2}mol dm^{-3} mercury solution prepared from Analar mercuric nitrate was equally satisfactory provided the solution was maintained at pH 2.

Standard metal solutions were prepared from Analar nitrate salts in the case of Pb and Cu and sulphate salts were used for Zn and Cd.

A 0.1mol dm^{-3} stock solution was prepared in 1 dm^3 or 500 cm^3 graduated flasks and a 10^{-3}mol dm^{-3} primary standard prepared by dilution on the day of the analysis. A 2 x 10^{-6} mol dm^{-3} working solution was then used for standardising the cell solution.

3.1.10. Nitric Acid Concentrated Analar nitric acid was diluted to 8mol dm^{-3} and used to lower the pH of natural water samples. The acid was sufficiently pure and did not warrant further purification.

3.1.11. Precautions to avoid contamination All water used in the making up of standard solutions and washing of the cell and electrodes was distilled twice, the second distillation being from a 0.2mol dm^{-3} Analar potassium permanganate solution. The water was stored in aged polyethylene containers to reduce any possible leaching of trace metal ions from the walls of the container.

The ASV cell and glassware used in the making up of standard solutions of metal ions were treated with Repelcote (Hopkins and Williams Ltd.). Later Desicote (Beckmann Instruments Inc.) a similar silicone hydrophobic surface coating was used to minimise adsorption and leaching phenomena associated with glass vessels. The glass vessel, after thorough washing is rinsed with acetone before treatment to allow the organo-silicone in acetone to 'wet' the surface and completely cover the glass.

CHAPTER 4.

PRELIMINARY EXPERIMENTS WITH GRAPHITE AND CARBON ELECTRODES

4.1. Experiments with graphite electrodes.

4.1.1. Electrode preparation In the initial work the cross section of the carbon or graphite electrode was smoothed with emery paper and polished but given no further pretreatment.

A literature survey revealed that most other workers impregnated graphite rods with wax. Matson (33) used ceresin wax whilst Clem et al (34) preferred paraffin wax. In this work it was therefore decided to impregnate the graphite rods with paraffin wax (BDH standard grade).

The graphite rods and molten paraffin wax were evacuated in separate side arm test tubes. After five minutes the molten wax was poured into the test tube containing the graphite rods. The vacuum of 0.01 to 0.1 mm mercury was maintained throughout the operation.

To ensure thorough impregnation of the rods with wax, they were left in the wax under vacuum and with gentle heating for a period of three hours. At the end of this period the vacuum was removed and the rods taken from the cooling, nearly set wax, so that a thick coating was left around them. The cross section of the rod was scraped clear and polished with medium grade emery paper, working down to finer grades and finishing off with 6μm and finally 1μm diamond abrasive paper. The polish was maintained by gentle wiping on a tissue paper.

The wax insulation was sufficient to prevent electrodeposition on any other area of the rod. The provision of a glass sleeve into which the carbon rod fitted shielded it from mechanical damage.

4.1.2. Plating procedure for a stationary (CMGE) electrode A $20cm^3$ sample of $0.1mol\ dm^{-3}$ KCl was made $2 \times 10^{-5}mol\ dm^{-3}$ with respect to mercuric nitrate. In all the experiments oxygen was purged from the solution, by bubbling a constant stream of nitrogen through the cell for ten minutes prior to plating and throughout the plating step.

The stationary graphite electrode was initially plated at an applied potential of -0.2V set between the calomel and graphite electrode. The duration of the plating step to deposit the mercury film was ten minutes. The electrode was then ready for use and an applied potential of -1.0V was set between the SCE and the graphite electrode to deposit the trace metals into the film. The circuit diagram of the initial arrangement is shown in (Fig.7).

4.1.3. Rest Period A rest period was observed for a stationary electrode in which the nitrogen purge gas was removed to flush the surface of the electrolyte and stirring was switched off for the stripping step.

After the quiescent period a linear potential scan was initiated from -1.0V to 0.4V to obtain the stripping voltammogram.

4.1.4. Problems arising from initial experiments The first attempts at plating a stationary electrode were performed in a supporting electrolyte of $0.1mol\ dm^{-3}$ KCl as used by Matson et al (35).

A film was formed but failed to give any voltammogram on a linear potential scan. A close examination of the film showed that it was a scum or precipitate of mercurous chloride rather than an active mercury film. This scum gave a smeared appearance on wiping with a tissue.

No results were obtained so potassium nitrate ($0.1 mol\ dm^{-3}$) was used as a supporting electrolyte with the result that an active mercury film which gave satisfactory voltammograms was produced. The film had a frosted appearance which did not smear on wiping, the droplet nature of the film was clearly visible under a (x 10) magnification hand lens.

Sodium acetate ($0.1 mol\ dm^{-3}$) also proved to be a successful supporting electrolyte from which active mercury films were deposited.

Figure 7.

Circuit diagram of the initial ASV apparatus.

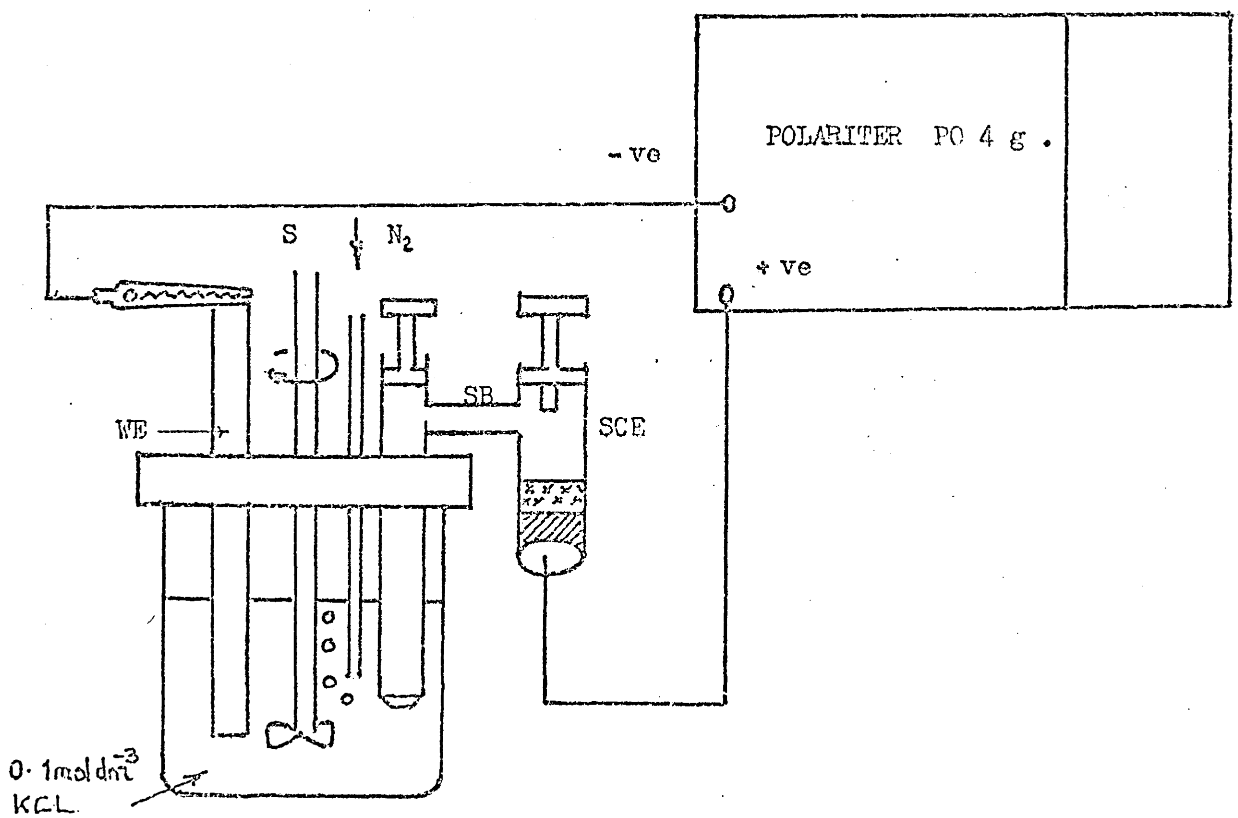

WE = working electrode .

SCE = saturated calomel electrode

S = stirrer

SB. = salt bridge

The voltammograms produced with unimpregnated Morgan Carbon Co. electrodes shown in (Fig.8) indicate the lack of sensitivity which these electrodes had even after a plating time of 70 minutes at -1.0V applied potential between SCE and the working electrode. The signal/noise ratio of the electrode was very low. Impregnation with wax increased the sensitivity of the electrode but the signals were still weak.

A Spectrographic graphite (National Carbon Co.) rod which had been impregnated with paraffin wax and used with an internal mercury pool reference electrode produced voltammograms with good peak resolution (Fig.10).

The very strong signals at applied potentials -0.80V, -0.37V and -0.25V in (Fig.10) show that the cell is heavily contaminated with three metals. The order in which the peaks appear in the anodic scan tentatively suggested the presence of Cd, Pb and Cu.

The source of such heavy contamination was probably the mercury pool reference electrode which covered the bottom of the cell.

4.1.5. Cell modification In an attempt to limit the number of cell components which are placed in solution and thus reduce the possibility of contamination, the graphite electrode was itself made to rotate at 2,550 r.p.m. thus dispensing with a stirrer. The effect of deaeration by the nitrogen bubbler is more uniform in its mechanically disturbing effect on the microstructure of the rotating electrode than on a stationary electrode and should make the electrode results more reproducible (Fig.11).

Florence has shown that it is advantageous to rotate an

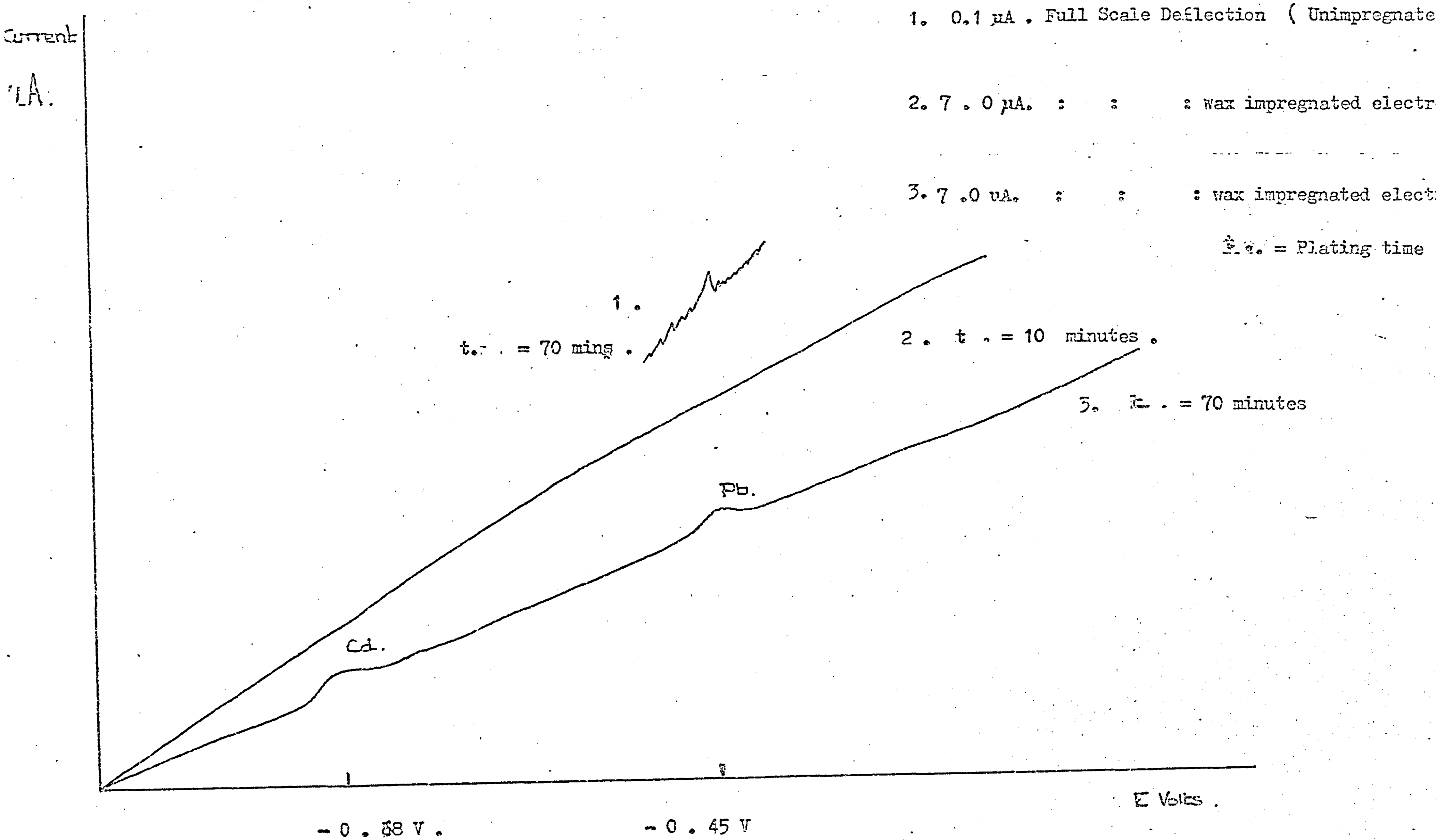

Figure 8.

Voltammograms produced with unimpregnated carbon electrodes.

electrode since the deposition and stripping currents are enhanced by the decrease in thickness of the diffusion layer which is the result of rotation.

4.1.6. Preparation of rotating wax impregnated graphite electrode.

The wax impregnated graphite (6mm=d) was machined down to 3mm and mounted in a 4mm diameter glass tube and sealed with some epoxy resin. The electrode was recoated with wax and the cross section scraped clear. After polishing, the electroactive surface was ready for use (Fig.9).

Figure 9.

Preparation of the rotating wax impregnated graphite electrode.

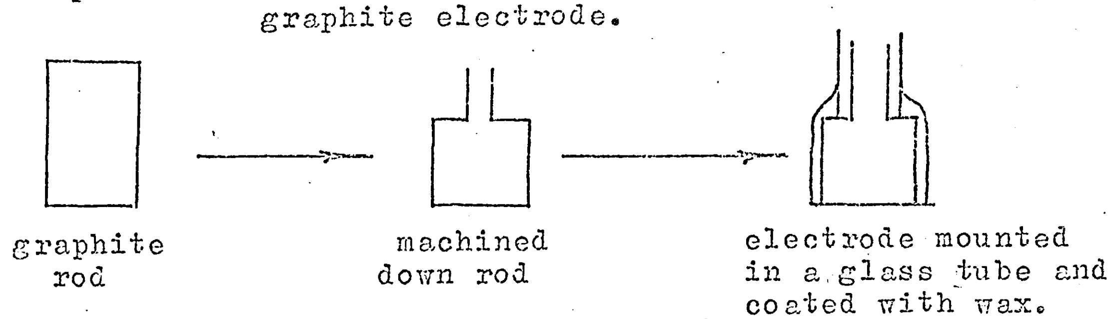

The glass tube was filled with mercury so that a wire dipping into it made electrical contact whilst allowing rotation. The electrode was mounted in the stirrer chuck.

4.1.7. Modified cell assembly results. The modified cell assembly with its rotating electrode was used with a saturated calomel electrode in place of a mercury pool in 0.1mol dm^{-3} KNO_3. Under these conditions the thin mercury film on a graphite support was found to malfunction and fail after 1 to 3 anodic scans.

The first voltammogram produced was normal but in later runs a process quoted by Clem et al 1973 (36), as cathodic

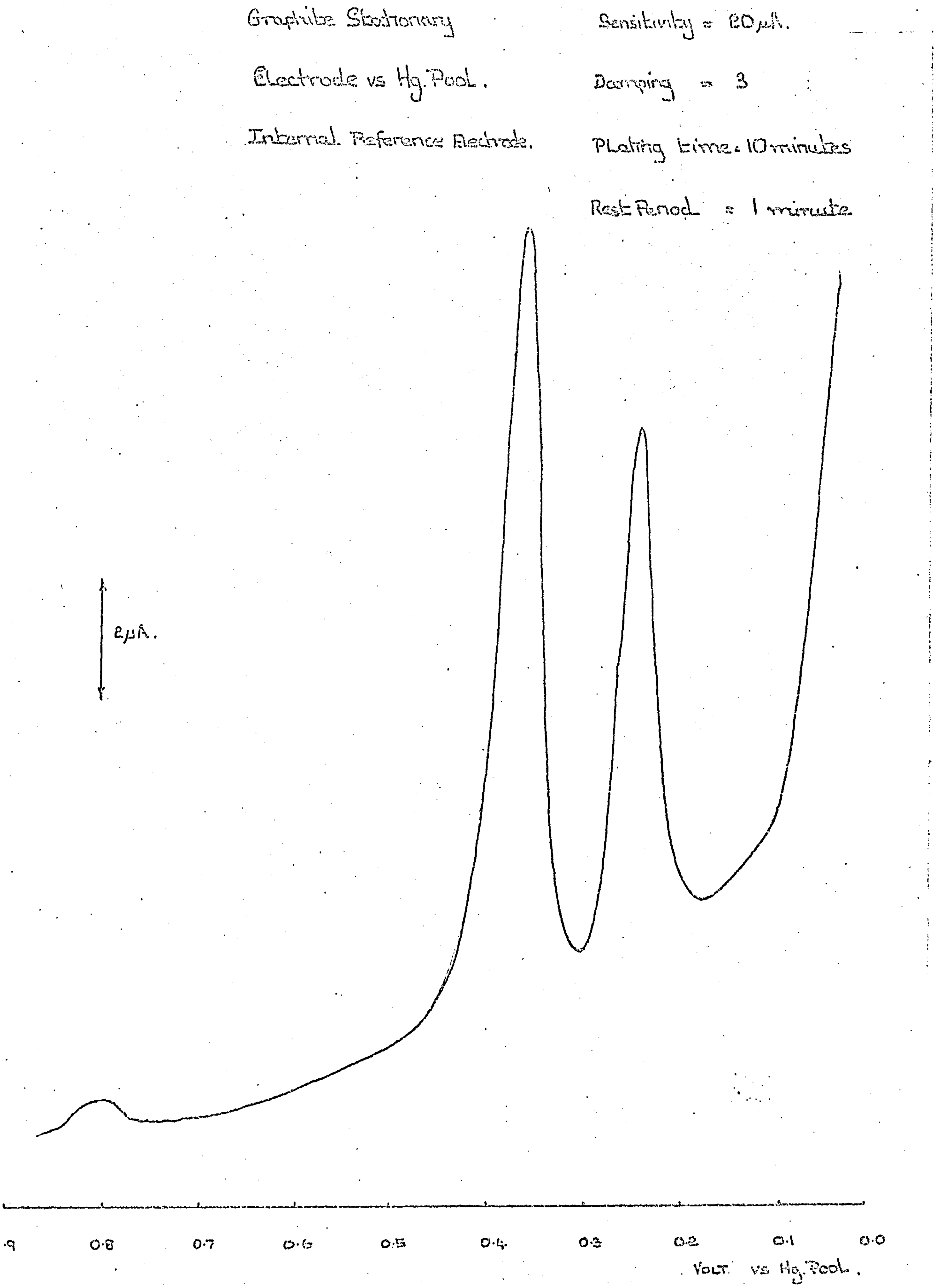
Graphite Stationary
Electrode vs Hg. Pool.
Internal Reference Electrode.
Sensitivity = 20 μA.
Damping = 3
Plating time = 10 minutes
Rest Period = 1 minute.
2 μA.
·9
0·8
0·7
0·6
0·5
0·4
0·3
0·2
0·1
0·0
Volt. vs Hg. Pool.

Figure 10

Figure 11.

Spectrographic graphite electrode.

Simplified Cell Assembly with

Rotating Electrode.

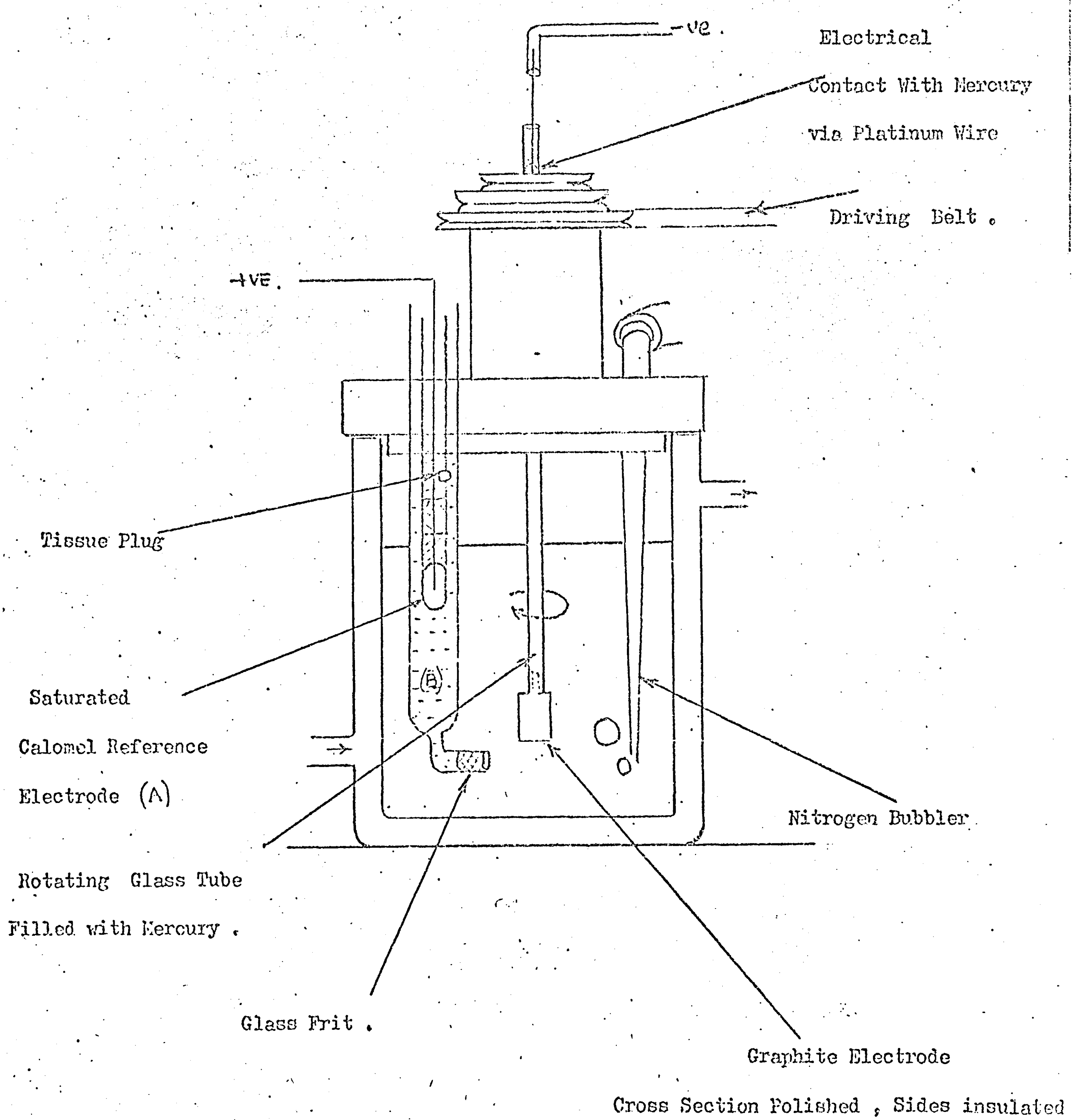

3 anodic scans after successive platings

showing a failing electrode.

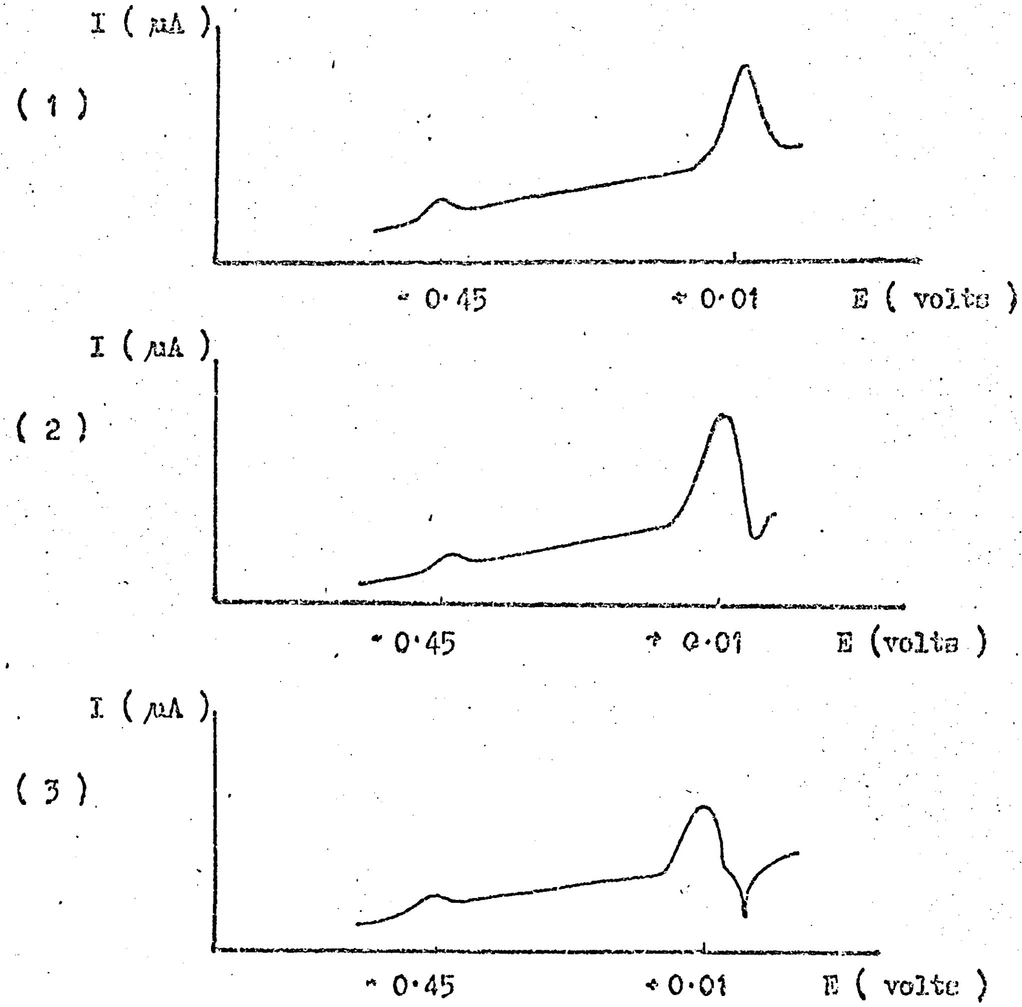

Figure 13.

Voltammograms to illustrate "humping".

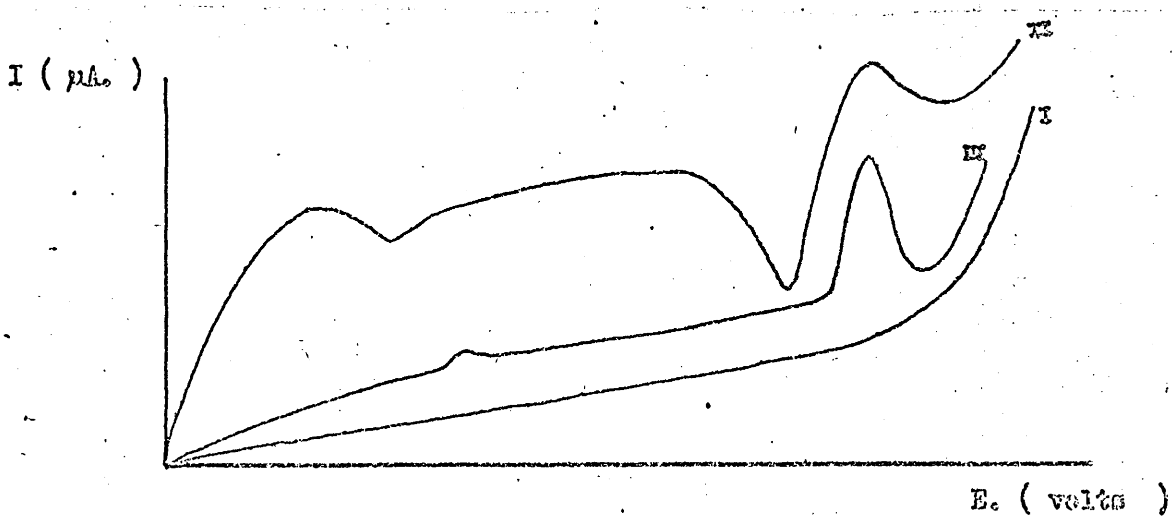

indentation, occurred. The lead peak at -0.45V was unaffected by cathodic indentation. The copper peak at 0.01V showed slight indentation initially on the anodic side of the peak; however, on further scans the copper peak became smaller and the trough so large that electrical compensation was necessary to keep the recorder pen on scale. The process is illustrated in (Fig.12).

This type of electrode behaviour has been attributed by Clem et al to poor impregnation of the electrode or to the use of inferior impregnating agents. The slow formation of a crystalline structure in the wax produces an irregular surface which may trap both gases and solution leading to abnormal electrode behaviour. On examination of the electrode surface after the experiment the film was seen to be in an inactive condition owing to the formation of mercurous chloride precipitate.

On another occasion the initial scan I (Fig.13) was smooth and gave the impression of extreme purity in the cell supporting electrolyte. Scan II in (Fig.13) is a successive scan following a further 5 minute plating in the same solution. The scan shows the occurrence of humping and high residual currents. Scan III shows the normal voltammogram produced when a mercury pool internal reference electrode was substituted for the SCE in the same solution.

4.1.8. <u>SCE Salt bridge</u>. Since the graphite electrode was the same in both cases it is concluded that the salt bridge of the SCE reference electrode was at fault in both the above experiments. The reference electrode salt bridge is a source of Cl^- ion and this has already been found to cause malfunction of the electrode when plating from a supporting electrolyte medium of 0.1mol dm^{-3} KCl. A salt bridge of agar gel was also found to be unsatisfactory owing to the prescence of Cl^- ion and the possible risk of introducing organic contaminants which may poison the electrode. A fluctuating potential from the SCE as a result of plating against the reference electrode may be an alternative explanation of the humping seen in the voltammograms shown in (Fig.13).

It was found that larger more symmetrical peaks were obtained when a laboratory made SCE was used instead of the Beckmann SCE (PL40E) (Fig.14). The laboratory made SCE was therefore used in all further experiments.

Figure 14.

Stripping voltammograms with commercial and a laboratory made calomel electrode.

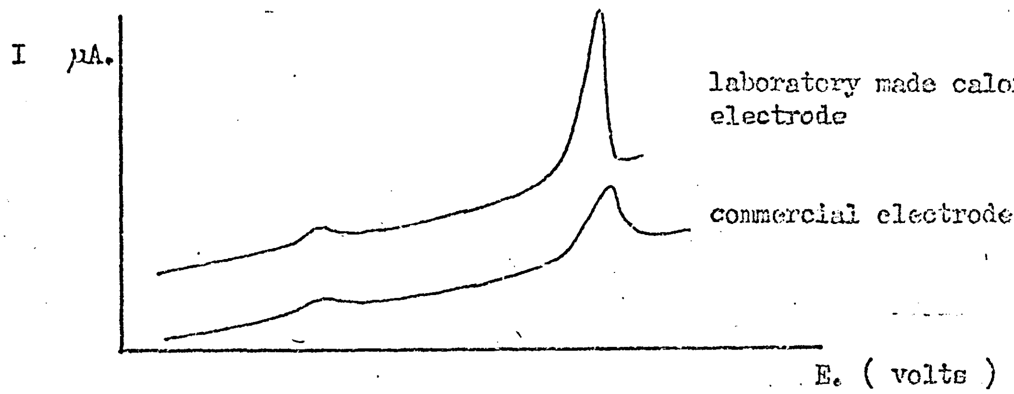

To overcome the problem of contamination from the SCE, it was put in a jacket type of salt bridge, the salt bridge was placed inside the cell and contained 0.2mol dm^{-3} KNO_3 to reduce the risk of Cl^- ion contamination.

Electrical contact between the SCE and the salt bridge was via a 2mm diameter tissue plug. The salt bridge made electrical contact with the solution via a ceramic plug. The apparatus is shown in (Fig.11). The cell geometry was maintained constant for all further experiments. The reference electrode was placed as near to the graphite working electrode as possible and thus kept the cell resistance to a minimum such that the ASV peak height above residual current is enhanced.

4.1.9. Copper contamination. The contamination of cell samples with Cu became very pronounced when samples were left in the cell for some time. In (Fig.15) the voltammograms recorded before and after a 16hr. period in which the cell contents were left in contact with the electrode assembly, show the serious leaching of Cu. The source of such contamination could be from the cell lid, the electrode chuck or from the cell itself.

Cell. The ASV cell was always washed with hot nitric acid and rinsed with doubly distilled water prior to the application of Desicote so that contamination from this source would be minimal.

Cell lid. The cell lid was made out of a black thermoplastic polymer which could have released significant amounts of copper.

Stirrer body and chuck. On close examination the chuck and stirrer body holding the rotating electrode were found to be made of brass or copper plate with a nickel finish.

The stirrer body could contaminate the cell contents if a mist produced by bubbling with nitrogen condensed on its surface and then dripped back into the cell solution.

The problem was overcome by covering the stirrer gland with parafilm and painting any metallic components with Desicote; the cell lid and cell body were also treated with Desicote at weekly intervals.

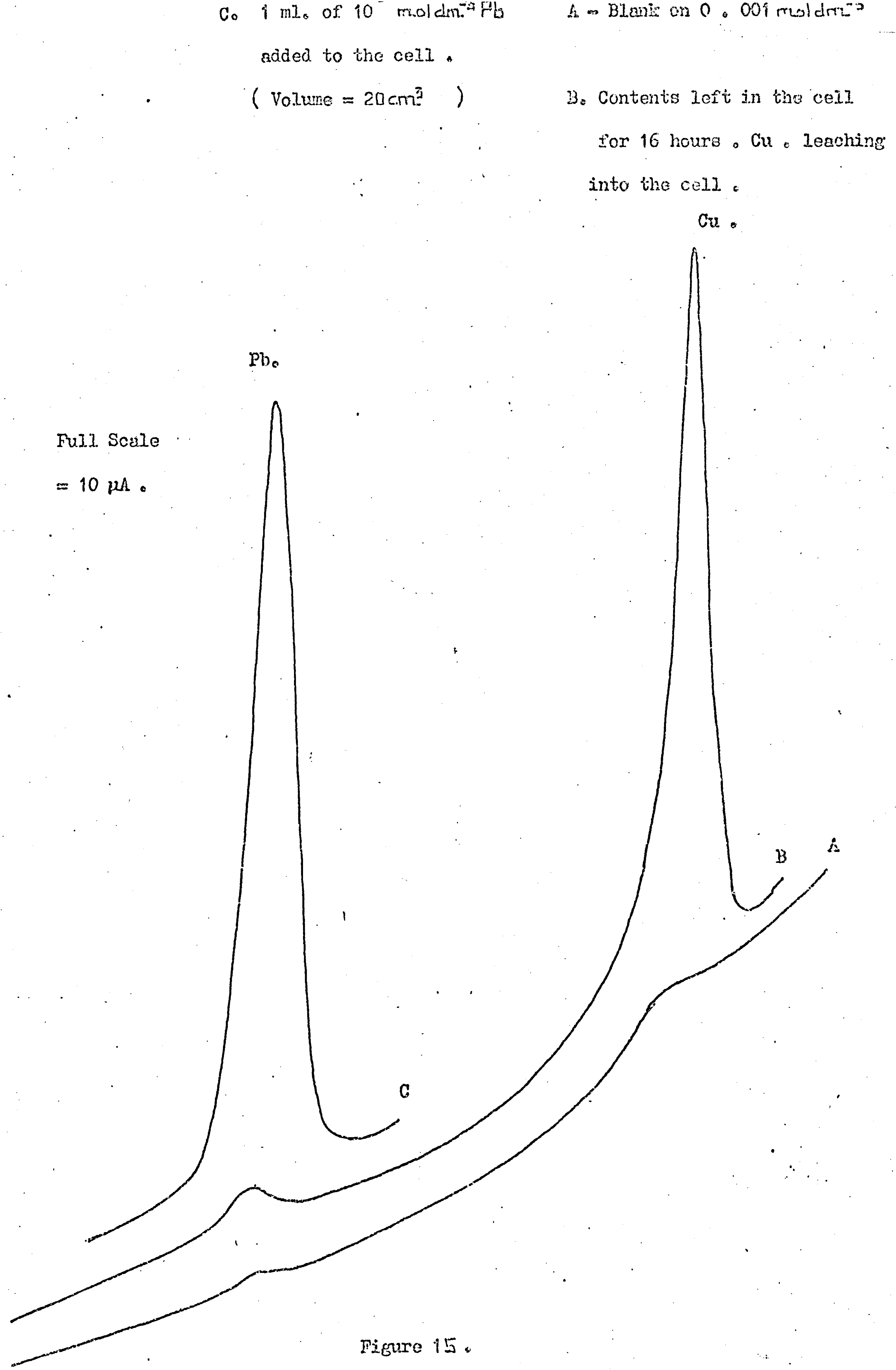

C. 1 ml. of 10^{-} moldm^{-3} Pb added to the cell. (Volume = 20 cm^{3})
A - Blank on 0.001 moldm^{-3}
B. Contents left in the cell for 16 hours. Cu. leaching into the cell.
Cu.
Pb.
Full Scale = 10 μA.
C
B
A

Figure 15.

4.1.10. Effect of Cu on the electrode. The electrode was adversely affected as a result of increased copper concentrations and produced voltammograms with high background currents.

After the potential between the MFE and SCE was set at -1.0V to plate the trace metals into the mercury film, the electrode behaved normally on the first anodic scan but on successive platings, increasingly erratic behaviour was observed as illustrated in (Fig.16)

Figure 16.

3 successive anodic scans with 10^{-6}mol dm^{-3} Cu in solution.

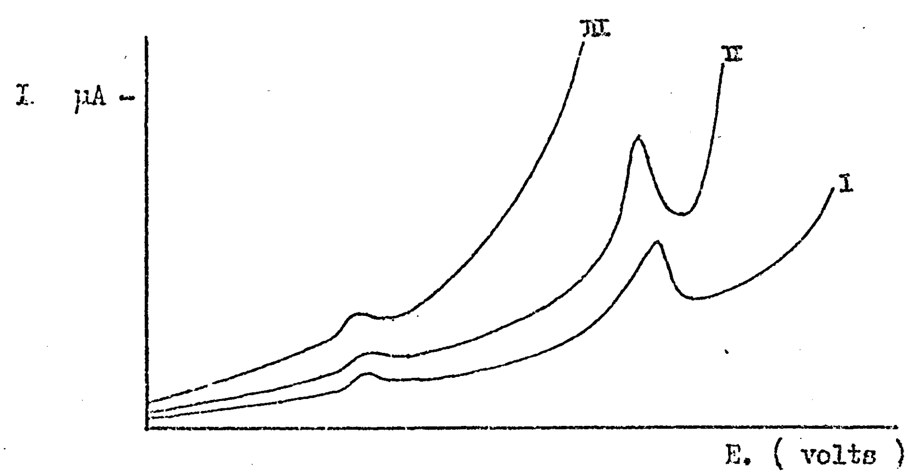

In the scans shown in Fig.16, the supporting electrolyte was 0.05mol dm^{-3} sodium acetate. Three plating and stripping runs were conducted on the same solution, the plating period being five minutes in each case (I, II & III, Fig.16).

The normal voltammogram shown in Fig.16 (I) shows a large anodic peak due to the presence of Cu. Scan II under the same conditions shows a pronounced Cu anodic peak on a steep slope caused by a high residual current, the recorder pen went off scale before reaching the mercury anodic peak at 0.45V vs. SCE. It is possible that the mercury peak merely moved in the cathodic direction which resulted in a high residual current following the Cu peak.

Scan III shows that the Cu peak has been obliterated by an uncontrollable high residual current following the anodic peak for Pb.

It has been suggested by I.M. Metters (37) at a research Symposium in May 1973 at Sheffield University that the plating out of copper in the mercury film at these high Cu concentrations lowers the potential at which hydrogen evolution occurs at the electrode. It is not easy to understand how this would cause the observed effect.

However, if a Cu/Hg amalgam is being formed then it is possible that the Cu and Hg stripping peaks are displaced and give rise to the steep current increase at 0.1V owing to oxidation of the intermetallic compound or amalgam.

4.1.11. <u>Residual current</u>. The use of the graphite wax impregnated electrode in supporting electrolytes of 0.1mol dm^{-3} concentration produced such a high residual current that instrument sensitivities below 10µA full scale deflection could not be used.

Perone and Kretlow (1965) (38) who also encountered this problem reduced the residual current by diluting the supporting electrolyte medium from 0.1mol dm^{-3} KCNS for the determination of 10^{-4} to 10^{-5}mol dm^{-3} Hg to 0.02mol dm^{-3} KCNS for the analysis of 10^{-7} to 10^{-9}mol dm^{-3} mercury, they found no significant variation in the analytical data and thus increased the working range of the electrode.

The dilution of 0.1mol dm^{-3} KNO_3 supporting electrolyte in our case allowed a sensitivity setting of 5µA full scale deflection to be used for the determination of trace metals in the 10^{-7}mol dm^{-3} to 10^{-9}mol dm^{-3} concentration range. The dilution of KNO_3 also reduced the Pb contamination from the supporting electrolyte as well as the residual current (Fig.17).

Figure 17.

The slopes of the residual current curves in different media.

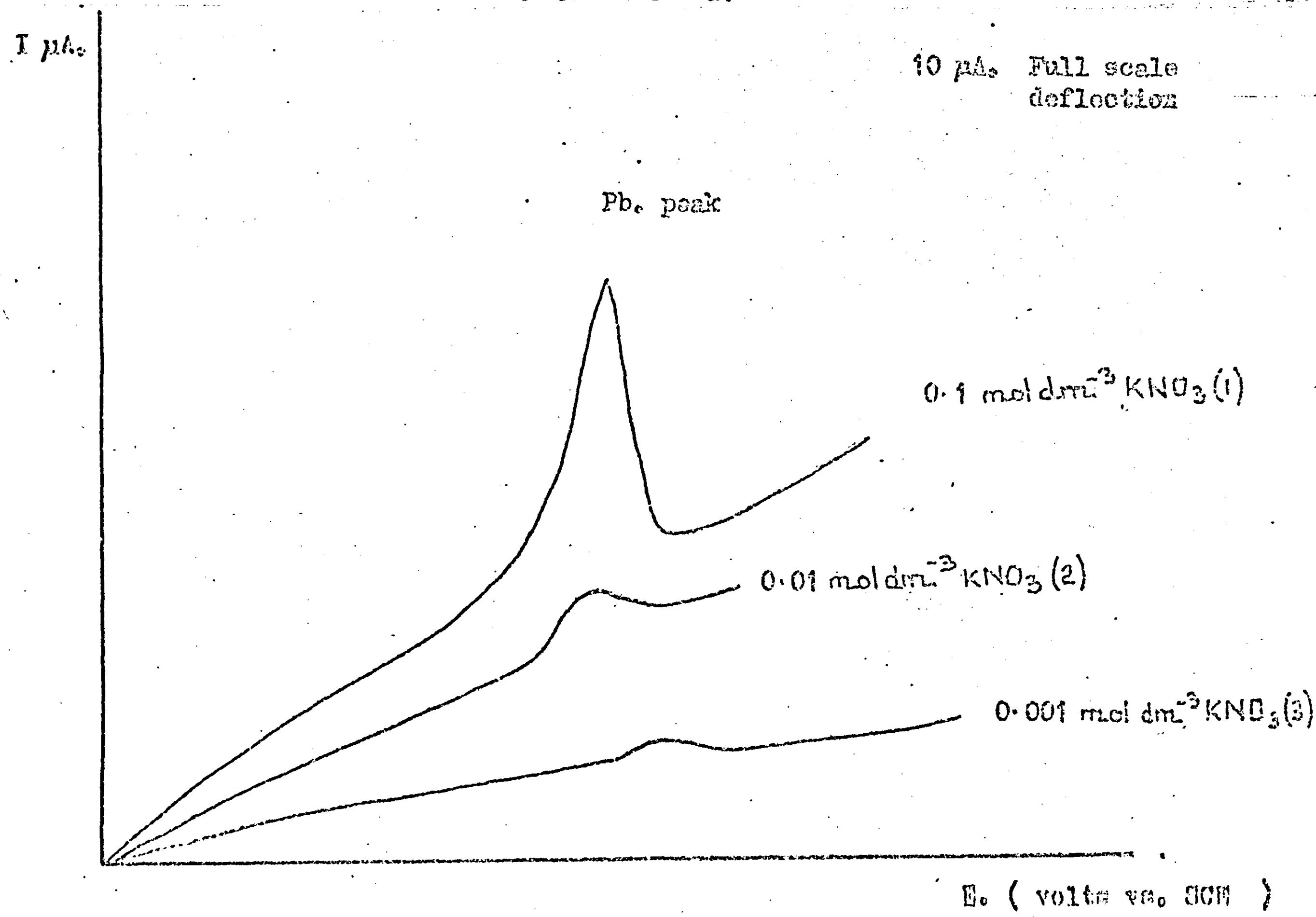

The slopes of the residual current curves in different media are tabulated in Table 3.

Table 3

Supporting Electrolyte	Residual Current
0.1mol dm^{-3} CH_3COONa	0.9 μA/V
0.1mol dm^{-3} KNO_3	1.1 μA/V
0.01mol dm^{-3} KNO_3	0.8 μA/V
0.001mol dm^{-3} KNO_3	0.4 μA/V

4.2. Experiments with glassy carbon electrodes

4.2.1. Electrode preparation. Glassy carbon is very hard and possesses good electrical conductivity, high hydrogen overpotential and chemical inertness. No wax impregnation procedure is necessary with this material. The polishing of the electrode with increasingly fine grades of emery and diamond paper finishing with 6µm and 1µm grade produced a superior mirror polish on this material as compared to a dull grey finish achieved with graphite.

A 1cm length of glassy carbon with a diameter of 0.3cm was inserted into a glass tube of 0.4cm diameter such that 0.2cm of the glassy carbon rod was left protruding from the end. The carbon rod was sealed in place with an epoxy resin. No other part of the rotating electrode assembly was altered from its use with graphite electrodes.

4.2.2. Plating procedure. The electrode is plated from a 2 x 10^{-5}mol dm^{-3} mercuric nitrate solution for 5 minutes as before. The mercury film is deposited at an applied potential of -1.0V vs. SCE with the simultaneous deposition of the trace elements in the sample. The first anodic potential scan is ignored and is used to condition the electrode.

Florence (11) pioneered this technique and claims film thicknesses of the order of 0.001μm to 0.01μm under the above conditions.

The electrode is rotated throughout the deposition and stripping phases of the analysis and deaeration of the sample are performed continuously.

The electrode is freshly plated in each analysis, the mercury deposit is completely removed after the analysis by wiping with a wet tissue, no mercury peak is observed on an anodic scan following the removal of the film.

The electrode was successfully plated with mercury from 0.1mol dm^{-3} KNO_3 containing 2 x 10^{-5}mol dm^{-3} mercuric nitrate solution and scanned from -1.0V to + 0.4V in a manual scan of the potential range without recording a voltammogram. After this conditioning run the potential could be re-set at -1.0V applied potential between SCE and the glassy carbon electrode to plate trace metals from the sample.

The voltammograms produced showed a low residual current contribution in 0.1mol dm^{-3} KNO_3 of less than 0.4μA V^{-1} on a 400mV min^{-1} scan rate. No dilution of supporting electrolytes was necessary to achieve sensitivity settings as high as 1.5nA full scale deflection.

The cell sample was made 10^{-7}mol dm^{-3} w.r.t Cd, In, Pb; sharp peaks were recorded at -0.64, -0.53 and -0.45V applied voltages vs. SCE. It was also found at this time that when a saturated KNO_3 salt bridge was used, sharper stripping peaks were obtained at the same peak potentials. A saturated KNO_3 bridge was therefore used in all further experiments.

The rotating electrode is particularly sensitive to oxygen

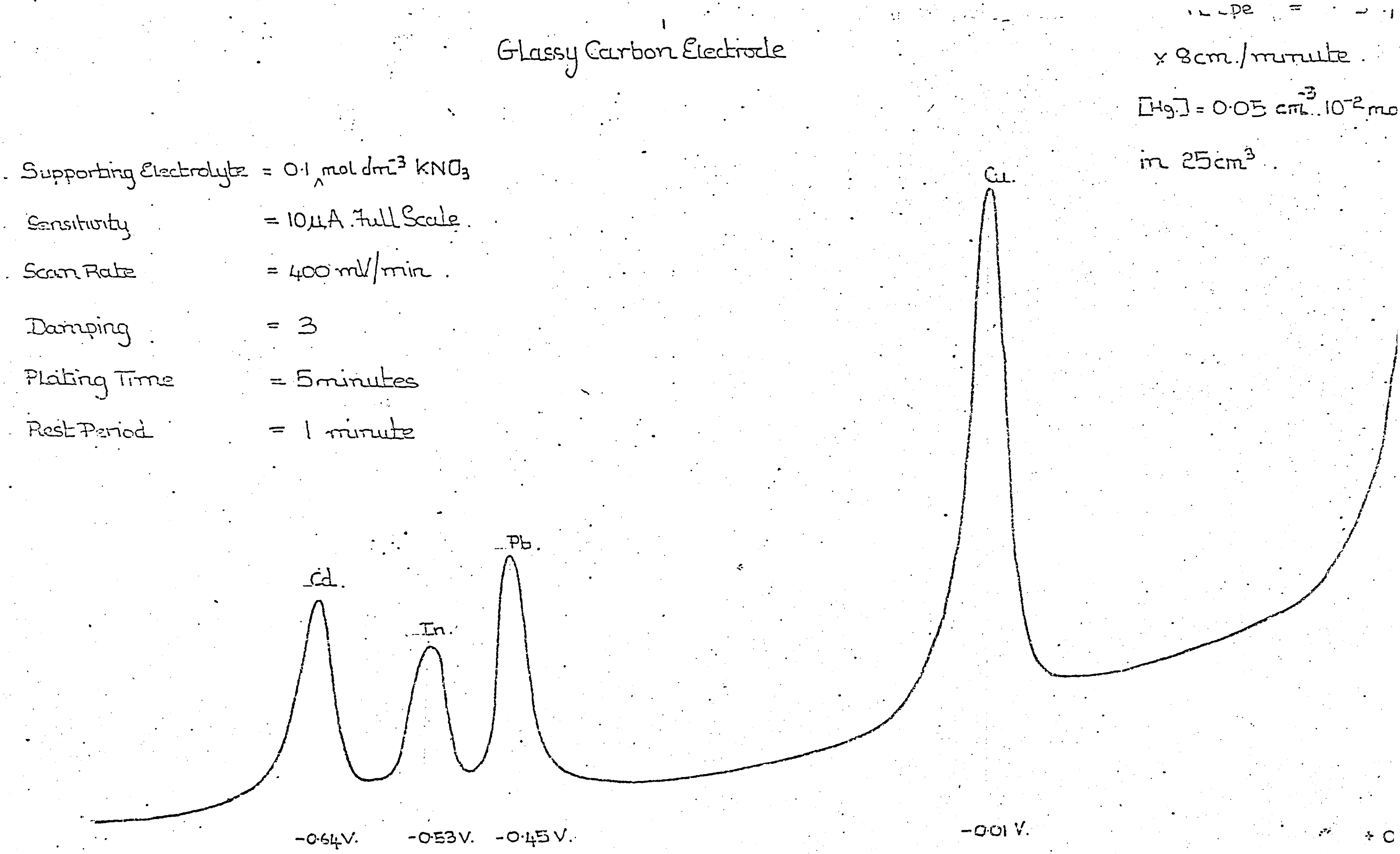

Figure 18.

Voltammogram produced with a glassy-carbon electrode.

Figure 12.

The 3-electrode cell and circuit.

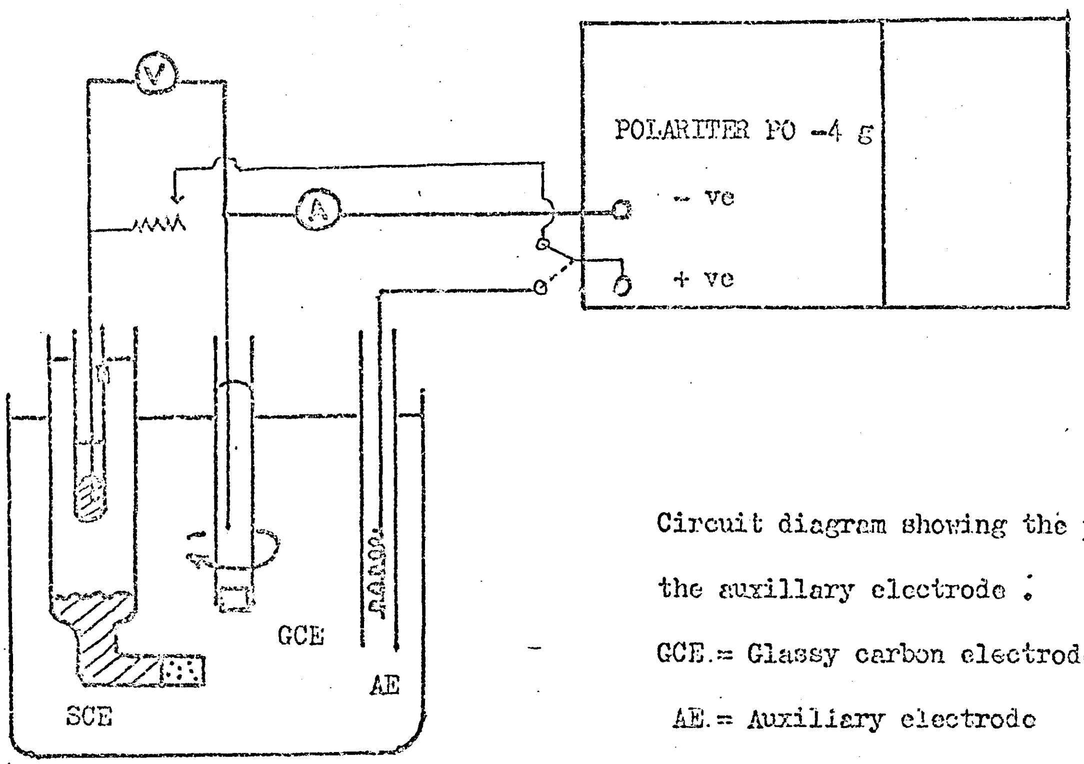

Circuit diagram showing the position of the auxillary electrode :

GCE.= Glassy carbon electrode

AE.= Auxiliary electrode

SCE.= Saturated calomel electrode and salt bridge .

in solution, a high rate of constant deaeration with nitrogen is necessary to keep the residual current to a minimum.

The glassy carbon electrode produces sharp peaks which allows the resolution of metals with adjacent peak potentials such as Cd and In or In and Pb (Fig.18).

4.2.3. <u>Development and evaluation of a 3 electrode cell</u>

The plating of the carbon cathode by applying a potential between it and a SCE is undesirable since trace metals in the salt bridge or mercury from the calomel electrode may also be plated into the film with the trace metals in the sample. The passing of current through the calomel reference electrode for the time associated with the plating step is also likely to cause a decrease in the reliability of the calomel electrode as a reference electrode.

A platinum auxiliary anode was therefore introduced to pass the current in the plating step and a SCE switched into the circuit for the anodic scan.

A high impedance voltmeter and an ammeter were introduced to monitor the voltage of the carbon electrode with respect to the SCE in the deposition step and the current passing between the platinum and glassy carbon electrode. The circuit is shown in Fig.19.

This combination was evaluated by varying the applied potential between the carbon and platinum electrodes in 0.5V steps from -3.0 to 0.5V and maintaining the potential of the platinum auxiliary electrode and the carbon electrode individually vs. the SCE.

The potential was scanned in both the anodic and cathodic direction. The cell contained $20cm^3$ of $0.1mol\ dm^{-3}$ KNO_3, the

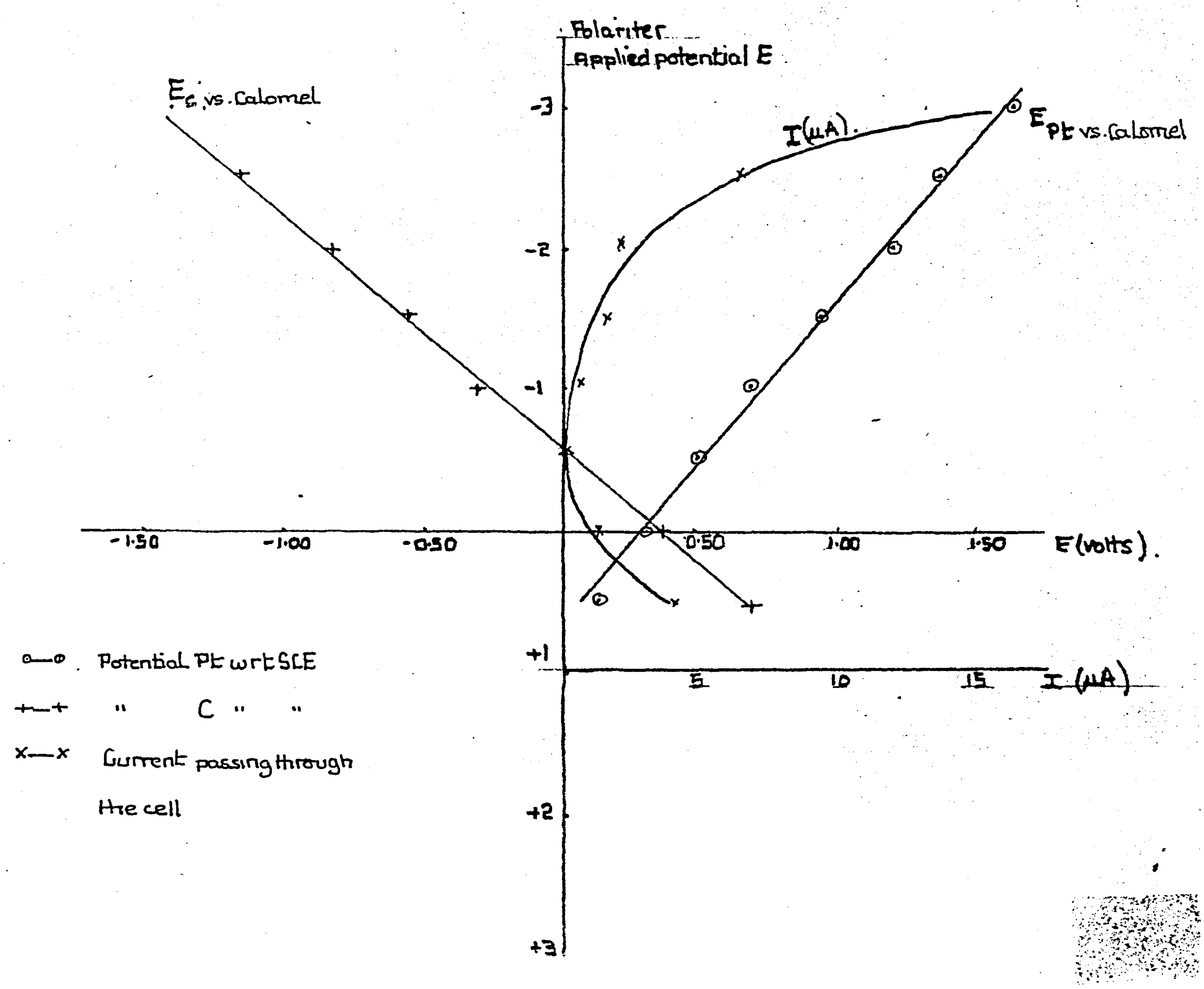
Polariter
Applied potential E
E_C vs. Calomel
I(µA).
E_{Pt} vs. Calomel
-3
-2
-1
+1
+2
+3
-1.50
-1.00
-0.50
0.50
1.00
1.50
E (volts).
5
10
15
I (µA)
Potential Pt wrt SCE
" C " "
Current passing through the cell

of the experiment. The results are recorded in Table 4 & Fig. 20.

Table 4 shows the difference of the potentials of these two electrodes is approximately equal to the applied potential as indicated by the Polariter voltage scale.

The carbon electrode changes in polarity at -0.5V (applied potential) and no current flows.

The platinum electrode shows no change in polarity w.r.t SCE and increases from 0.159V to 1.650V vs. SCE.

The results from a cathodic scan starting at 3.0V vs, SCE are erratic since at this potential, electrolysis of the cell solution is occurring with the evolution of oxygen at the

Table 4

Record of carbon and platinum electrode potentials and deposition current at different applied potentials

	Polariter applied potential	Current passing through cell	Potential platinum w.r.t SCE	Potential carbon w.r.t SCE
	Volt	µA	Volt	Volt
Cathodic Scan	0.50	4.00	+0.159	0.681
	0.00	1.00	+0.315	0.345
	-0.50	0.00	+0.520	0.00
	-1.00	0.05	+0.710	-0.320
	-1.50	1.50	+0.970	-0.580
	-2.00	2.00	+1.210	-0.820
	-2.50	6.50	+1.380	-1.160
	-3.00	21.50	+1.650	-1.400
Anodic Scan	-3.00	20.08	+1.61	-1.44
	-2.50	3.00	+1.31	-1.25
	-2.00	0.03	+0.88	-1.16
	-1.50	0.10	+0.445	-1.09
	-1.00	1.00	+0.185	-0.850
	-0.50	3.50	+0.090	-0.450
	0.00	4.00	+0.050	-0.005
	0.50	4.50	+0.030	0.500

platinum anode and hydrogen at the carbon electrode.

Since polarization of the anode is inevitable it cannot be used as a reference electrode in the stripping step. In the 3-electrode cell the SCE can be switched into the plating circuit prior to the anodic scan.

The platinum electrode is jacketed to prevent any oxygen evolved from contaminating the whole cell contents.

4.2.4. <u>ASV with a 3-electrode cell.</u> The plating current was passed by the auxiliary electrode and plating performed at a carbon electrode potential of -1.0V vs. SCE. The potential of the carbon electrode was maintained constant by manual alteration of the applied potential as set by the Polariter between the carbon and platinum electrodes.

A $20cm^3$ volume of $0.1mol\ dm^{-3}$ KNO_3 was made $2.5 \times 10^{-5} mol\ dm^{-3}$ in mercuric nitrate and plating performed for five minutes. The calomel electrode which had been used to monitor the carbon electrode potential was then switched into the plating circuit and the platinum counter electrode disconnected immediately. A conditioning anodic scan was then performed followed by a recorded scan after a further plating period of five minutes. A smooth voltammogram was produced with the mercury oxidation peak at + 0.45V vs. SCE.

The solution was then made $10^{-6} mol\ dm^{-3}$ w.r.t Pb and Cu.

The addition of these two metal standards yielded sharp peaks in the stripping voltammograms at -0.45V and -0.05V for Pb and Cu respectively.

The results of the experiment are shown in Table 5.

The plating current was monitored both by an ammeter in series in the plating circuit and by the Polariter chart recorder.

The chart recorder has a slight time lag otherwise agreement between the readings was good.

Table 5

Results of initial plating experiment

using a 3-electrode cell

Polariter reading (V)	Time in minutes	Deposition Current μA (meter)	μA (chart)	Carbon electrode vs. Calomel (V)
-2.36	0	3.00	3.00	-1.0
-2.36	1	2.50	2.45	-1.0
-2.38	2	2.35	2.38	-1.0
-2.38	3	2.25	2.24	-1.0
-2.38	4	2.26	2.25	-1.0
-2.38	5	2.26	2.26	-1.0

Results of a Linear potential scan

at 800mV min^{-1}

Peak	E_p(V)	i_p(μA)	$b_{\frac{1}{2}}$(mV) (half peak width)
Pb	-0.45	7.90	55
Cu	-0.05	6.60	40

4.2.5. Use of carbonic acid (H_2CO_3) as supporting electrolyte.

The cell geometry and apparatus shown in Fig.11 was maintained constant and the use of carbon dioxide to replace nitrogen as the purge gas investigated.

The use of CO_2 to deaerate a distilled water sample not only removes oxygen from that sample but provides a supporting electrolyte from which sharp quantitative anodic stripping

Figure 21

Voltage of the Pt. electrode monitored w.r.t. the glassy carbon electrode .from the onset of de - gassing with CO_2. The sample was $2{\cdot}5 \times 10^{-5}$ mol dm^{-3}. w.r.t. Hg^{II}. and had a pH. of 3·80 after 10 minutes .

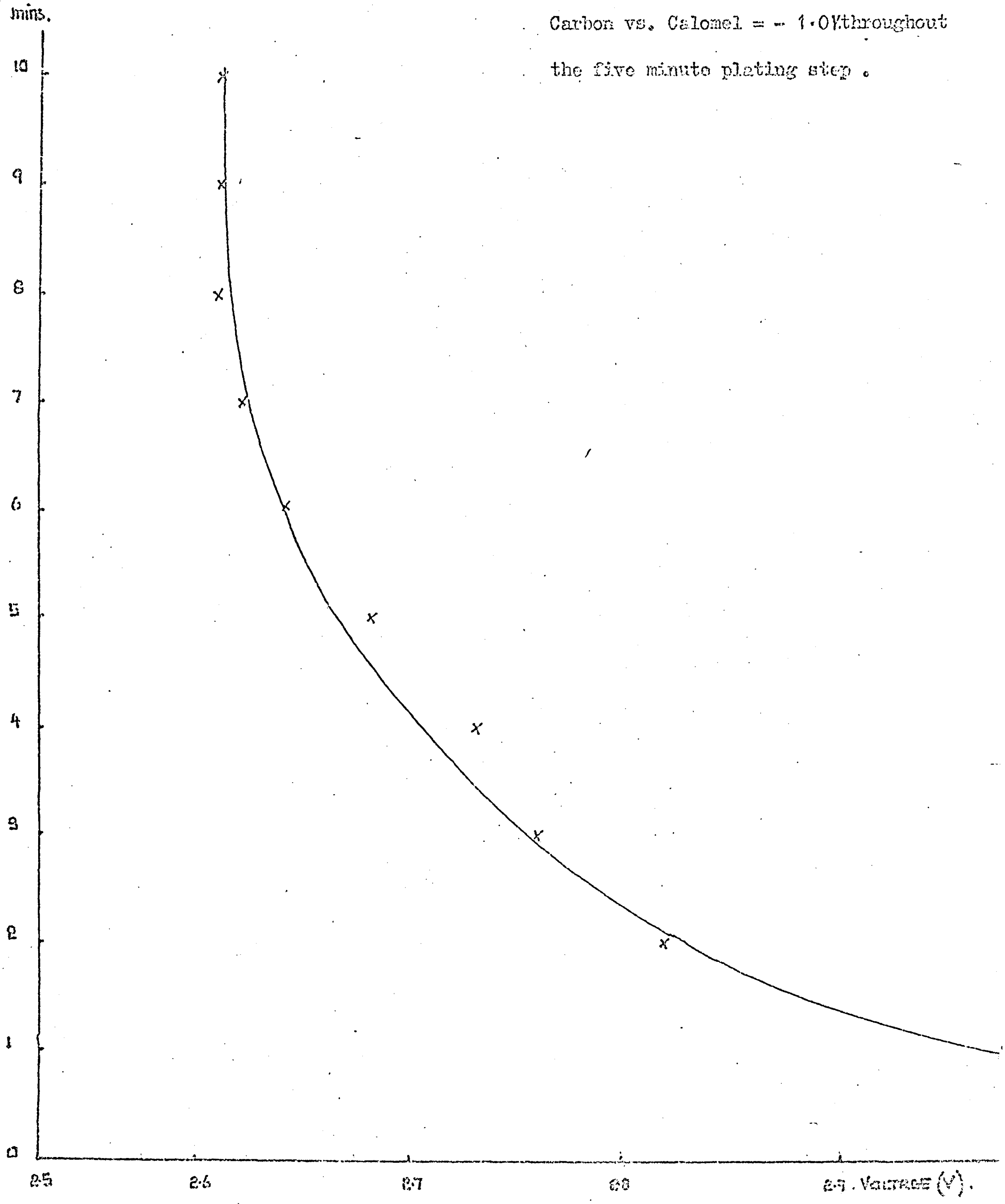

Figure 22

Deposition current monitored with time whilst de - gassing a 20 cm^3 sample of doubly distilled water with CO_2 . The sample was 2·5 X 10^{-5} mol dm^{-3}. w.r.t. Hg^{II}. and had a pH. of 3·80 after 10 minutes .

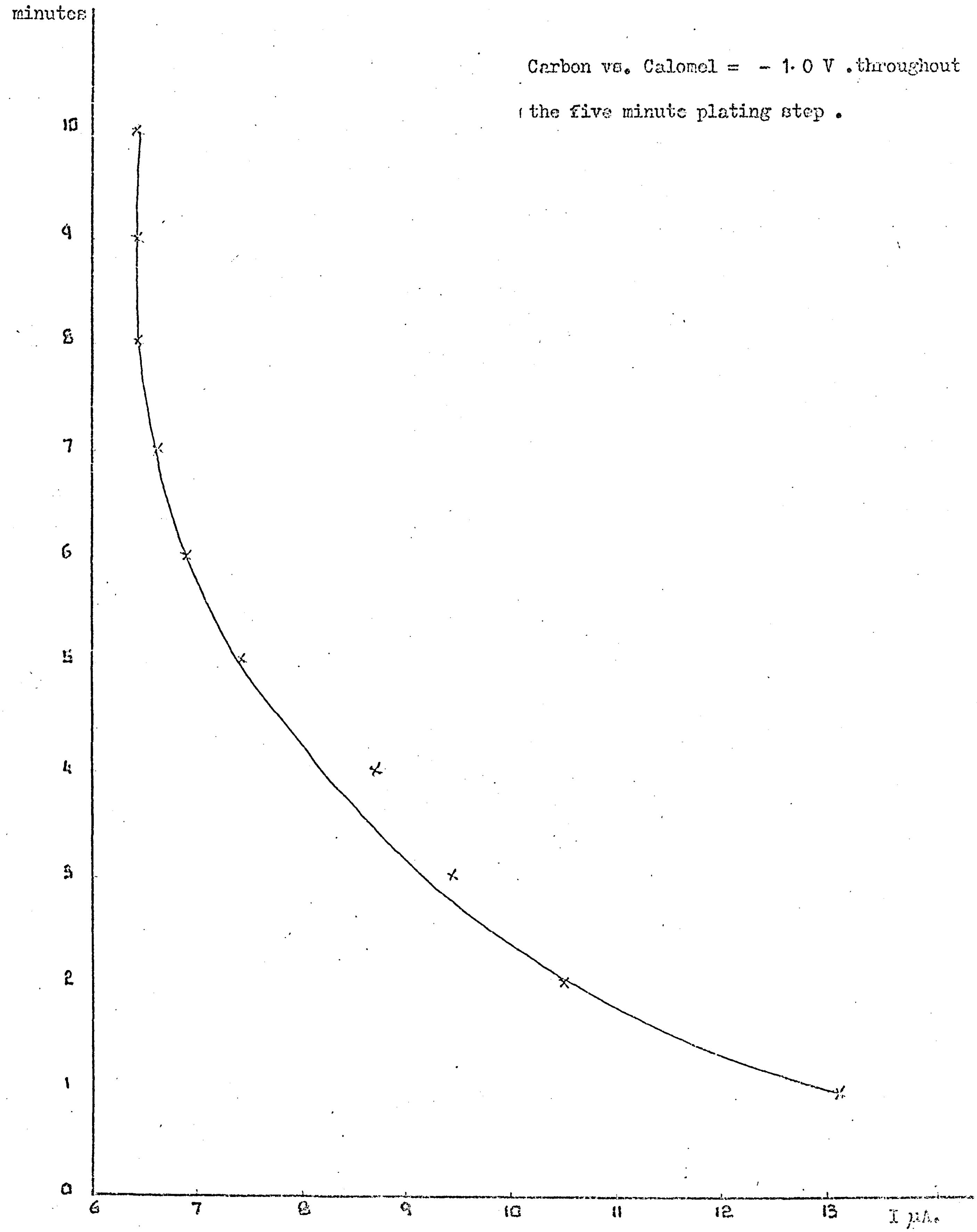

peaks are produced.

There is an added advantage in providing a supporting electrolyte in this manner in that no contamination from an added salt is possible. The number of manipulative operations prior to analysis is also reduced.

The time for the 20cm^3 solution of distilled water to be thoroughly degassed is between 8 to 10 minutes as can be seen from (Figs. 21 and 22) in which the deposition current is monitored from the onset of degassing, together with the Polariter applied potential.

The current is high (13µA) at the onset of degassing owing to the presence of oxygen in solution and its participation in the electrode reactions; also mercury film coverage is minimal.

The solution gradually becomes saturated with carbonic acid and oxygen is dispelled. The removal of oxygen and the build up of the carbonic acid supporting electrolyte results in an overall decrease in current to 6.40µA where it stays constant, (mercury now covers all the sites available). The pH of the solution after bubbling with CO_2 stabilises at pH 3.8.

In all further experiments involving carbonic acid as the supporting electrolyte the degassing period was therefore fixed at 10 minutes to ensure complete saturation of the solution and complete film coverage.

It was also possible to obtain voltammograms using nitrogen as the purge gas and without the addition of any supporting electrolyte other than mercuric nitrate used for plating. Nitrogen degassing for a period of ten minutes prior to plating from the sample also produced good voltammograms. The pH of the distilled water was found to drift upward from 5.8 to 6.2

during nitrogen degassing but stabilised after ten minutes at the higher value.

The electrode area decreases as plating of mercury commences and this contributes to the declining deposition current as shown in Fig.22. The conditioning scan prior to recording an anodic scan ensure that both degassing and film coverage is adequate. The plateau current condition can thus be achieved quickly in consecutive scans so that reproducibility is not impaired.

The deposition current under nitrogen stabilised at 6.2μA and in acidic media at 7.3μA.

CHAPTER 5.

Investigation of ASV parameters

5.1. Scan rate (ν)

The equation (10) in the theory section (Ch.2.) shows that the peak current i_p is proportional to the scan rate (ν).

There are four scan rates possible on the Polariter PO-4g: 100mV min^{-1}, 200mV min^{-1}, 400mV min^{-1} and 800mV min^{-1}. The 100mV min^{-1} scan is possible on the slow chart speed of 0.5V cm^{-1}, whilst the others are on the 0.1V cm^{-1} setting (Table 1).

The use of two different chart speeds in the same experiment necessitates a correction to the i_p value since the time required to scan to the E_p value will be greater for the slower chart speed.

The E_p value becomes more anodic, the faster the scan, so a similar time correction must be applied to scans on the same chart speed.

If a plating time of 6 minutes is used then a correction of $\left(\frac{6}{6+t}\right) \times i_p$ (peak height) is necessary to correct for the extra plating time (t) taken to scan to the E_p value. An experiment to investigate the relationship was performed where the cell solution of 20cm^3 of 0.1mol dm^{-3} KNO_3 was made 5.10^{-7}mol dm^{-3} with respect to Pb and after a 6 minute plating and manual anodic scan the i_p values at different scan rates were recorded. The results are shown in Table 6.

A plot of i_p vs. scan rate is shown in (Fig.23) and verifies the predicted linear relationship.

The use of the fastest scan rate is maintained for further experiments to gain maximum sensitivity and reduce total analysis time to a minimum.

<u>Figure 23.</u>

Anodic\scan rate vs. anodic peak* height. (*corrected)

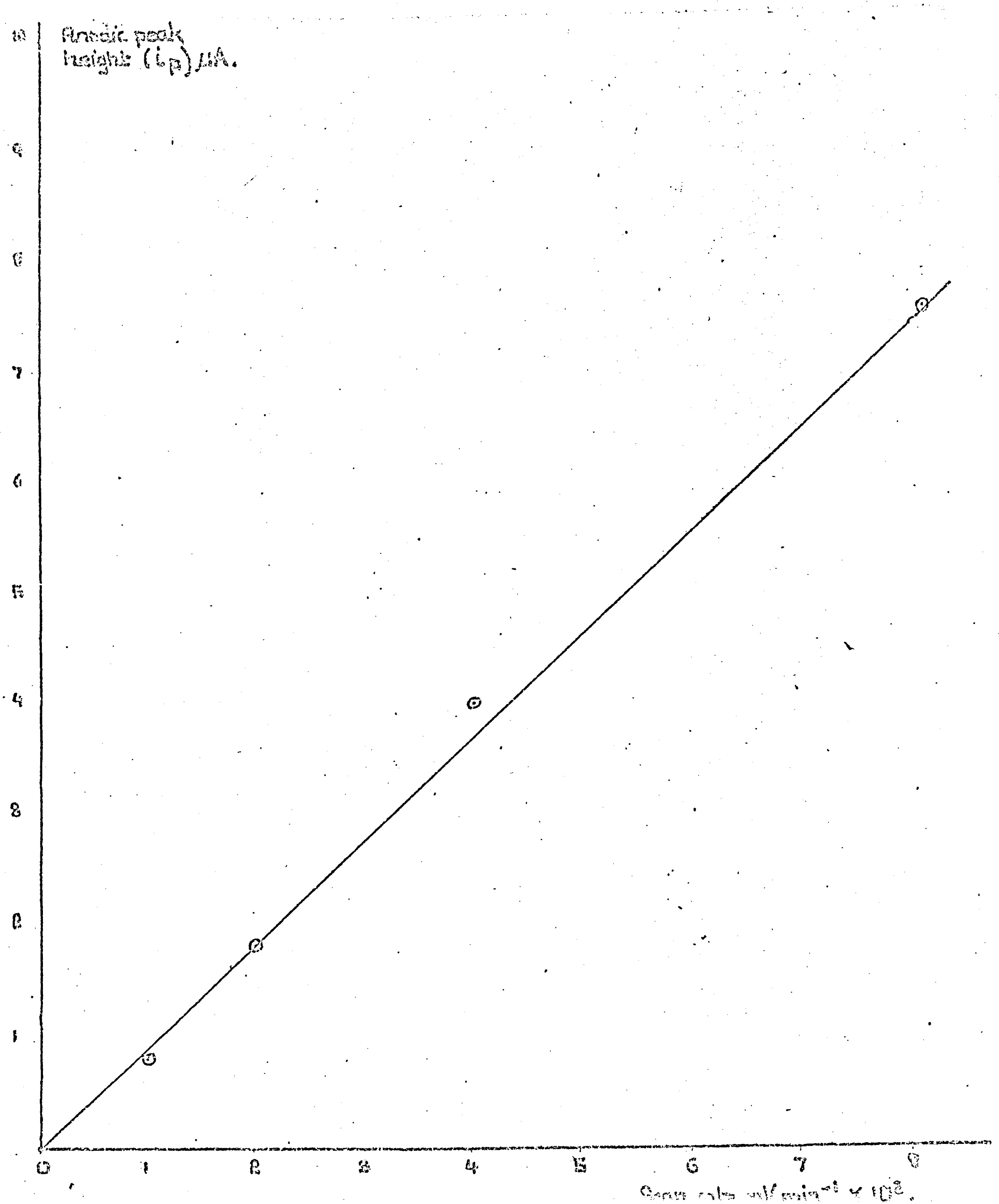

Table 6

Scan Rate mV min^{-1}	Chart Speed Volt cm^{-1}	Pb(E_p) V vs. SCE	Peak Height i_p(μA)	Time to scan to E_p: t (min)	Corrected i_p(μA)
100	0.05	-0.510	1.50	4.90	0.83
200	0.10	-0.470	2.70	2.65	1.87
400	0.10	-0.465	4.95	1.34	4.05
800	0.10	-0.440	8.40	0.70	7.52

5.2. The relationship between peak current (i_p) and rotation speed (ω).

Florence has shown that for glassy carbon electrodes the peak current (i_p) is proportional to the (rotation speed)$^{\frac{1}{2}}$ of the electrode.

An experiment was performed to verify these findings.

A 20cm^3 sample of 0.1mol dm^{-3} KNO_3 was made 5 x 10^{-7}mol dm^{-3} w.r.t. Pb; using plating times of five minutes, separate analyses were performed at four different rotation speeds (Fig.24).

The results are shown in Table 7.

Table 7

Rotation speed (r.p.m)	(r.p.m)$^{\frac{1}{2}}$	Peak Current i_p(μA)	$i_p r^{-\frac{1}{2}}$ μA min
2550	50.50	7.80	0.154
1432	37.84	5.05	0.133
952	30.05	3.53	0.114
764	27.64	2.85	0.103

A linear relationship is obtained between the Pb peak current and the (rotation speed)$^{\frac{1}{2}}$ of the electrode (Fig.24).

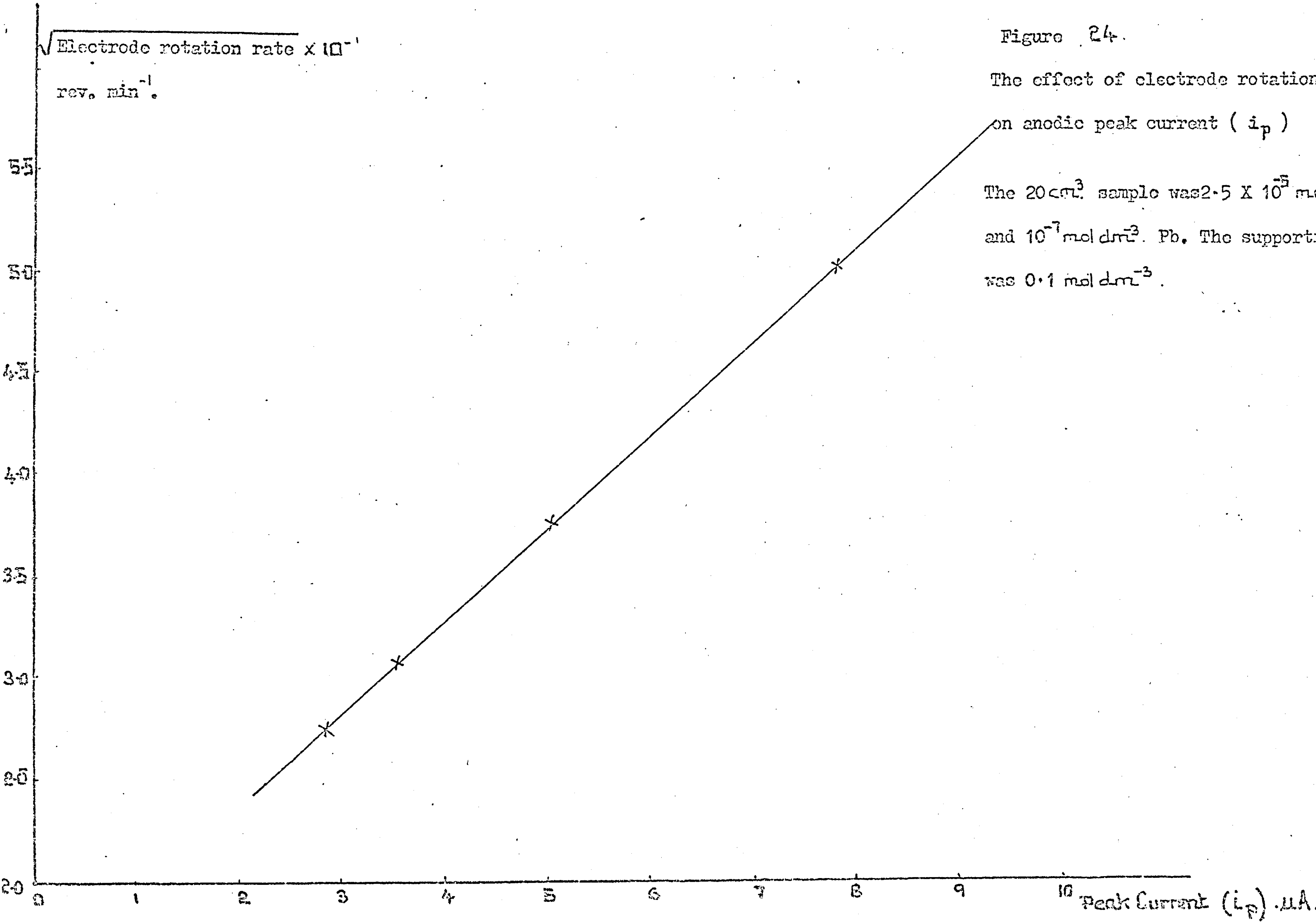

Figure 24.

The effect of electrode rotation speed(w
on anodic peak current (i_p)

The 20 cm^3 sample was 2·5 X 10^{-5} mol dm^{-3} Hg^{II}
and 10^{-7} mol dm^{-3}. Pb. The supporting electr
was 0·1 mol dm^{-3}.

5.3. The effect of scan rate on band width ($b_{\frac{1}{2}}$)

The band width at half peak height is a function of scan rate (ν). The plot of $b_{\frac{1}{2}}$ vs. ν varies according to the mercury film thickness as shown by Van Dalen's (39) plot illustrated in Figure 25. The $b_{\frac{1}{2}}$ values increased with faster scan rates.

Thin films of between 4 and 25µ were relatively unaffected however, films of between 50 and 200µ produced a curved response as the magnitude of $b_{\frac{1}{2}}$ increased from 38mV to 101.9mV correspondingly.

An experiment in which an 0.1mol dm^{-3} KNO_3 solution was made 10^{-7}mol dm^{-3} w.r.t Pb was performed to investigate the $b_{\frac{1}{2}}$ values of the Pb anodic peak at 200, 400 and 800 mV min^{-1}. The glassy carbon was plated insitu and used in successive scans without wiping the electrode. The values of $b_{\frac{1}{2}}$ after a five minute plating were recorded in Table 8 and plotted with van Dalen's results in (Fig.25).

Table 8

Scan Rate (mV min^{-1})	$b_{\frac{1}{2}}$	E_p(Pb)(V)	$E_p - E_{\frac{1}{2}}$(mV)
800	40	-0.437	-52
400	35	-0.455	-70
200	30	-0.480	-95

Results. The lowest value of $b_{\frac{1}{2}}$: 30.00mV is below that of van Dalen's plot at 200mV min^{-1}; on the next successive scan at 400mV min^{-1} the $b_{\frac{1}{2}}$ vs. scan rate (ν) curve of glassy carbon is below the 10 and 25µ film of van Dalen's plot. The $b_{\frac{1}{2}}$ value at 800mV min^{-1} lies between the 10 and 25µ film thickness.

The results indicate that the film is growing in thickness with successive scans since the $b_{\frac{1}{2}}$ vs. scan rate plot crosses

Figure 25

Plot of b½(mV.) vs . Scan Rate (m

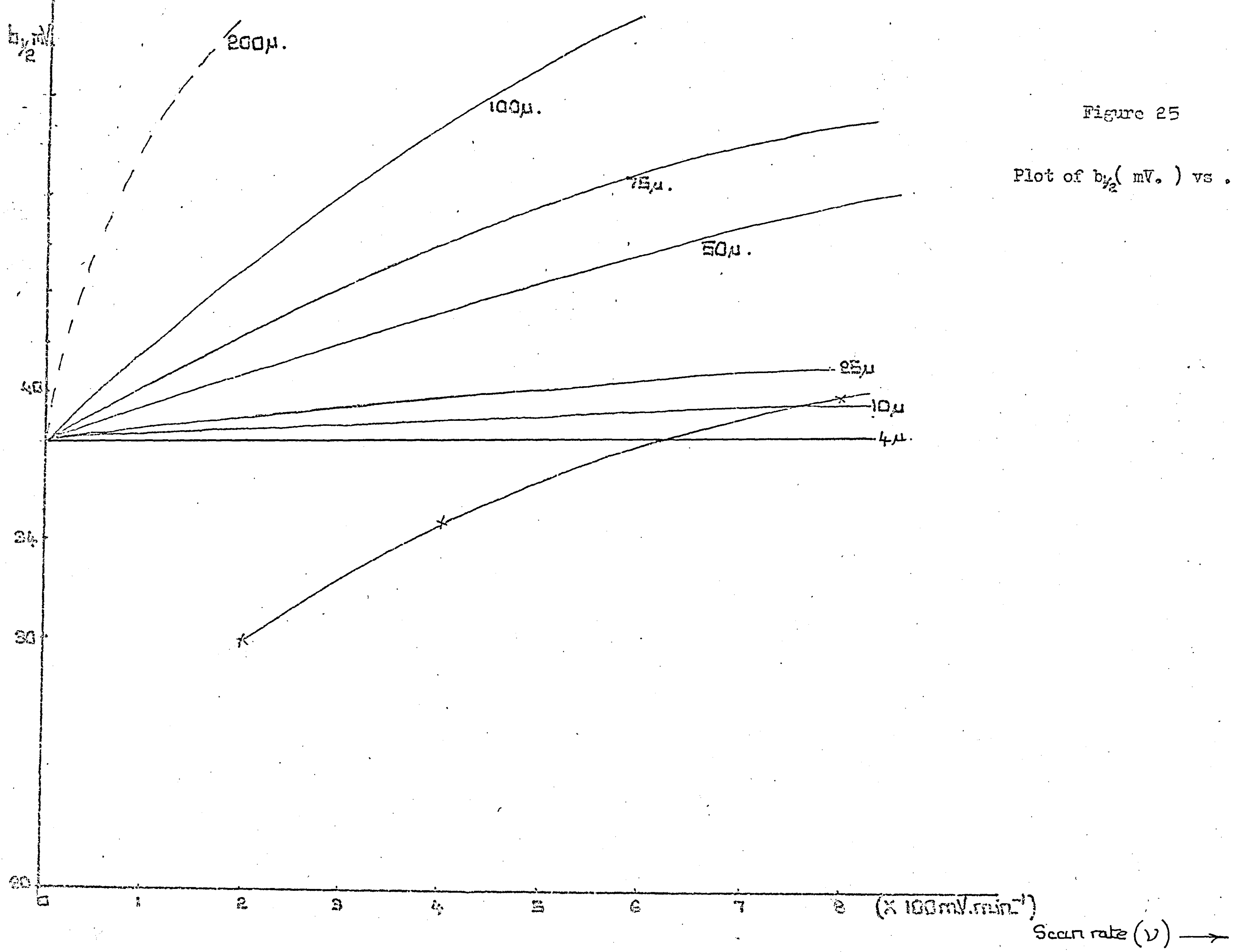

the van Dalen plots at different film thicknesses (i.e. 4 and 10μ).

From our experiments, the conclusion that maximal sensitivity is achieved if very thin films of between 4 and 25μ are used at relatively fast sweep rates is valid provided the number of consecutive analyses is small. Selectivity may be preserved and peak current enhanced by increasing the scan rate when using these thin films. However the advantage would be lost if too many analyses were performed without wiping the mercury film off the electrode. Thick mercury films make the diffusion process of the reduced metal in the film to the surface of the film a comparatively lengthy process such that at fast scan rates it is often incomplete by the time the appropriate potential has been scanned. The resulting peaks are very broad with large $b_{\frac{1}{2}}$ values and selectivity is poor.

5.4. <u>The effect of scan rate on $(E_p - E_{\frac{1}{2}})$ values</u>.

At large values of scan rate (ν) and film thickness (ℓ), the difference between peak potential and half wave potential $(E_p-E_{\frac{1}{2}})$ in volts was found by van Dalen to approach asymptotically a value of 14.3mV.

In the experiment performed above to investigate band width the E_p values were also recorded (Fig.26).

The $(E_p-E_{\frac{1}{2}})$ values were plotted against scan rate together with the corresponding van Dalen plot.

A curved response was obtained which was below the $(E_p-E_{\frac{1}{2}})$ vs. scan rate plot of van Dalen for 4μm films. A value of 95mV was obtained at the slowest scan rate of 200mV min^{-1} and increased on consecutive scans at 400 and 800mV min^{-1} as might be expected with increased film thickness.

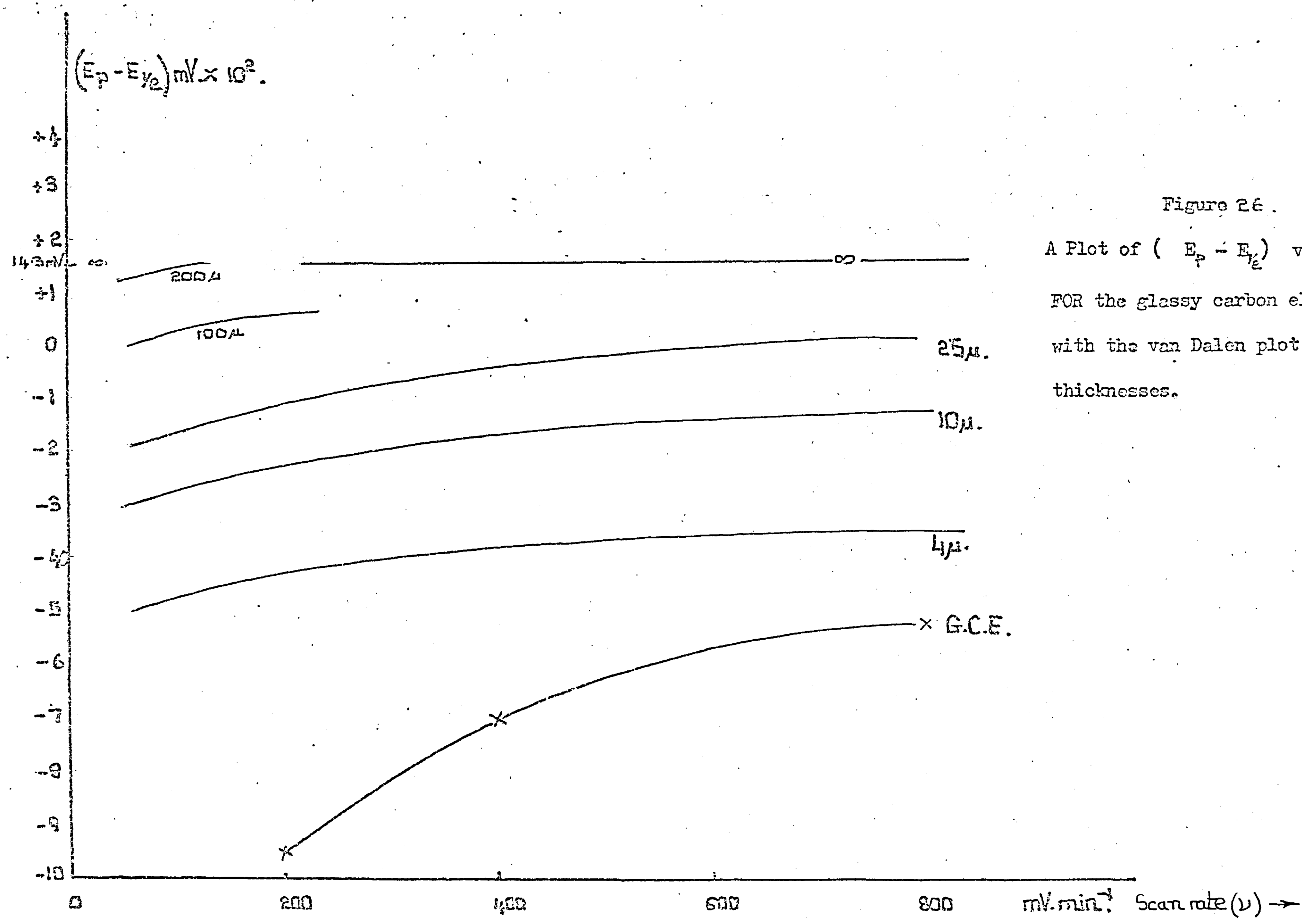

Figure 26.

A Plot of ($E_p - E_{1/2}$) vs. Scan Ra

FOR the glassy carbon electrode to

with the van Dalen plot for differ

thicknesses.

5.5. Deposition Period (t).

The peak current (i_p) has been shown by equation (10) to be proportional to the plating period (t) providing the area of the electrode surface, stirring rate and procedure are maintained constant for a particular solution.

The linearity of the relationship was investigated by plating from a solution of 8 x 10^{-8}mol dm^{-3} Pb for times ranging between 5 and 25 minutes.

The supporting electrolyte was 0.05mol dm^{-3} KNO_3; i_p values were corrected for the time taken to scan from the deposition potential of -1.0V to the peak potential of the lead anodic peak.

The electrode assembly was that shown in (Fig.11) with a wax impregnated graphite electrode with constant rotation.

Initially the electrode was kept in the solution throughout the successive depositions, then the experiment was repeated with a similar Pb solution and the electrode wiped with a tissue after each plating step. Linearity was observed between i_p and plating times of up to 20 minutes duration.

A curve was produced in the first experiment when the electrode was used continuously and without wiping between successive plating steps (Fig.27).

This curve agrees with the peak height (i_p) vs. plating time curves illustrated by Dr. Griffin (40) of 'Environmental Science Associates' in a seminar on ASV in Manchester (1973). It was shown that 96% of the metal ion in solution is reduced in ca. 30 minutes in a particular case and he quoted a time when 50% of the metal is reduced on to the electrode from solution as $t_{\frac{1}{2}}$ minutes.

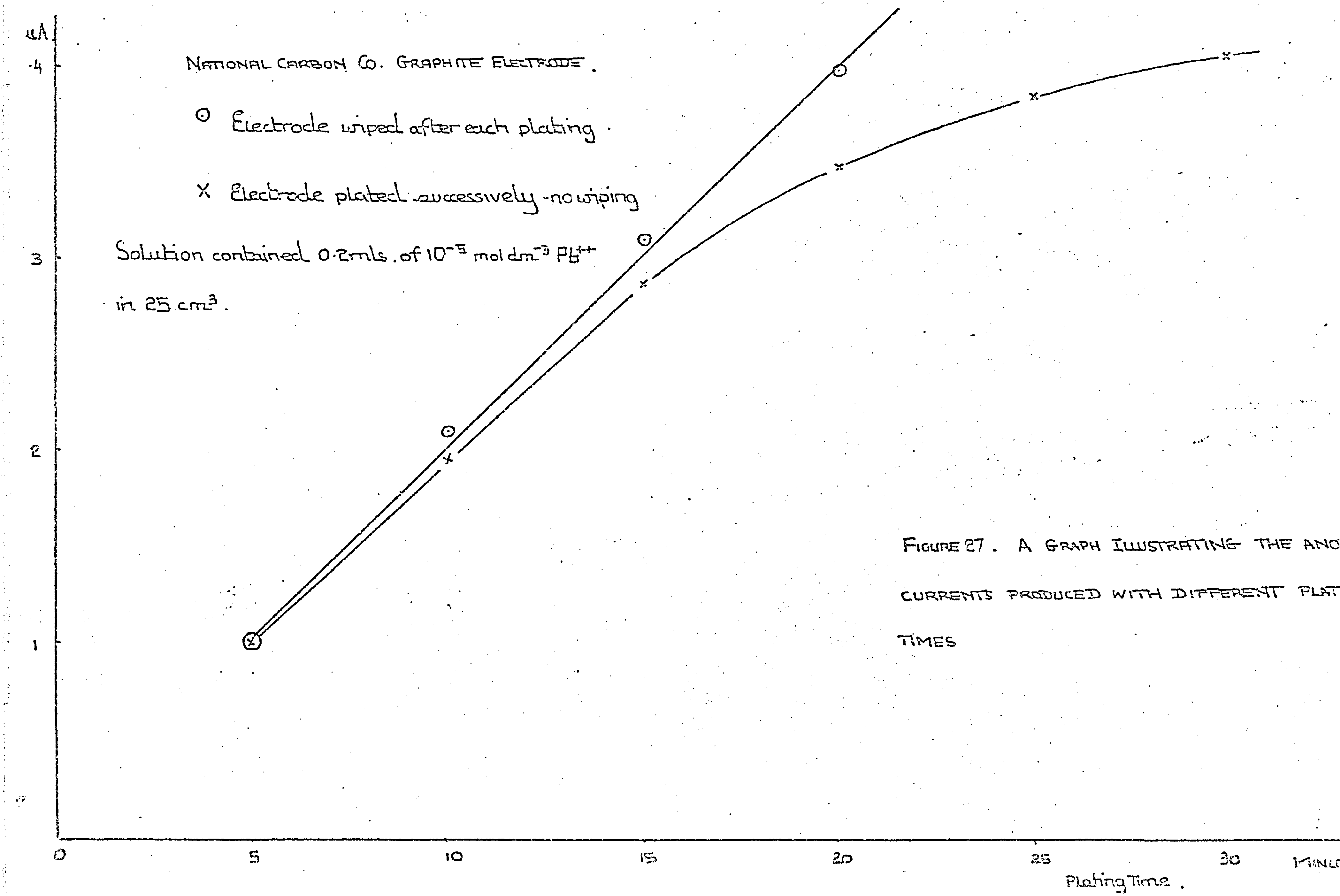

FIGURE 27. A GRAPH ILLUSTRATING THE ANO
CURRENTS PRODUCED WITH DIFFERENT PLAT
TIMES

A further period of $t_{\frac{1}{2}}$ minutes plating duration would only plate out 50% of the metal ion left in solution and continued plating would thus produce a curve with an infinite time for total reduction of the metal ion in solution. It would not be advantageous to plate out the metal ion from solution for periods far in excess of $t_{\frac{1}{2}}$ minutes as the increase in signal would not warrant the extra time taken for the analysis.

The mercury film is growing in thickness and as van Dalen has shown $b_{\frac{1}{2}}$ increases with film thickness; this might account for the curved response with an unwiped electrode where there is a simultaneous deposition of mercury with the trace metal concerned. Diffusion of the trace metal from an ever increasing mercury film thickness would thus be an explanation for peak broadening ($b_{\frac{1}{2}}$) and reduced peak height (i_p).

Dr. Griffins experiments were performed with the Matson CMGE where film thickness is constant, therefore time is a factor. In the simultaneous plating technique by wiping the electrode with a tissue before each plating step the linear relationship between i_p and concentration is obtained in accordance with equation (10). The electrode in each plating step is fresh and is plated for five minutes and scanned manually to condition the film prior to plating the metal.

The advantage of using long electrodeposition times is that sensitivity is improved and this allows analyses of very dilute solutions of trace metals in the 10^{-9} to 10^{-11}mol dm^{-3} concentration range. However the linear response between i_p and concentration may be lost at these levels of concentration which would necessitate the use of special calibration curves and model solutions.

5.6. Ionic strength effect.

The addition of 0.03cm^3 of concentrated HNO_3 (16mol dm^{-3}) was necessary to bring the pH of the distilled water to 2 in the (i_p) calibration of the Cd, Pb and Cu at this lower pH.

The sensitivity of the electrode to the metal under examination increased in each case at the lower pH.

The increase in sensitivity is attributed either to the effect of pH or ionic strength on the system.

To investigate the effect of ionic strength 0.3cm^3 of 1.6mol dm^{-3} KNO_3 was added to the cell and a calibration for Cu performed.

The sensitivity showed no significant increase in 1.6mol dm^{-3} KNO_3, the solution was degassed with CO_2 which produced a stable pH of 3.81.

The results are shown in Table 9.

Table 9

pH	Supporting Electrolyte	Sensitivity µA (5 x 10^{-8}mol dm^{-3} Cu)
3.80	H_2CO_3	0.80
3.81	KNO_3/H_2CO_3	0.82
2.00	HNO_3	0.92

The other explanation for the increased sensitivity in pH 2 solutions is that the size of the mercury droplets plated on the electrode are smaller in diameter and thus provides a higher effective surface area for reduction of metal in solution. Stulikova found that hydrogen evolution at glassy carbon electrodes decreased the size of the mercury droplets and made their distribution more uniform on the electrode surface.

5.7. Standard addition technique.

The standard addition technique allows the concentration of a trace metal ion to be measured without reference to calibration curves.

The sample is first analysed by plating for a given time and obtaining a signal for the metal ion in the sample. A standard is then added and the procedure repeated to obtain a peak from the standard plus the original metal ion concentration. Further additions of standards and subsequent analyses produce a linear response between peak current and concentration. The intercept of this line on the current axis is the original peak current of the sample and may be converted into a concentration by finding the slope of the line which gives the peak current per aliquot of standard.

If the sample contains complexing ligands the standard addition technique will not produce a linear response since the organic complexes or flocculates will tie up a fraction of the added metal by complexation or adsorption processes.

The technique was used to determine Pb in a tap water sample taken from the laboratory. The original peak current was measured and successive $0.5 cm^3$ aliquots of $2.5 \times 10^{-7} mol\ dm^{-3}$ Pb were added and voltammograms recorded after each addition. The results are shown in Table 10.

$$1.35 \mu A - 0.05 \mu A \text{ (Blank)} = 1.30 \mu A$$

$$\text{Pb in tapwater} = \frac{1.30}{3.57} \times 10^{-6} mol\ dm^{-3}\ \text{Pb}$$

$$= \underline{3.64 \times 10^{-7} mol\ dm^{-3}\ \text{Pb}}$$

The concentration of Pb in laboratory tapwater was found to be $3.64 \times 10^{-7} mol\ dm^{-3}$ Pb or 0.08ppm.

FULL SCALE = 5 μA.

DAMPING = 3.

SCAN RATE = 400 mV/MIN.

Figure 28.

Voltammogram of tapwater.

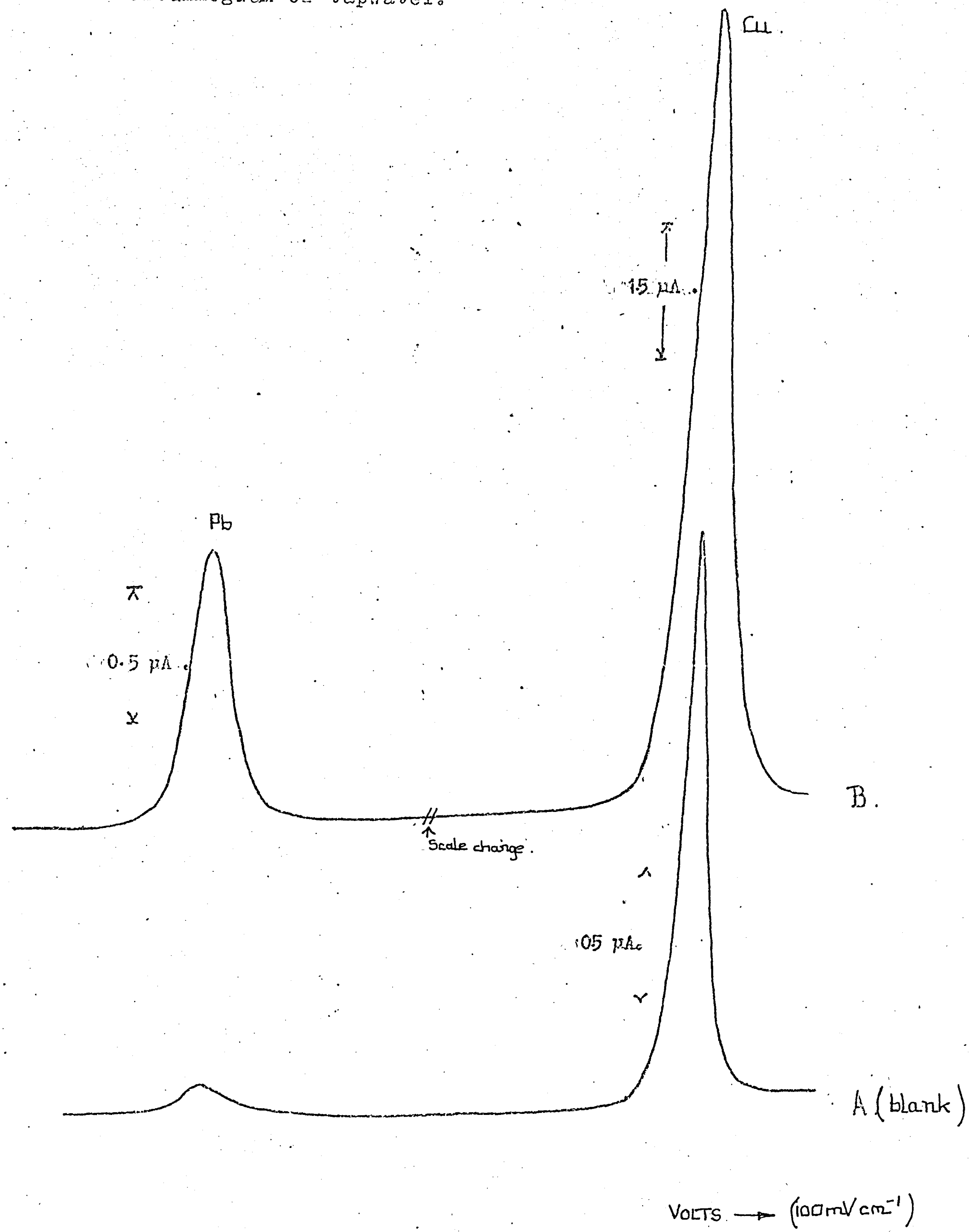

STANDARD ADDITION OF LEAD STANDARDS

$2{\cdot}5 \times 10^{-7}$ mol dm^{-3} Pb in $0{\cdot}5$ cm^{3}.

Aliquots.

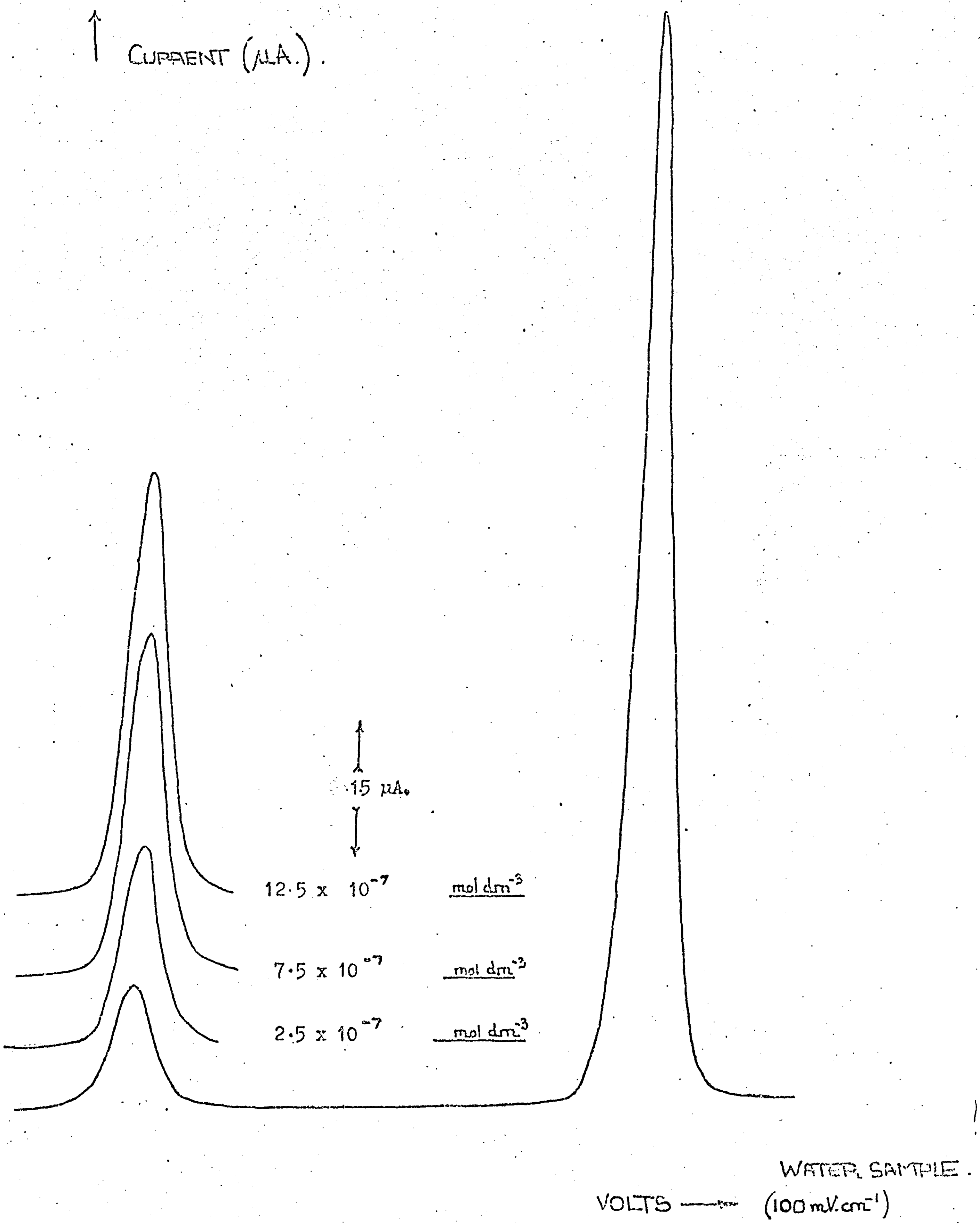

Figure 30

The Standard Addition Technique applied to laboratory tap - water in the analysis of lead by ASV .

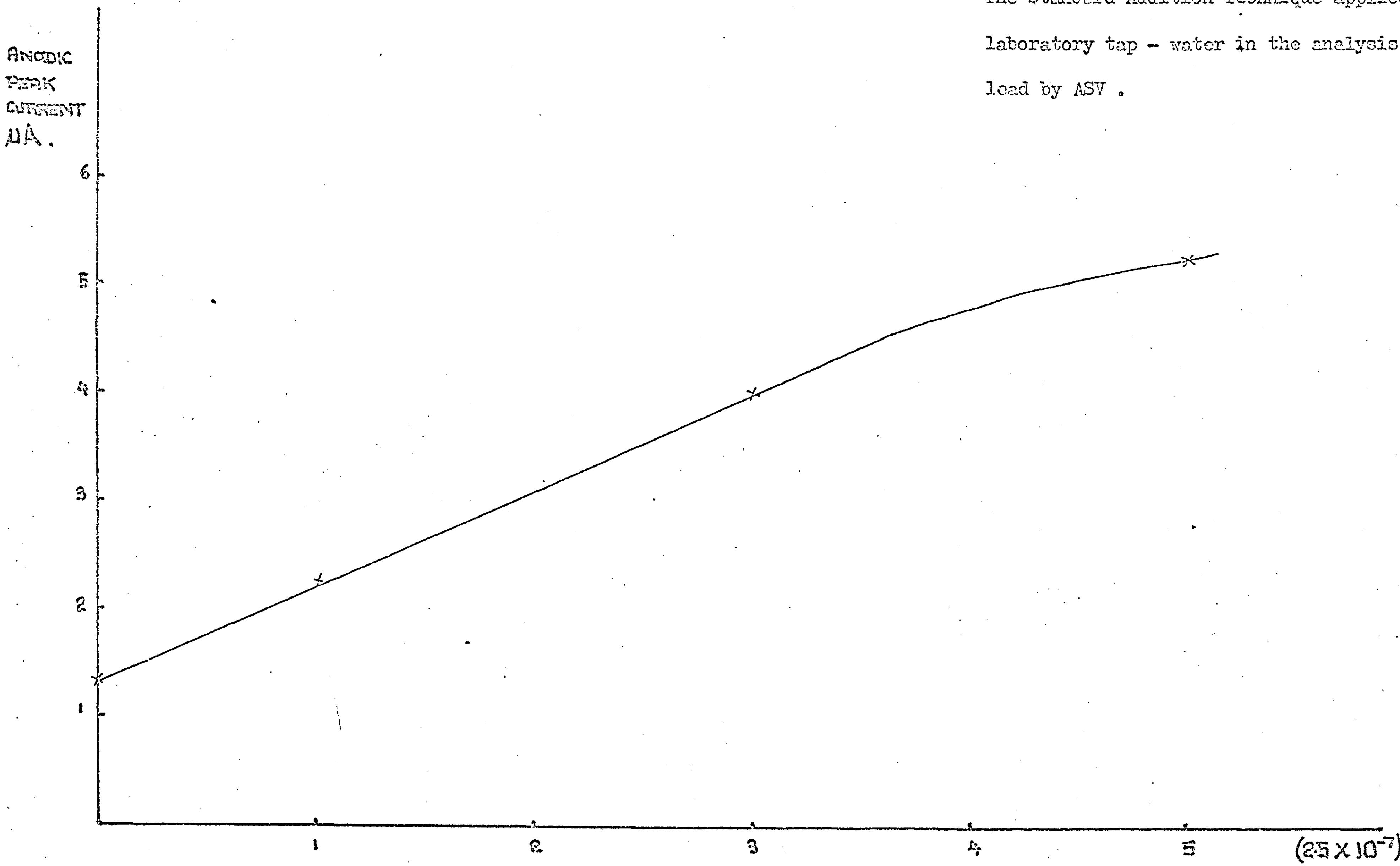

Table 10

ASV analysis of Pb in tapwater

using the standard addition technique.

Sample	Peak Current i_p (μA)	$0.25\mu mol\ dm^{-3}$ Pb	$\mu A/\mu mol\ dm^{-3}$ Pb
Tapwater	1.35		
" $0.25\mu mol\ dm^{-3}$ Pb	2.24	0·890	0·893 = 3·57
" $0.75\mu mol\ dm^{-3}$ Pb	4.03	0·895	
" $1.25\mu mol\ dm^{-3}$ Pb	5.32	0·630	

5.8. <u>Sensitivity comparison between glassy carbon mercury plated insitu and wax impregnated graphite electrodes (CMGE).</u>

The relationship between peak current (i_p) for a particular metal and the concentration of the metal ion in solution was investigated for glassy carbon and CMGE electrodes by keeping the procedure and cell geometry constant, together with the plating time.

A $0.05cm^3$ aliquot of a Pb standard was added to the cell solution and plating performed for five minutes at -1.0V. Four determinations were made on each sample at one particular concentration.

The graphite electrode was plated with mercury for 10 minutes at -0.2V applied potential with respect to the SCE prior to being placed in $20cm^3$ of $0.1mol\ dm^{-3}$ KNO_3. The standards were then added to the KNO_3. The glassy carbon electrode was plated insitu from a $2 \times 10^{-5} mol\ dm^{-3}$ Hg(II) solution and the standards added to the same solution for both electrodes (i.e. KNO_3). The electrodes were both rotated at the same speed in the solution which was buffered to pH 4 with HNO_3

and 0.05mol dm^{-3} NaAc.

The area of the electroactive surface of the electrode exposed to the solution differs. It is therefore necessary first to find the sensitivity of the electrodes to Pb and then to calculate the effective sensitivity per unit area to determine which of the two electrodes is most desirable for ASV. The results of the experiment are shown in Table 11.

Table 11

Comparison of Electrode Sensitivity between the GCE and CMGE.

Electrode	Glassy carbon	Wax impregnated graphite
Area	0.071cm^2	0.282cm^2
Auxiliary electrode	Pt	Pt
Sensitivity to a µmol dm^{-3} Pb solution	3.25µA	5.00µA
Sensitivity per unit area of electrode surface µA cm^{-2}	45.8	17.8
Electrolyte: 0.1mol dm^{-3} KNO_3 at pH 4 degassed with N_2		

The superior sensitivity of the glassy carbon and the insitu mercury plating procedure, were used in further work.

5.9. Calibration of glassy carbon electrode in stream water.

The glassy carbon electrode* was calibrated for Zn, Cd, Pb and Cu in aged stream water, using carbonic acid supporting electrolyte and in a stream water sample acidified to pH 2 with HNO_3.

The fact that mercuric nitrate was present in the solutions together with the ions found in the natural water allowed sufficient conductance so that voltammograms could be obtained

* A= 0.4cm^2

Table 12

Calibration data for Zn.

Medium	Conc. [Zn] mol dm^{-3}	Peak Current (μA)	Corr. Peak Current (μA)	Sensitivity $\mu A(\mu mol\ dm^{-3}\ Zn)^{-1}$	E_p Volts	$b_{\frac{1}{2}}$ (mV)
Natural water	nil.	0.04			-1.03	49
degassed with	1×10^{-8}	0.200	0.16	16.00	-1.03	49
nitrogen	5×10^{-8}	0.790	0.750	14.00	-1.04	48
pH = 5.50	1×10^{-7}	1.560	1.520	15.20	-1.05	42
	5×10^{-7}	6.94	6.900	13.80	-1.06	42
	1×10^{-6}	15.34	15.300	15.30	-1.08	40
				Mean = 14.86		
Natural water/	nil.	0.04			-1.01	48
carbonic acid	1×10^{-8}	0.210	0.170	17.00	-1.01	48
pH = 3.82	5×10^{-8}	0.760	0.720	14.40	-1.02	46
	1×10^{-7}	1.670	1.630	16.30	-1.04	43
	5×10^{-7}	7.74	7.700	15.20	-1.05	42
	1×10^{-6}	15.86	15.820	15.82	-1.06	41
				Mean = 15.74		

Table 13

Calibration data for Cd.

Medium	Conc. [Cd] mol dm^{-3}	Peak Current (μA)	Corr. Peak Current (μA)	Sensitivity μA(μmol dm^{-3} Cd)$^{-1}$	E_p Volts	$b_{\frac{1}{2}}$ (mV)
Natural water	nil.	0.01			-0.58	49
degassed with	1×10^{-8}	0.15	0.14	14.00	-0.58	48
nitrogen	5×10^{-8}	0.65	0.64	12.80	-0.60	44
pH = 5.50	1×10^{-7}	0.142	0.132	13.20	-0.61	42
	5×10^{-7}	6.62	6.61	13.22	-0.62	41
	1×10^{-6}	13.31	13.30	13.30	-0.65	40
				Mean = 13.30		
Natural water/	nil.	0.01			-0.54	48
carbonic acid	1×10^{-8}	0.160	0.150	15.00	-0.54	48
pH = 3.82	5×10^{-8}	0.700	0.690	13.80	-0.55	46
	1×10^{-7}	1.401	1.391	13.91	-0.56	45
	5×10^{-7}	7.11	7.100	14.20	-0.58	44
	1×10^{-6}	13.79	13.78	13.78	-0.60	42
				Mean = 14.14		
Natural water	nil.	0.01			-0.52	48
+ addition of	1×10^{-8}	0.170	0.160	16.00	-0.53	48
HNO_3	5×10^{-8}	0.780	0.770	15.40	-0.53	46
pH = 2.00	1×10^{-7}	1.540	1.530	15.30	-0.54	43
	5×10^{-7}	7.560	7.55	15.10	-0.55	42
	1×10^{-6}	15.01	14.91	14.91	-0.58	40
				Mean = 15.34		

Table 14

Calibration data for Pb.

Medium	Conc. [Pb] mol dm^{-3}	Peak Current (μA)	Corr. Peak Current (μA)	Sensitivity μA(μmol dm^{-3} Pb)$^{-1}$	E_p Volts	$b_{\frac{1}{2}}$ (mV)
Natural water	nil.	0.03			-0.44	48
degassed with	1×10^{-8}	0.20	0.17	17.00	-0.44	48
nitrogen	5×10^{-8}	0.81	0.78	15.60	-0.45	46
pH = 5.50	1×10^{-7}	1.67	1.64	16.40	-0.46	44
	5×10^{-7}	8.13	8.10	16.20	-0.46	42
	1×10^{-6}	16.47	16.40	16.40	-0.47	40
				Mean = 16.32		
Natural water/	nil.	0.04			-0.43	49
carbonic acid	1×10^{-8}	0.22	0.180	18.00	-0.43	48
pH = 3.82	5×10^{-8}	0.86	0.820	16.40	-0.43	46
	1×10^{-7}	1.75	1.71	17.10	-0.44	43
	5×10^{-7}	8.29	8.25	16.50	-0.44	38
	1×10^{-6}	17.24	17.20	17.20	-0.45	33
				Mean = 17.04		
Natural water	nil.	0.06			-0.42	48
+ addition of	1×10^{-8}	0.24	0.18	18.00	-0.42	48
HNO_3	5×10^{-8}	0.99	0.930	18.60	-0.43	44
pH = 2.00	1×10^{-7}	1.91	1.85	18.50	-0.43	40
	5×10^{-7}	9.56	9.50	19.00	-0.45	38
	1×10^{-6}	18.48	18.42	18.42	-0.45	37
				Mean = 18.50		

Table 15

Calibration data for Cu.

Medium	Conc. [Cu] mol dm^{-3}	Peak Current (μA)	Corr. Peak Current (μA)	Sensitivity μA(μmol dm^{-3} Cu)$^{-1}$	E_p Volts	$b_{\frac{1}{2}}$ (mV)
Natural water	nil.	0.05			-0.05	55
degassed with	1×10^{-8}	0.20	0.15	15.00	-0.06	53
nitrogen	5×10^{-8}	0.72	0.67	13.40	-0.06	49
pH = 5.50	1×10^{-7}	1.45	1.40	14.00	-0.07	48
	5×10^{-7}	7.26	7.21	14.40	-0.08	44
	1×10^{-6}	14.25	14.20	14.20	-0.08	40
				Mean = 14.20		
Natural water/	nil.	0.05			-0.04	54
carbonic acid	1×10^{-8}	0.19	0.16	16.00	-0.04	54
pH = 3.82	5×10^{-8}	0.80	0.75	15.00	-0.05	53
	1×10^{-7}	1.45	1.40	14.00	-0.05	50
	5×10^{-7}	7.15	7.10	14.20	-0.06	44
	1×10^{-6}	15.00	14.95	14.95	-0.06	41
				Mean = 14.62		
Natural water	nil.	0.08			-0.03	48
+ addition of	1×10^{-8}	0.25	0.17	17.00	-0.03	48
HNO_3	5×10^{-8}	0.91	0.83	16.60	-0.04	44
pH = 2.00	1×10^{-7}	1.73	1.65	16.50	-0.04	43
	5×10^{-7}	8.00	7.92	15.84	-0.05	42
	1×10^{-6}	16.28	16.20	16.20	-0.05	42
				Mean = 16.42		

after degassing with N_2 and without the addition of further supporting electrolytes. The solution was buffered with citrate to pH 5.50.

CO_2 degassed the solution of oxygen and buffered the solution to a pH of 3.8 ($\pm$ 0.1) within 30 seconds.

The calibration in a pH 2 solution was necessary since in a natural water sample the possible release of trace metal from acid labile complexes is to be examined. In this solution it is not possible to measure Zn.

The calibrations are shown in Table 12-15. Aged stream water rather than distilled water was used since ligands and ionic composition characteristic of a particular water body alter the mol dm^{-3} sensitivities of the trace elements in an ASV analysis. Four measurements were made on each metal ion concentration and the mean of the readings tabulated. Periodic checking of the original calibration curves was performed by standard addition techniques on various random samples from the trout stream. A deposition potential of -1.3V vs. SCE was used to plate the metals from the natural water.

5.10. <u>Limit of detection</u>

The limit of detection was estimated by measuring the peak currents for Zn, Cd, Pb and Cu in seven aliquots of aged stream water which showed very low peak currents for the trace metals under investigation. A 5 minute deposition period was used and a scan rate of 800 mV min^{-1} with an electrode rotation speed of 2550 r.p.m. Longer plating times would be possible to increase the limit of detection but would become impractical and too time consuming in routine analysis.

The blanks were measured on an 0.5µA full scale setting on the chart recorder. The solution was made 2 x 10^{-5}mol dm^{-3} with mercuric nitrate and buffered with citrate to pH 5.6 before degassing with nitrogen. The sample was then analysed in carbonic acid at a pH of 3.8 and finally at pH 2 after the addition of HNO_3. The limit of detection was expressed as the mean blank reading + (3 x the standard deviation of the blank). The results are shown in Table 16.

Table 16

Limits of detection

Metal	Solution degassed with N_2 pH 5.6		Carbonic acid solution pH 3.8		HNO_3 pH 2	
	Mean i_p (μA)	Limit of detection mol dm^{-3}	Mean i_p (μA)	Limit of detection mol dm^{-3}	Mean i_p (μA)	Limit of detection mol dm^{-3}
Zn	0.004±50%	6.7×10^{-10}	0.010±20%	1×10^{-9}	——	——
Cd	0.005±40%	8.2×10^{-10}	0.012±33%	1.7×10^{-9}	0.015±26%	1.76×10^{-9}
Pb	0.005±40%	8.5×10^{-10}	0.018±28%	1.9×10^{-9}	0.02 ±30%	2.1×10^{-9}
Cu	0.006±33%	8.4×10^{-10}	0.02'±30%	2.6×10^{-9}	0.03 ±33%	3.65×10^{-9}

Florence (11) recorded 10^{-9} mol dm^{-3} as the limit of detection for lead. Matson (17) and Hume (18) recorded similar limits of detection in the 10^{-10}mol dm^{-3} concentration range for the four elements concerned. Deposition periods in excess of 15 minutes were often used to determine the limits of detection.

The residual current which increases the slope of the base line of the i-E trace increases in carbonic acid and HNO_3 with the result that the limit of detection falls from 10^{-10} to the 10^{-9}mol dm^{-3} concentration range in these media.

5.11. Precision of measurement in aged stream water.

This was estimated by analysing five separate aliquots of

5×10^{-8} mol dm^{-3}, 1×10^{-7} mol dm^{-3} and 10^{-6} mol dm^{-3} solution of Zn, Cd, Pb and Cu in aged stream water using carbonic acid as the supporting electrolyte. The peak currents with their relative standard deviations are recorded in Table 17.

Table 17

	5×10^{-8} mol dm^{-3}	10^{-7} mol dm^{-3}	10^{-6} mol dm^{-3}
Zn	0.770µA ± 5.5%	1.69µA ± 3.4%	15.80µA ± 1.9%
Cd	0.700µA ± 8.5%	1.41µA ± 4.8%	13.34µA ± 2.1%
Pb	0.85 µA ± 4.8%	1.77µA ± 3.0%	17.10µA ± 1.7%
Cu	0.82 µA ± 7.9%	1.46µA ± 3.7%	14.70µA ± 2.4%

A similar range of precision was encounted after degassing the sample with nitrogen and after the addition of HNO_3 in the final stage of the analysis. Precision deteriorates with a lowering of concentration of the trace metal concerned. Cadmium is particularly sensitive to oxygen in solution and is the worst affected. Copper contamination in the cell itself may account for the comparatively high standard deviation of 7.9% encountered for this element at the 5×10^{-8} mol dm^{-3} level.

5.12. <u>The disappearance of Zn anodic peak signal under nitrogen.</u>

The degassing of a natural water sample under nitrogen caused an increase in pH with degassing time as shown in Figure 31.

Above a pH of 7.60 the natural water sample showed a rapid decrease in the Zn anodic peak with successive analyses.

At a pH of 8.01 the Zn anodic peak was only slightly reduced. Between pH 8.01 and 8.4 a 50% reduction occurred. A similar drop occurred at pH 8.50 and above that pH the signal remained constant at 0.06µA.

Degassing with CO_2 caused a drop in pH to 3.75 and restored

Figure 31 The disappearance of Zn^{++} anodic peak signals in a natural water sample

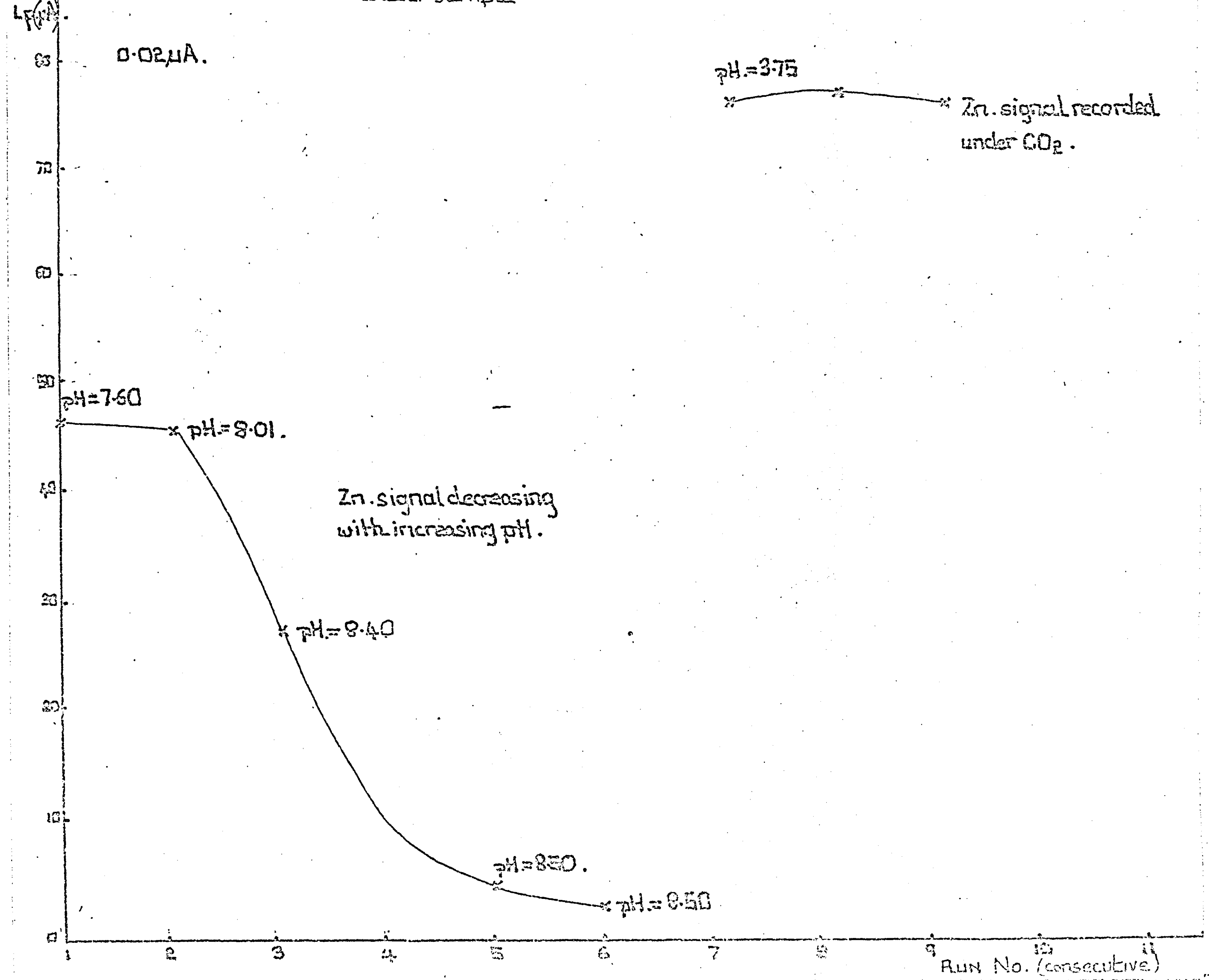

the Zn anodic peak to a value of 1.60μA, this was higher than the original signal. The Zn peak remains constant at pH of 3.75 in consecutive runs.

Zirino and Healey (21) proposed the existence of a neutral species of $Zn(OH)_2$ or $Zn(CO_3)$ at high pH values in seawater. In Figure 31 the Zn anodic peak decrease from pH 8.01 to pH 8.50 may be the result of the formation of a neutral species in the freshwater sample. The concentration of Zn^{++} in solution will thus be reduced with increase of pH in consecutive analyses as more of the neutral species is formed. The above workers have also shown that Zn may be adsorbed on to particulate matter which could be present or form in high pH solutions as a result of precipitation.

The increased Zn anodic peaks in carbonic acid illustrates the importance of pH in controlling Zn concentrations in solution. The drop in pH to 3.75 alters the speciation of Zn such that the free ion is once again the dominant species plus any contribution from adsorbed or complexed metal which is pH labile at pH 3.75.

Zn is the most sensitive of the metals in high pH solutions with regard to loss of anodic peak current; Pb and Cu anodic peaks measured from the same sample were unaffected. Cd was not recorded in this sample

5.13. Double peak phenomena associated with the Cu anodic peak.

5.13.1. Introduction. Double peak phenomena for lead in natural water have been attributed to the presence of free metal and a metal complex with some organic chelator by Matson.

Clem (42/43) has attributed copper doublets to the following reaction.

$$Cu/Hg \longrightarrow Cu^{+} + e$$
$$2Cu^{+} \longrightarrow Cu^{o} + Cu^{2+}$$

Copper is stripped as the univalent species followed by disproportionation. The Cu^{2+} is then re-reduced at the electrode.

Zirino and Healy observed a small Zn peak 100mV less negative than the main Zn peak in seawater at high pH's and suggested that it was caused by the adsorption of $ZnCO_3$ or $Zn(OH)_2$ or a mixed zinc hydroxy carbonate on the electrode as the zinc/mercury amalgam is oxidised.

Hume and Carter (18) have shown that doublet peaks for lead can be caused by stripping of the metal from different sites on the electrode surface. The CMGE when plated at potentials more positive than -0.2V vs. Ag/AgCl reference electrode gave one large and one much smaller peak while those plated at more negative potentials up to -1.0V always gave single peaks. The electrode film is made up of mercury droplets on bare carbon; the higher plating potential ensures that all the sites are plated simultaneously whilst the lower plating potentials allow plating of mercury on the most active sites only thus creating the two sites for deposition and stripping of lead which result in a doublet being formed on an anodic scan.

In this work a plating potential of -1.0V vs. SCE was used to plate the electrode since this ensures that all the sites on the electrode surface are covered with mercury.

Copper was the only trace metal to be associated with double peak phenomena in the analysis of stream water. Double peaks were observed after degassing with nitrogen and these changed shape but persisted in carbonic acid. A singlet peak was observed at pH 2.

5.13.2. Character of the Cu-doublet.

Variation with Plating Time. In the carbonic acid supporting electrolyte a natural water sample of initial pH 5.3 produced a copper doublet which when plated for twice the initial plating time (Fig.32) produced a corresponding increase in the less anodic peak at -0.07V whilst the more anodic peak remained unchanged.

Figure 32.

The effect of increasing the duration of plating time on the copper doublet.

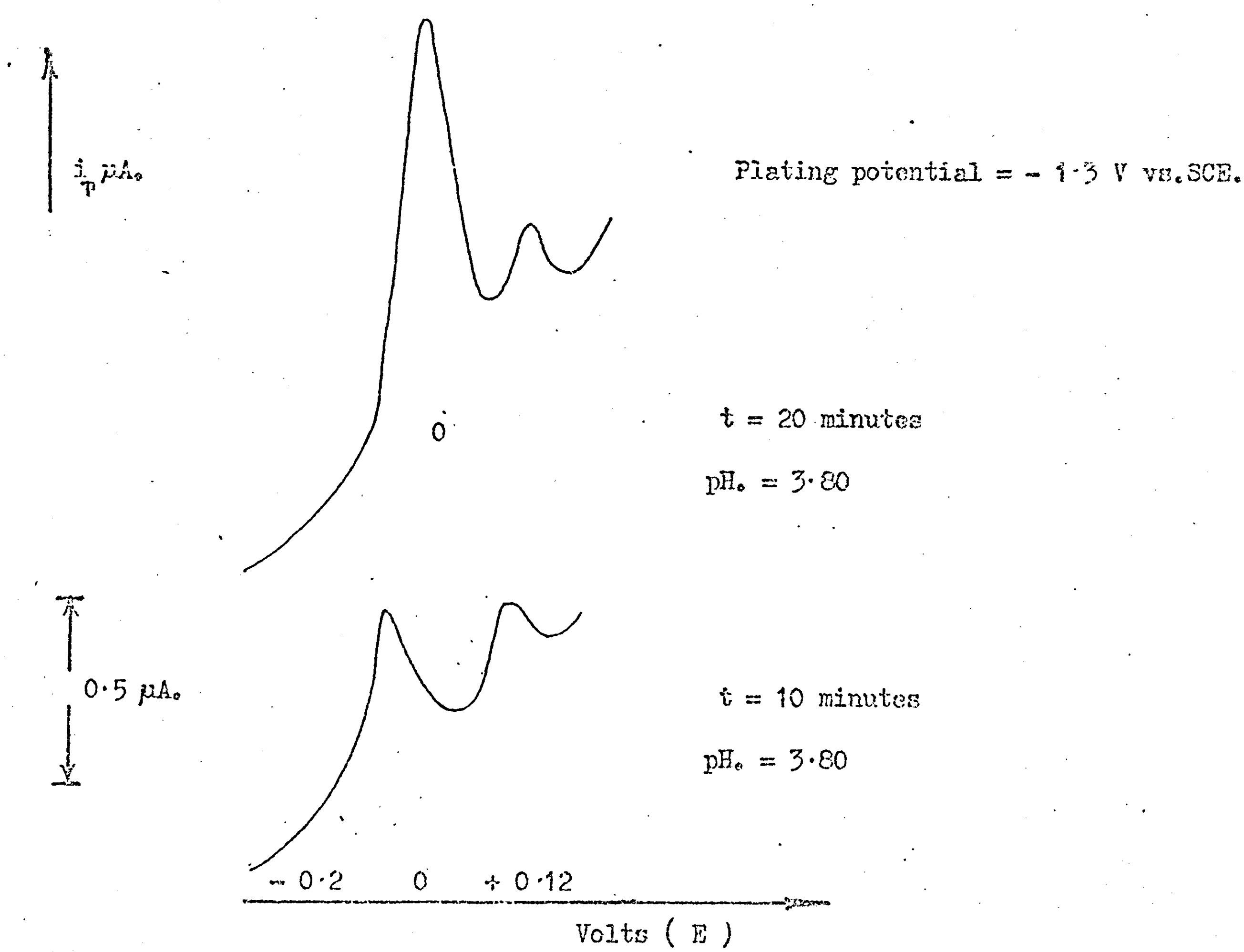

The less anodic peak appears to represent the oxidation of copper from the electrode surface while the more anodic peak could be an adsorbed species associated with organic surface active material in the natural water. Further plating fails to reduce more of the species responsible for the second peak on to the electrode which suggests that it reaches a saturation value.

The electrode may be subjected to some sort of interference or poisoned by organic compounds in the natural water sample. An intermetallic compound could have formed on the electrode surface where copper metal and the intermetallic compound at its optimum concentration oxidise at different potentials.

Carter and Hume have shown that in the case of doublet peaks being the result of stripping metal from different sites on the electrode, the less anodic peak in Figure 32 represents metal being stripped from the bare carbon surface while the second peak is produced from metal being stripped from adjacent mercury droplets. In an anodic scan the oxidation of metal occurs first from the bare carbon sites and is replated into the mercury droplets before the scan reaches the potential at which the metal is once again oxidised from the mercury to produce the second more anodic peak. This explanation however fails to account for the fact that the more anodic peak of the doublet does not increase with longer plating times. Faster scan rates than 400mV min^{-1} in successive analyses simply resulted in loss of resolution between the peaks as a result of slow recorder response after the main oxidation peak; investigation using this variable did not provide further information on the copper doublet.

5.13.3. <u>Cu doublet measured under N_2, CO_2.</u> The voltammogram of a natural water sample taken at a pH of 4.5 and analysed under nitrogen produced a doublet peak for copper in which the anodic peak of the doublet was larger than the more negative peak Fig. 33(1). When the pH of the sample was lowered to 3.8 by bubbling CO_2 through the sample the doublet remained but was not so resolvable since the Ep's were closer to each other. The more negative peak was at -0.03V, whilst the anodic peak was at + 0.12V under nitrogen and in carbonic acid they were at -0.02 and + 0.11V respectively.

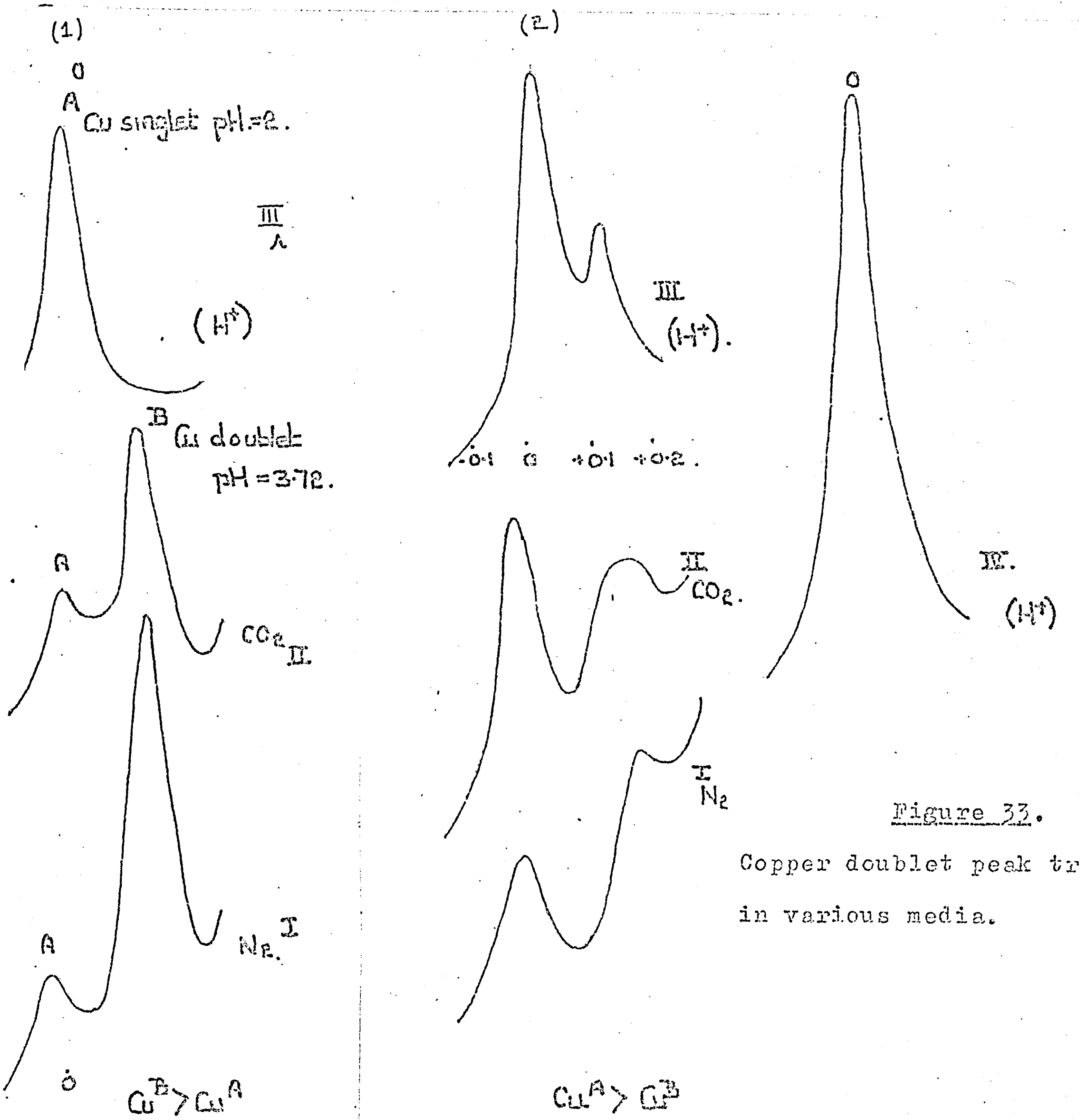

<u>Figure 33.</u>

Copper doublet peak traces in various media.

When the sample was acidified to pH 2 with HNO_3 the doublet disappeared and a singlet peak was produced at -0.015V Fig. 33(1)(III).

The more negative peak moved in an anodic direction as the pH was lowered whilst the more anodic peak behaved in a reverse manner and moved cathodically on lowering the pH.

In a natural water sample where the more -ve peak and anodic peak were nearly equivalent under nitrogen, Fig. 33(2), the anodic peak at + 0.18V moved to + 0.15V under CO_2 whilst the cathodic peak moved from -0.015 to -0.02V and increased in height (i_p).

5.13.4. <u>Cu doublet disappearance on acidification.</u> The copper doublet in the samples did not completely disappear after acidification with HNO_3 Fig. 33(2) (III & IV). If anodic stripping runs were performed immediately after adding acid the doublet was still seen on the first scan.

On the second scan the anodic peak was observed at + 0.11V situated on a slope of a more negative peak at 0.00V. A further scan resulted in a singlet peak being formed at 0.00V, this then remained constant in height and peak potential on further scans.

5.13.5. <u>Addition of copper standards to the Cu doublet.</u> Background observations in odd samples led to a controlled experiment. The addition of a copper standard to a distilled water sample which produced a copper doublet in carbonic acid on a previous voltammogram resulted in the merging of the two peaks by interfering with the more cathodic peak, a blunt more humped peak was formed, the more anodic peak remained well formed Fig. 34. The configuration of the Cu doublet remained

5.13.5. The addition of a Cu standard to a natural water sample at pH. 3.8 in H_2CO_3 which originally gave a singlet peak at - 0 . 18 V resulted in a more negative peak of approximately 0 . 19 µA . The two peaks were quite distinct as illustrated in(Fig. 35 p.98) and resembled the Cu doublet peak seen in other natural water samples . At higher concentrations the distinct nature of the peaks is lost . The Cu metal peak dominates the more anodic peak at higher concentrations . The small more anodic peak does not increase in height with increased plating times and resembles the second peak shown in Figure 32 .

constant; throughout 3 further consecutive scans the peaks failed to resolve themselves.

I. Fraser (43) (of Env. Sci. Associates) recommended using lower plating potentials for elements which produced overlapping and adjacent peaks.

By plating at a potential of -0.5V vs. SCE the two copper peaks did resolve themselves. However, they were reduced in size (Fig. 34).

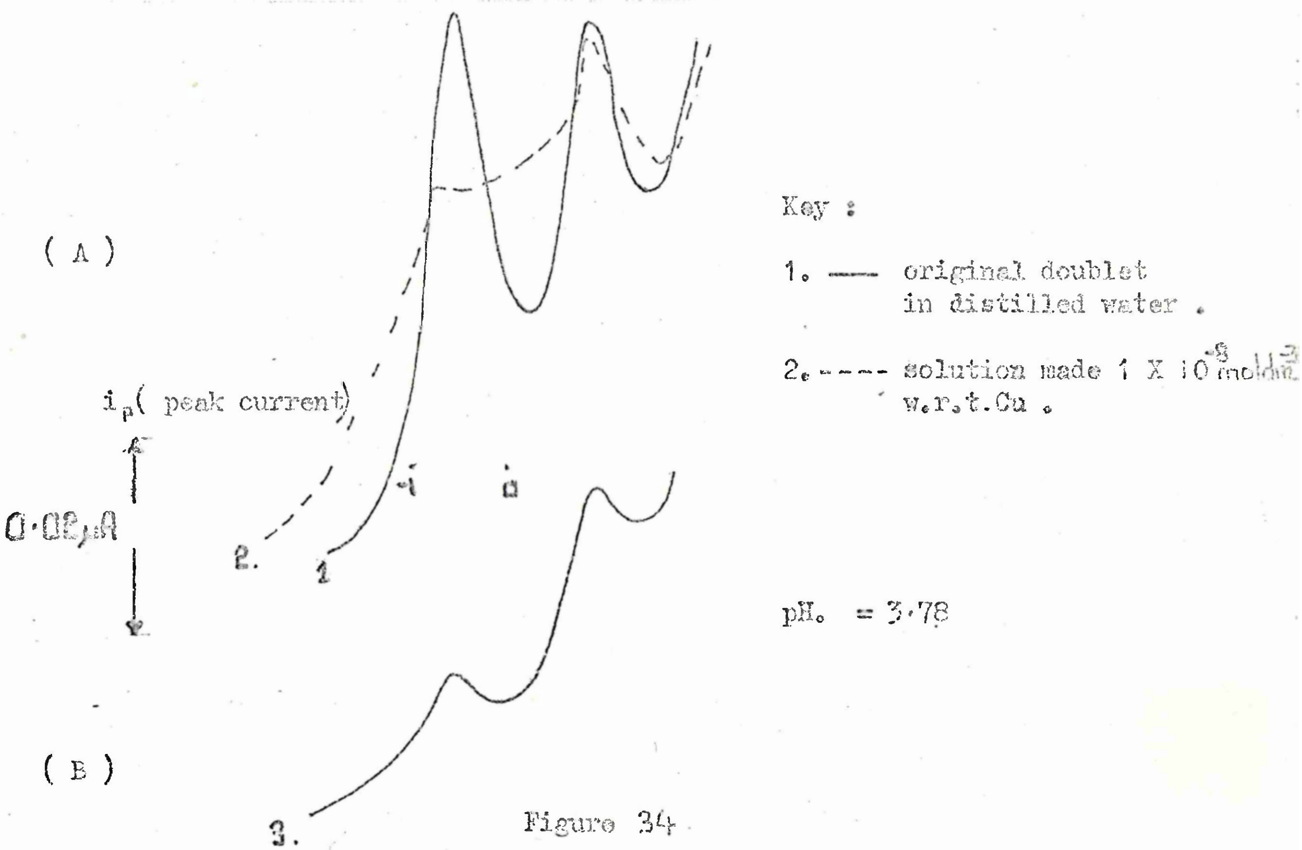

Figure 34

In trace (B) the Cu peaks were resolved by lowering the deposition potential to - 0·5 V vs. SCE .

5.13.6. <u>Conclusion.</u> All the experimental evidence points to the double peak effect being characteristic of the individual electrode because doublet phenomena are apparent in blank solutions but only at high resolution (slow scan rates and high sensitivity settings combined with long plating times).

The addition of a copper standard to investigate doublet phenomena.

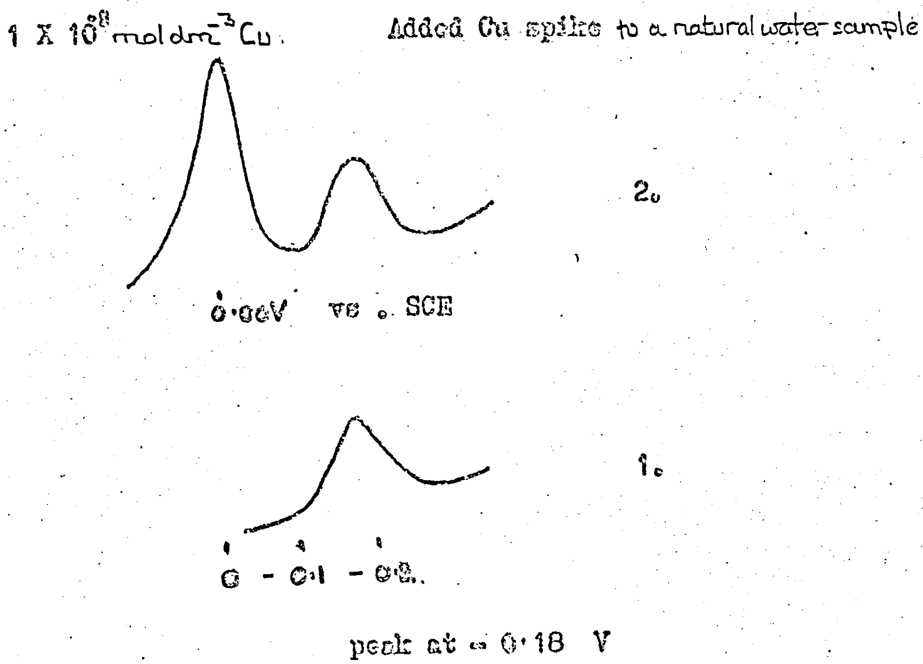

The role of the composite nature of the mercury film being one of mercury droplets and bare carbon sites has already been implicated by Hume et al to be involved in doublet peak formation, but only for those electrodes plated at positive potentials to -0.2V vs. Ag/AgCl. The electrode used in this work was plated at -1.0V vs. SCE and must by Hume's definition have all its carbon sites plated with mercury. It is necessary therefore to modify Hume's theory with respect to the GCE.

The droplet nature of the MFE must inevitably mean that there are bare sites between the droplets; even in low pH solutions where hydrogen evolution and mercury plating are occurring together to produce the advantageous plating conditions referred to by Stulikova where very fine mercury droplets plate evenly on the carbon surface. The ratio of bare sites to plated sites would be small and stripping from the bare sites comparatively unimportant. Singlet peaks are observed in pH 2 solutions; the stripping of the metal is predominantly from the mercury droplets. In Fig. 33(2) (III & IV) it can be seen that the production of a singlet peak is not instantaneous but occurs within two consecutive runs in pH 2 solutions. The electrode structure will itself be changing with hydrogen evolution in the plating periods prior to recording these voltammograms as outlined above; the ratio of bare:mercury plated sites will be reduced with the result that the more cathodic peak becomes dominant and finally a singlet.

The soluble organic material within the water sample could modify the GCE characteristics and prevent mercury deposition on bare active sites adjacent to those already plated with mercury by becoming adsorbed onto the electrode. The result would be that the ratio of bare to mercury plated sites would increase and that mercury would deposit on mercury and increase the droplet size rather than population. The bare sites would now become important in deposition and stripping of copper leading to doublet formation and the production of intermetallic compounds to further distort the more anodic peak of the doublet. The modification of the electrode structure by the sample and plating conditions could provide an explanation for the 'memory' effect observed by Hume et al when he transferred his CMGE from a humic acid solution to a clean solution where it continued to behave as though it were in the humic acid solution with respect to shifts in position, height and shape of the Pb and Cu peaks he was studying.

5.14. The role of chloride ion in producing abnormal electrode behaviour.

The use of potassium chloride as a supporting electrolyte for ASV was discontinued early in this work because it was difficult to produce reliable MFE's in it and very often the mercury film was completely inactive. The film had a scum like appearance of a mercurous chloride precipitate. To investigate the problem further a GCE was plated from 2×10^{-5}mol dm^{-3} mercuric nitrate in 0.1 mol dm^{-3} KCl at a pH of 4.5 for five minutes at -1.0V vs. SCE.

The electrode was examined after plating and was observed to have the frosty appearance of an active mercury film. The potential was scanned manually to + 0.45V vs. SCE to condition the electrode as recommended by Florence (11) however, on examining the electrode surface with a hand lens after the scan; the droplet nature of the surface was seen to have changed to a grey precipitate. The electrode had been damaged in the conditioning scan. On using the electrode to plate 10^{-6}mol dm^{-3} Cu and Pb, the resulting anodic scan showed abnormal electrode behavior with both metal anodic peaks being distorted and present on an irregular base line. The same procedure when performed in 0.1mol dm^{-3} KNO_3 produced normal electrode behavior.

Chlorine evolution can occur at the GCE at positive potentials in the anodic scan with the result that a scum like precipitate of mercurous chloride is formed which inactivates the mercury film. Chlorine will also attack the glassy carbon surface, the polish is lost and the surface etched if the electrode is left inadvertently at + 0.45V for any length of time.

The irregular surface may trap gases and solution which will continue to cause electrode malfunction if replating of a fresh mercury film is attempted.

To avoid damaging the mercury film the anodic scan should be stopped before reaching positive potentials where chlorine evolution can occur. The electrode behaved normally when this procedure was adopted and both peaks for Cu and Pb were normal in subsequent scans following the normal plating procedure. The technique of wiping the mercury film off the electrode with a damp tissue rather than oxidising the mercury is preferable since this avoids chlorine attack on the electrode substrate.

Clem (42) has pointed out that workers using ASV for trace metal analysis in chloride supporting electrolytes and seawater could have unknowingly minimised the danger of chlorine attack by their procedure or technique. The scan may be stopped before chlorine evolution occurs or the mercury film may be renewed after each analysis. When an electrode does fail, poor wax impregnation or the suitability of the substrate material is called into question rather than the problem of chlorine evolution in chloride electrolytes. The problem is seldom mentioned in the literature and yet knowledge of it is vital in maintaining reliable ASV electrodes.

5.15. <u>ASV analysis following centrifugation of an aged water sample</u>.

The settling out of particulate matter in the sample bottles was a slow process and was most noticeable after a period of 8 days in samples of high pH.

Aged samples in polyethlene sampling bottles were shaken

<u>Figure 36.</u>

Peak current plots for Pb and Cu in centrifuged samples plotted against time.

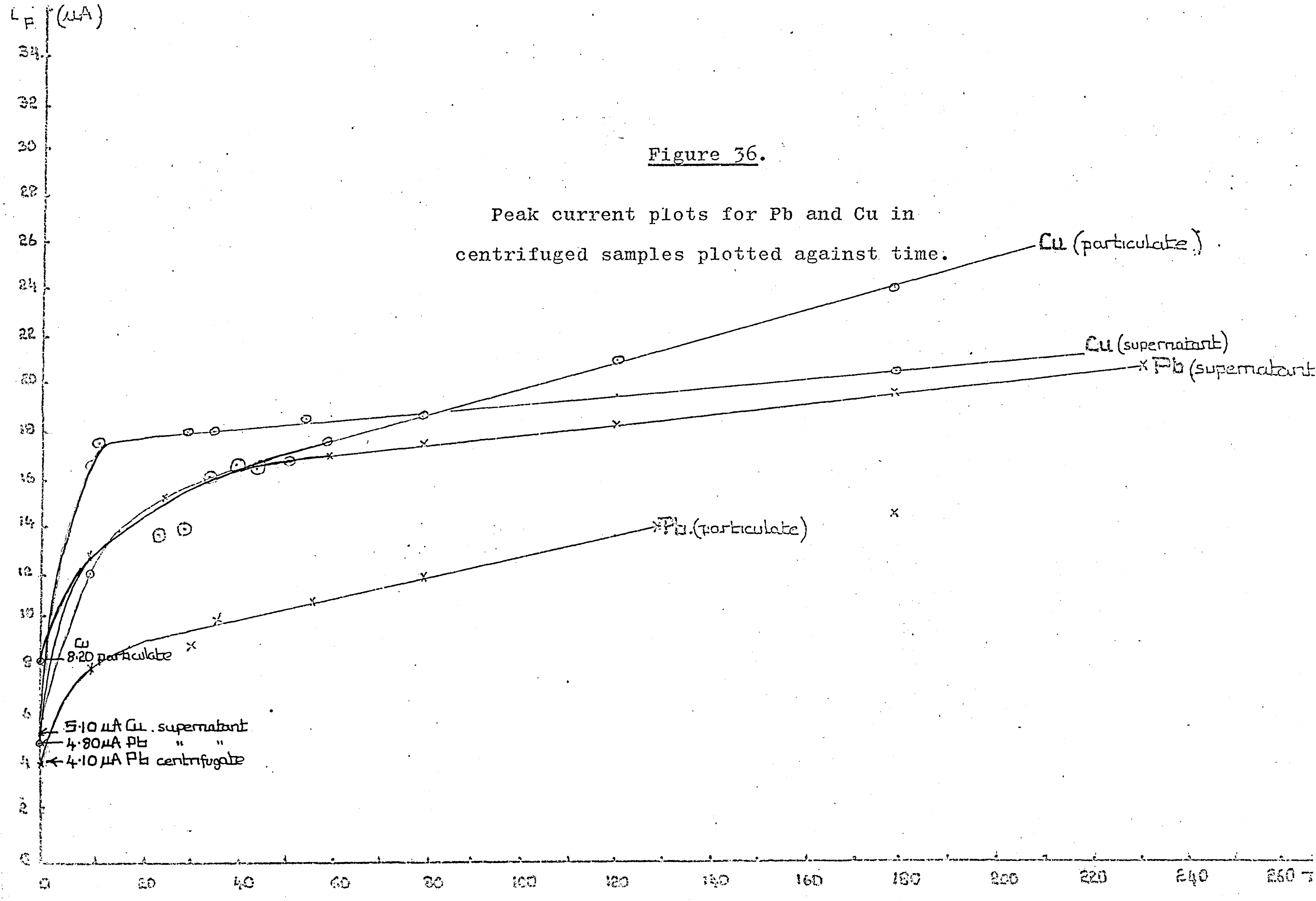

and then poured into 200cm^3 centrifuge tubes and centrifuged at 1,500 rpm for ten minutes. The top 100cm^3 or supernatant was decanted from the portion containing the centrifugate. 20cm^3 samples from supernatant and centrifugate were analysed separately by ASV using CO_2 as the purge gas. The samples were then acidified to pH 2 by adding 0.03cm^3 of concentrated HNO_3 and any release of trace metal observed with time by performing successive ASV analyses on the same sample.

The graph in Figure 36 illustrates the release of metal with time after acidification to pH 2. The start of each curve represents the peak current recorded in carbonic acid prior to acidification to pH 2. (For Pb 4.10μA in the centrifugate and 4.80μA in the supernatant and for Cu 5.10μA in the supernatant and 8.20μA in the particulate fraction.) Cu appears to be complexed or associated with the particulate matter and is released in two phases after acidification, an initial release which is complete after 35 minutes followed by a steady release over the following three hour period. The supernatant shows an initial release which approaches completion after 10 minutes.

Pb is found in higher concentration in solution than associated with particulate matter. Acid release of Pb in solution is near completion after 40 minutes. Like Cu, the Pb associated with particulate matter continues to be released over the following three hour period.

The occurrence of settling out was rare in the samples since the analyses were completed within two days of sample collection. The importance of allowing the sample to equilibriate after the addition of acid is important if one is to get an accurate measure of total acid labile metal concentration.

In practice 20 minutes was allowed for this purpose prior to the initial analysis after acidification.

5.16. Comparison of ASV with Atomic Fluorescence Spectroscopy (AFS).

Natural water samples were first subjected to ASV analysis prior to AFS methods. The samples were analysed by simply deaerating the sample with nitrogen and adding no supporting electrolyte other than mercuric nitrate. A further analysis was performed on the same sample by purging with CO_2 which brought the pH to 3.8 ± 0.15. An addition of 0.03cm^3 concentrated HNO_3 lowered the pH of the sample to 2 and thus allowed a further measurement using ASV to determine any acid labile metal; this final measurement was then compared with the results of the analysis performed by using AFS since in the latter technique the total metal content of the sample is being determined.

The metals analysed by AFS were Zn and Pb. Zn cannot be measured at pH 2 by ASV since its anodic peak is more cathodic than the potential of hydrogen evolution at the mercury film electrode. The total metal as measured by AFS is compared with the results under nitrogen and CO_2 in the ASV analysis of Zn.

The samples were taken from stations on the small tributary supplying the Trout hatchery at Ladybower reservoir. The sample points are those designated and numbered later in the chapter (Fig.37).

The pH of the samples was measured before analysis and prior to each stage of the analysis. When degassing with nitrogen it is necessary to measure the pH after analysis to ensure that no significant increase in pH has occurred (pH 5.6±0.2).

The samples were measured unfiltered to eliminate any manipulative operation and risk of contamination. Turbid samples were rejected.

Although no filtering process was performed on the samples every effort was made in their collection to limit the incorporation of plant or animal particulate matter since it is recognised that their incorporation can hasten metal removal through adsorption as emphasised by Hume.

The results of the ASV and AFS measurements are shown in Tables 18 and 19.

Table 18

Analysis of Zn by AFS and ASV on stream water.

Station	Zn_{AFS} x 10^{-7} mol dm^{-3}	$Zn_{ASV(N_2)}$ x 10^{-7} mol dm^{-3}	$Zn_{ASV(CO_2)}$ x 10^{-7} mol dm^{-3}
pH 5.5 I	2.54	0.95	1.04
pH 5.40 II	1.777	0.81	0.90
pH 4.55 III	5.34	2.35	2.23
pH 4.59 IV	4.66	2.21	2.04

Station	$\frac{Zn_{ASV(N_2)} \times 100}{Zn_{AFS}}$ %	$\frac{Zn_{ASV(CO_2)} \times 100}{Zn_{AFS}}$ %
I	37.4%	41.0%
II	45.8%	50.8%
III	44.0%	41.8%
IV	47.4%	43.8%

peak current (i_p) mean of 4 readings corrected for blanks. AFS units corrected for blank in bottles. Standard corrected for doubly distilled water blank.

Table 19

Comparison of Pb measurement by AFS and ASV.

Station	$Pb_{AFS} \times 10^{-7} mol\ dm^{-3}$	$Pb_{ASV_H} \times 10^{-7} mol\ dm^{-3}$	$\frac{Pb_{ASV_H}}{Pb_{AFS}} \times 100$
pH 5.50 I	0.99	0.63	63.6%
pH 5.40 II	1.58	1.10	69.6%
pH 4.55 III	2.57	2.26	87.9%
pH 4.59 IV	7.12	2.83	39.8%

The Pb concentration as measured by ASV after acidification represents between 39 and 88% of the concentration measured by AFS. The slow release of Pb as illustrated in the 'centrifugation' experiment may account for the discrepancy between the two analytical techniques, since after acidification Pb continues to be released from particulate matter over a three hour period. In the above analysis the sample was allowed to equilibrate for 20 minutes only.

The low concentration of Pb as determined at station IV by ASV compared with the AFS analysis indicates that much of the Pb in solution was either adsorbed onto particulate matter or not acid labile. Station IV is composed of acid run-off water only and could have an increased particulate matter content because of this. Lead adsorbed onto particulate matter would be measured by the AFS technique and might account for the apparent discrepancy between the AFS and ASV techniques.

CHAPTER 6.

Analysis of natural waters for trace metals.

6.1. Introduction.

The analysis of natural water by ASV is often preceeded by filtration through an 0.45μ filter to remove any particulate matter which nearly always constitutes a problem.

The trace elements in a natural water system are frequently associated with the particulate phases; organic and inorganic, living and non-living.

Hume (44) has pointed out that the removal of suspended mineral particles or living organisms may simplify the analytical procedure but destroy the significance of the results.

Zirino and Healy in their analyses of oceanic water have shown that as much as 10^{-7} mol dm^{-3} Zn may be leached from filter papers and to overcome the problem the filters had first to be prefiltered with 1 dm^3 of dilute HNO_3 followed by several cubic decimetres of open ocean water.

The disturbing contribution of Zn, Cd, Pb and Cu from filter papers and the lengthy and hazardous way of prefiltering with natural water led us to avoid filtration in this work. This was possible since the water was optically clear and little precipitation occurred in storage of the samples in polyethylene bottles prior to analysis.

No salts other than mercuric nitrate were added to the natural water samples to provide a supporting electrolyte since good voltammograms were obtained after deaerating the solutions with N_2 and CO_2. No manipulative operations were performed on the samples prior to pouring them into the ASV cell.

Contamination or adsorptive loss was thus restricted to the sampling bottles, the purge gases and from the ASV cell and electrode itself.

The addition of HNO_3 to determine any acid labile material in the final stages of the ASV analysis necessitated a blank reading for the addition and involved possible contamination from the pipette. The lowering of the pH in the cell may release metals adsorbed onto the glass surface of both electrodes and cell and this could introduce a possible error into the final stage of the analysis.

6.2. Sampling Bottles.

The loss of trace metal ions on the walls of containers used for collection and storage of water samples can become important at the low concentrations (10^{-6} to 10^{-11} mol dm^{-3}) found in environmental samples, Struempler (45). The collection of water samples in this work was done with 200cm^3 polyethylene sampling bottles which had been subjected to a thorough acid washing treatment outlined by Struempler.

6.2.1. Bottle washing procedure. 200cm^3 polyethylene bottles were cleaned by a detergent wash followed by a tap rinse. The bottles were then completely filled with chromic acid, the screw tops were submerged in a separate container of chromic acid. After 12 hours the bottles were emptied and rinsed with distilled water before refilling with concentrated HNO_3. After a further 12 hours, the bottles were rinsed with distilled water and finally washed out with de-ionised water.

6.2.2. Blank bottles. To determine the dissolution of ions from the bottle walls the containers were filled with doubly distilled water and any build up of Zn, Cd, Pb or Cu observed by repeated ASV analyses at 2 hourly intervals for a period of 8 hours, a further analysis was performed at 24 hours after the start of the experiment and at 24 hour intervals up to 72 hours. The results are shown in Table 20.

Table 20.

Hours	Zn	Cd	Pb	Cu
0	0.05µA	0.01µA	0.01µA	0.02µA
2	0.06µA	"	0.02µA	0.02µA
4	0.04µA	"	0.03µA	0.03µA
6	0.05µA	"	0.03µA	0.04µA
8	0.04µA	"	0.03µA	0.04µA
24	0.03µA	"	0.04µA	0.04µA
48	0.01µA	"	0.04µA	0.05µA
72	0.01µA	"	0.04µA	0.05µA

Each value is the mean of four readings on a $10cm^3$ sample (2.5×10^{-5} mol dm^{-3}) w.r.t. mercuric nitrate in H_2CO_3 supporting electrolyte at pH 3.85.

The blank reading for Zn of 0.05µA decreased to 0.01µA in a 72 hour period of standing which shows that Zn is adsorbed onto the container walls to a significant degree when compared with the standard deviation* (± 20%) of the Zn blank measurement in Section 5.10.

The Cd peak current remained at less than 0.01µA throughout the experiment.

Lead and copper peak currents were found to increase by 0.03µA for both elements in 72 hours which is indicative of

* Relative standard deviation

leaching from the container walls. Blank measurements were found to vary between 28% and 30% for Pb and Cu respectively in Section 5.10.

6.2.3. <u>Standard Bottles</u>. In another experiment, bottles used for sample collection were filled with 10^{-8}mol dm^{-3} Cd and Cu, 2 x 10^{-8}mol dm^{-3} Zn together with 3 x 10^{-8}mol dm^{-3} Pb. The bottles were monitored for a 72 hour period as above, the results are shown in Table 21.

<u>Table 21</u>.

ASV analysis on polyethylene bottles containing standards.

Hours	x10^{-8} mol dm^{-3}	2	1	3	1	% Deviation from original i_p			
	Metal	Zn	Cd	Pb	Cu	Zn	Cd	Pb	Cu
0	—	0.46	0.18	0.58	0.22	-	-	-	-
2	—	0.45	0.17	0.57	0.23	-2.2	-5.6	-1.7	4.6
4	—	0.46	0.19	0.55	0.22	0.0	-5.6	- 5.2	0.0
6	—	0.44	0.18	0.56	0.23	-4.4	0.0	- 3.5	4.6
8	—	0.43	0.17	0.54	0.24	-6.50	-5.6	- 6.9	9.1
24	—	0.42	0.18	0.53	0.23	-8.70	0.0	- 8.6	4.6
48	—	0.41	0.17	0.52	0.24	-10.9	-5.6	-10.3	9.1
72	—	0.40	0.19	0.50	0.26	-13.00	5.6	13.8	15.4

The aliquots taken were analysed in carbonic acid supporting electrolyte (pH = 3.80). Each peak current value is the mean of four measurements.

The bottles adsorbed Zn from the standard solution, a process which continued throughout the 72 hour period giving a maximum % deviation of 10.2% at the 2 x 10^{-8}mol dm^{-3} level, a value nearly double the precision of measurement standard deviation at the 5 x 10^{-8}mol dm^{-3} concentration (Section 5.11).

Cadmium was once again unaffected by leaching or adsorption phenomena at the pH of 5.82 of the bottles.

The Pb signal decreased in contrast to the blank solution. Pb was adsorbed from the standard solution giving a range of negative deviations (%) of -1.7% to -13.8% at the 2 hour and 72 hour periods. The precision of measurement at the 5 x 10^{-8}mol dm^{-3} level was ± 4.8%.

The copper peak current increased in the bottles containing a 1 x 10^{-8}mol dm^{-3} standard from 0.22 to 0.26μA between 2 and 72 hours producing a positive deviation of between 4.6 to 15.4% at this concentration. This is slightly in excess of the precision of measurement at the 5 x 10^{-8}mol dm^{-3} concentration of ± 7.9%.

Struempler points out that analysis of trace metal concentrations in the p p b range necessiates that the sample should be acidified to pH 2 to minimise adsorption on container walls. In this work this is not desirable as the possible acid release of metal on acidification is to be examined after analysis of the sample at the insitu pH of the sample.

In the work described later to encompass the varying adsorption effects at the different pH's of the water samples in the bottles, they were analysed in sequence.

6.3. Sampling.

The collection of natural water samples was carried out by taking subsurface samples in 200cm^3 polyethylene bottles. The bottles remained full of doubly distilled water prior to

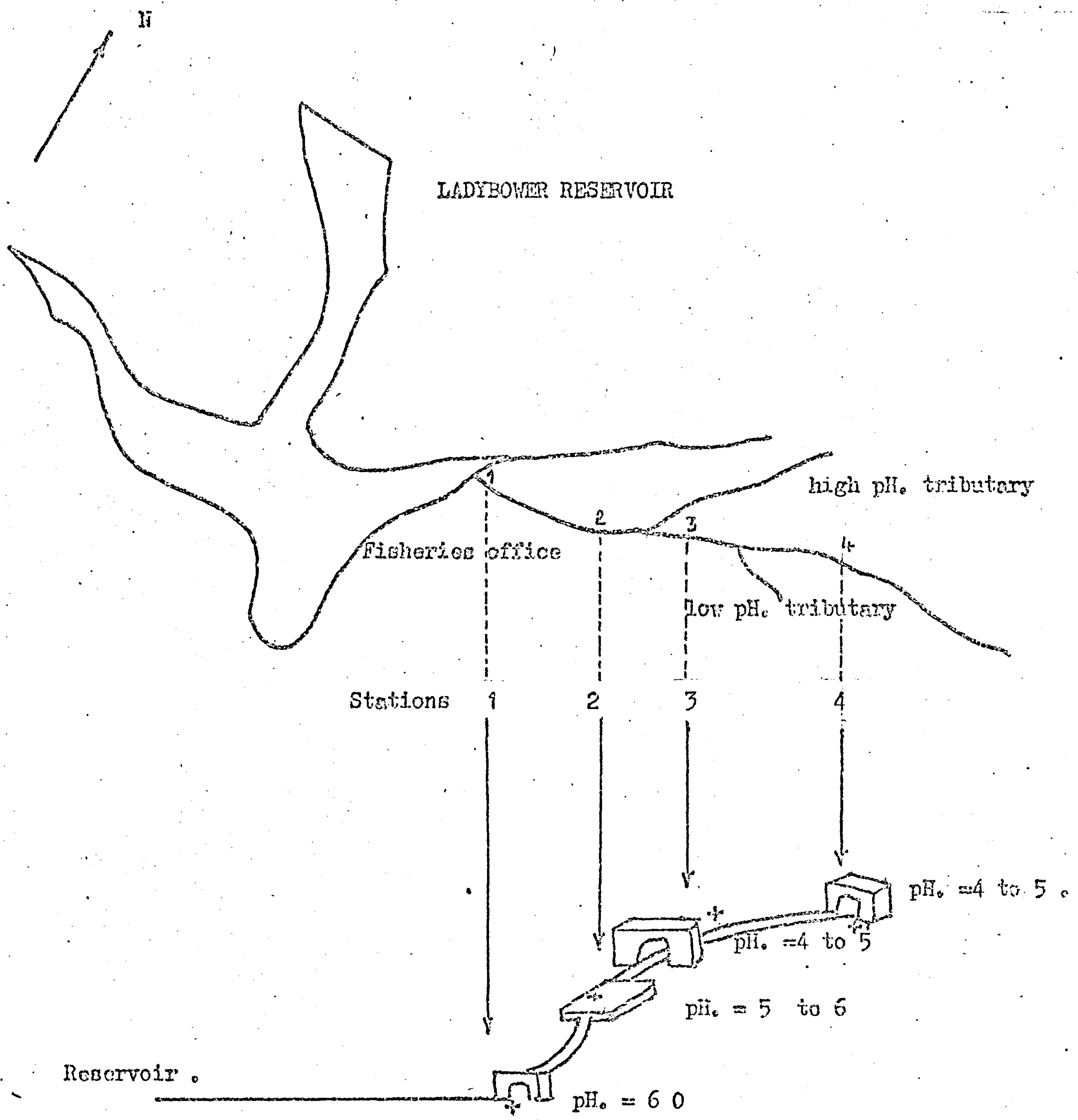

Figure. 37.

To show the location of the sampling stations on the stream supplying the Trout Hatchery.

sampling and were rinsed out six times with natural water before the sample was taken. Two blank bottles were filled with doubly distilled water before the collection of samples and analysed with the samples. No reagents were added to prevent adsorptive losses in the natural water samples since this can disrupt the natural distribution of constituents between the particulate matter and solution and might significantly alter the trace metal ion concentration in solution.

6.4. <u>Sampling stations.</u>

The sampling stations were situated on a small tributary supplying the trout hatchery at Ladybower reservoir and are shown in Figure 37. The tributary was chosen as a sampling point because of the variation in pH which was encountered at the four sampling stations situated on it. The range of pH was from 6.0 to 4.0. The effect of pH on the trace metal concentrations found in the tributary could be investigated and observations made over a period of months.

A report from the fisheries officer that young trout-fry mortality was high after heavy rainfall also aroused an added interest in this stream.

6.5. <u>Procedure for sample collection.</u>

The samples were collected in two 200cm^3 polyethylene bottles from each of the 4 stations (Fig.37). The range of samples were analysed by taking aliquots from one of each of the bottles in succession. After the complete range of samples had been analysed the second sample bottle of the pair was analysed in the same order as the first series so that any adsorption effects occurring in storage whilst the samples were being analysed were easily identified. Uncertainty about metal ion removal was thus limited to the period between sampling and commencement of analysis of a sample which was limited to 72 hours.

CHAPTER 7.

Results of the four series of ASV analyses performed on 'The Trout Stream' water.

7.1. Introduction.

The tributary supplying the Trout Hatchery was sampled on four occasions in the months of April, May and June (1973).

The stream was in flood in both April and May and was fast flowing. In June the flow of the stream was reduced to a trickle and it became divided up into numerous shallow pools along its length. In late June the water level had risen slightly.

The results obtained from the ASV measurements made on the tributary are shown in Tables 22 to 25.

Two sample bottles were used on each station and analysed in two series such that the second bottle was stored until one bottle from each station had been analysed. Complications arising from storage would be apparent if the anodic peak currents differed considerably from those measured from the first bottle. Each bottle was sub-sampled twice for ASV analysis so that 4 readings for each station were obtained in each phase of the analysis and the mean value* recorded in the table of results.

In the table of results the metals analysed have their peak current (i_p) and the corresponding concentration at the three pH values of the sample as it undergoes each phase of the analysis:

pH_1 = natural water pH

pH_2 = pH after degassing with N_2

pH_3 = pH after degassing with CO_2

* (Maximum S.D. = ± 0·05 μA)

pH_4 = pH after the addition of $0.03 cm^3$ HNO_3 acid.

Blank bottles containing aged stream water with no detectable trace metals levels were run through the sampling and analysis procedure to monitor possible leaching phenomena throughout the time that samples were stored or in transit.

7.2. Results.

The results will be summarised under each individual metal heading. The variation in metal concentrations will be compared for individual stations on a particular sampling date and also over the period of sampling.

Table 22.

Result of an ASV analysis performed on stream water sampled on April 22nd.

pH Station	Zn $i_p(\mu A)$, mol dm^{-3}	Cd $i_p(\mu A)$, mol dm^{-3}	Pb $i_p(\mu A)$, mol dm^{-3}	Cu-1 $i_p(\mu A)$, mol dm^{-3}	Cu-2 $i_p(\mu A)$, mol dm^{-3}
Station 1					
pH_1=5.30					
pH_2=6.50	0.425, 2.86×10^{-8}	0.010, 0.75×10^{-9}	1.108, 6.79×10^{-8}	0.201, 1.43×10^{-8}	0.055, 3.88×10^{-9}
pH_3=3.80	0.540, 3.44×10^{-8}	0.010, 0.71×10^{-9}	1.251, 7.35×10^{-8}	0.401, 2.75×10^{-8}	0.025, 1.71×10^{-9}
pH_4=2.00	- -	0.08, 5.23×10^{-9}	1.855, 1.01×10^{-7}	0.610, 3.72×10^{-8}	- -
Station 2					
pH_1=5.40					
pH_2=6.55	0.625, 4.21×10^{-8}	0.005, 0.38×10^{-9}	1.408, 8.65×10^{-8}	- -	0.250, 1.76×10^{-8}
pH_3=3.80	0.740, 4.71×10^{-8}	0.005, 0.35×10^{-9}	1.460, 8.56×10^{-8}	0.810, 5.55×10^{-8}	0.025, 1.71×10^{-9}
pH_4=2.00	- -	0.005, 3.27×10^{-10}	1.875, 1.11×10^{-7}	0.913, 5.56×10^{-8}	- -
Station 3					
pH_1=6.10					
pH_2=6.80	0.390, 2.62×10^{-8}	- -	0.250, 1.54×10^{-8}	- -	- -
pH_3=3.81	0.330, 2.10×10^{-8}	0.01, 0.71×10^{-9}	0.350, 2.05×10^{-8}	0.200, 1.37×10^{-8}	0.05, 3.42×10^{-9}
pH_4=2.00	- -	0.01, 0.65×10^{-9}	0.600, 3.24×10^{-8}	0.300, 1.83×10^{-8}	- -

Table 22 (continued)

pH	Zn	Cd	Pb	Cu-1	Cu-2
Station 4	i_p(μA), mol dm^{-3}	i_p(μA), mol dm^{-3}	i_p(μA), mol dm^{-3}	i_p(μA), mol dm^{-3}	i_p(μA), mol dm^{-3}
pH_1=4.50					
pH_2=4.80	0.625, 4.21×10^{-8}	0.01, 0.75×10^{-9}	1.550, 9.51×10^{-8}	0.364, 2.56×10^{-8}	0.180, 1.27×10^{-8}
pH_3=3.72	0.540, 3.44×10^{-8}	0.01, 0.71×10^{-9}	1.656, 9.70×10^{-8}	0.430, 2.94×10^{-8}	- -
pH_4=2.00	- -	0.08, 5.22×10^{-9}	2.775, 1.50×10^{-7}	0.611, 3.72×10^{-8}	- -
Blanks					
pH_1=5.72					
pH_2=5.85	0.200, 1.35×10^{-8}	- -	- -	0.04, 2.82×10^{-9}	0.02, 1.41×10^{-9}
pH_3=3.85	0.280, 1.79×10^{-8}	- -	0.10, 5.87×10^{-9}	0.076, 5.20×10^{-9}	
pH_4=2.00	- -	- -	0.12, 6.49×10^{-9}	0.100, 6.10×10^{-8}	

Table 23.

Result of an ASV analysis performed on stream water sampled on May 17th.

pH Station 1	Zn $i_p(\mu A)$, mol dm^{-3}	Cd $i_p(\mu A)$, mol dm^{-3}	Pb $i_p(\mu A)$, mol dm^{-3}	Cu-I $i_p(\mu A)$, mol dm^{-3}	Cu-2 $i_p(\mu A)$, mol dm^{-3}
$pH_1=5.20$					
$pH_2=6.51$	0.35 , 2.35×10^{-8}	- -	1.20 , 7.36×10^{-8}	0.15 , 1.06×10^{-8}	0.06 , 1.42×10^{-8}
$pH_3=3.81$	0.48 , 3.06×10^{-8}	0.012 , 0.86×10^{-9}	1.41 , 8.26×10^{-8}	0.55 , 3.76×10^{-8}	0.025, 1.71×10^{-9}
$pH_4=2.00$	- -	- -	2.05 , 1.11×10^{-7}	0.72 , 4.39×10^{-8}	- -
Station 2					
$pH_1=5.90$					
$pH_2=6.45$	0.24 , 1.61×10^{-8}	- -	1.32 , 8.10×10^{-8}	0.16 , 1.13×10^{-8}	0.25 , 1.76×10^{-8}
$pH_3=3.80$	0.32 , 2.10×10^{-8}	0.008 , 0.56×10^{-9}	1.53 , 8.96×10^{-8}	0.71 , 4.86×10^{-8}	0.03 , 1.83×10^{-9}
$pH_4=2.00$	- -	- -	1.98 , 1.07×10^{-7}	0.85 , 5.19×10^{-8}	- -
Station 3					
$pH_1=5.90$					
$pH_2=6.70$	0.24 , 1.61×10^{-8}		0.12 , 7.36×10^{-9}	0.18 , 1.27×10^{-8}	
$pH_3=3.85$	0.30 , 1.53×10^{-8}	0.015 , 1.06×10^{-9}	0.26 , 1.53×10^{-8}	0.35 , 2.40×10^{-8}	0.05 , 3.42×10^{-9}
$pH_4=2.00$	- -		0.31 , 1.68×10^{-8}	0.48 , 2.93×10^{-8}	

Table 23 (continued)

pH Station	Zn i_p(µA) mol dm^{-3}	Cd i_p(µA) mol dm^{-3}	Pb i_p(µA) mol dm^{-3}	Cu-1 i_p(µA) mol dm^{-3}	Cu-2 i_p(µA) mol dm^{-3}
4 $pH_1=4.40$					
$pH_2=4.95$	0.64 , 4.30×10^{-8}	- -	1.46 , 8.95×10^{-8}	0.410 , 2.89×10^{-8}	0.190 , 1.34×10^{-8}
$pH_3=3.79$	0.47 , 2.99×10^{-8}	0.02 , 1.42×10^{-9}	1.74 , 1.02×10^{-8}	0.580 , 3.97×10^{-8}	-
$pH_4=2.00$	- -		2.81 , 1.52×10^{-7}	0.650 , 3.96×10^{-8}	
Blanks					
$pH_1=4.82$					
$pH_2=5.40$	0.10 , 0.67×10^{-8}			0.016 , 1.13×10^{-9}	
$pH_3=3.80$	0.18 , 1.46×10^{-8}	0.002 , 1.42×10^{-10}	0.004 , 2.34×10^{-10}	0.030 , 2.06×10^{-10}	0.008 , 5.46×10^{-10}
$pH_4=2.00$			0.02 , 1.08×10^{-9}	0.10 , 6.10×10^{-8}	

Table 24.

Result of an ASV analysis performed on stream water sampled on June 3rd.

pH Station	Zn $i_p(\mu A)$ mol dm^{-3}	Cd $i_p(\mu A)$ mol dm^{-3}	Pb $i_p(\mu A)$ mol dm^{-3}	Cu-1 $i_p(\mu A)$ mol dm^{-3}	Cu-2 $i_p(\mu A)$ mol dm^{-3}
Station 1 pH_1=6.50					
pH_2=7.45	0.790 , 5.30×10^{-8}	- -		0.02 , 1.41×10^{-9}	
pH_3=3.90	1.13 , 7.20×10^{-8}	0.01 , 0.71×10^{-9}	0.040 , 2.34×10^{-9}	0.018 , 1.23×10^{-9}	0.064 , 4.38×10^{-9}
pH_4=2.00	- -		0.070 , 3.79×10^{-9}	0.190 , 1.59×10^{-8}	- -
Station 2					
pH_1=6.39					
pH_2=7.50	0.144 , 0.97×10^{-8}	- -	- -	0.050 , 3.52×10^{-9}	- -
pH_3=3.80	0.370 , 2.36×10^{-8}	0.004 , 2.84×10^{-10}	0.01 , 5.87×10^{-9}	0.400 , 2.74×10^{-8}	- -
pH_4=2.00	- -	- -	0.110 , 5.95×10^{-9}	0.670 , 4.08×10^{-8}	- -
Station 3					
pH_1=4.51					
pH_2=4.30	2.025 , 1.38×10^{-7}	0.030 , 2.23×10^{-9}	2.360 , 1.45×10^{-7}	0.500 , 3.52×10^{-8}	0.425 , 2.99×10^{-8}
pH_3=3.70	1.450 , 9.24×10^{-8}	0.035 , 2.48×10^{-9}	2.450 , 1.44×10^{-7}	1.050 , 7.20×10^{-8}	0.440 , 3.01×10^{-8}
pH_4=2.00	- -	0.03 , 1.96×10^{-9}	3.55 , 1.92×10^{-7}	1.900 , 1.59×10^{-7}	- -

Table 24 (continued)

pH Station 4	Zn i_p(µA)	Zn mol dm^{-3}	Cd i_p(µA)	Cd mol dm^{-3}	Pb i_p(µA)	Pb mol dm^{-3}	Cu-1 i_p(µA)	Cu-1 mol dm^{-3}	Cu-2 i_p(µA)	Cu-2 mol dm^{-3}
pH_1=4.59										
pH_2=4.55	1.815	1.22×10^{-7}	0.025	1.88×10^{-9}	3.05	1.87×10^{-7}	0.325	2.29×10^{-8}	1.305	9.20×10^{-8}
pH_3=3.72	1.510	9.61×10^{-8}	0.05	3.55×10^{-9}	3.40	1.99×10^{-7}	0.850	5.81×10^{-8}	1.810	1.23×10^{-7}
pH_4=2.00	-	-	0.04	2.61×10^{-9}	4.66	2.52×10^{-7}	1.870	1.14×10^{-7}	-	-
Blanks										
pH_1=4.80										
pH_2=5.40	0.14	0.94×10^{-8}	-	-	-	-	0.020	1.41×10^{-9}		
pH_3=3.80	0.210	1.38×10^{-8}	0.002	1.42×10^{-10}	0.004	2.34×10^{-10}	0.030	2.06×10^{-9}	0.008	5.46×10^{-10}
pH_4=2.00	-	-			0.02	1.08×10^{-9}	0.100	6.10×10^{-9}		

Table 25.

Result of an ASV analysis performed on stream water sampled on June 20th.

pH Station	Zn $i_p(\mu A)$	Zn mol dm^{-3}	Cd $i_p(\mu A)$	Cd mol dm^{-3}	Pb $i_p(\mu A)$	Pb mol dm^{-3}	Cu-1 $i_p(\mu A)$	Cu-1 mol dm^{-3}	Cu-2 $i_p(\mu A)$	Cu-2 mol dm^{-3}
Station 1										
$pH_1=6.64$										
$pH_2=7.50$	1.42	9.53×10^{-8}	–	–	–	–	0.03	2.16×10^{-9}	0.06	4.23×10^{-9}
$pH_3=3.80$	1.60	1.07×10^{-7}	0.015	1.06×10^{-9}	0.15	8.81×10^{-9}	0.04	2.74×10^{-9}	0.100	6.85×10^{-9}
$pH_4=2.00$			–	–	0.26	1.41×10^{-8}	0.20	1.20×10^{-8}	–	–
Station 2										
$pH_1=6.30$										
$pH_2=7.30$	1.21	8.12×10^{-8}	–	–	0.04	2.46×10^{-9}	0.15	1.06×10^{-8}	–	–
$pH_3=3.80$	1.40	9.40×10^{-8}	0.01	0.71×10^{-9}	0.12	7.05×10^{-9}	0.35	2.40×10^{-8}	–	–
$pH_4=2.00$					0.21	1.13×10^{-8}	0.45	2.74×10^{-8}	–	–
Station 3										
$pH_1=4.50$										
$pH_2=4.40$	3.50	2.35×10^{-7}	–	–	2.38	1.46×10^{-7}	0.43	3.12×10^{-8}	0.45	3.17×10^{-8}
$pH_3=3.79$	3.50	2.22×10^{-7}	0.043	3.05×10^{-9}	2.60	1.53×10^{-7}	0.76	5.20×10^{-8}	0.43	3.29×10^{-8}
$pH_4=2.00$	–	–	–	–	3.50	1.89×10^{-7}	0.91	5.55×10^{-8}	–	–

Table 25 (continued)

pH Station	Zn i_p(µA)	Zn mol dm^{-3}	Cd i_p(µA)	Cd mol dm^{-3}	Pb i_p(µA)	Pb mol dm^{-3}	Cu-I i_p(µA)	Cu-I mol dm^{-3}	Cu-2 i_p(µA)	Cu-2 mol dm^{-3}
4										
pH_1=4.55										
pH_2=4.50	3.30	2.22×10^{-7}	-	-	3.20	1.96×10^{-7}	0.310	2.18×10^{-8}	1.30	9.16×10^{-8}
pH_3=3.80	3.21	2.16×10^{-7}	0.06	4.20×10^{-9}	3.49	2.05×10^{-7}	0.730	5.0×10^{-8}	1.80	1.23×10^{-8}
pH_4=2.00	-	-	-	-	4.50	2.44×10^{-7}	0.880	5.36×10^{-8}	-	-
Blanks										
pH_1=4.80										
pH_2=5.42	0.15	1.01×10^{-8}	-	-	-	-	0.019	1.34×10^{-9}	-	-
pH_3=3.80	0.20	1.34×10^{-8}	0.002	1.42×10^{-10}	0.005	2.94×10^{-9}	0.018	1.37×10^{-9}	0.009	6.16×10^{-10}
pH_4=2.00					0.05	1.62×10^{-9}	0.10	6.10×10^{-9}	-	-

Peak Current profiles for Zn

over the sampling period.

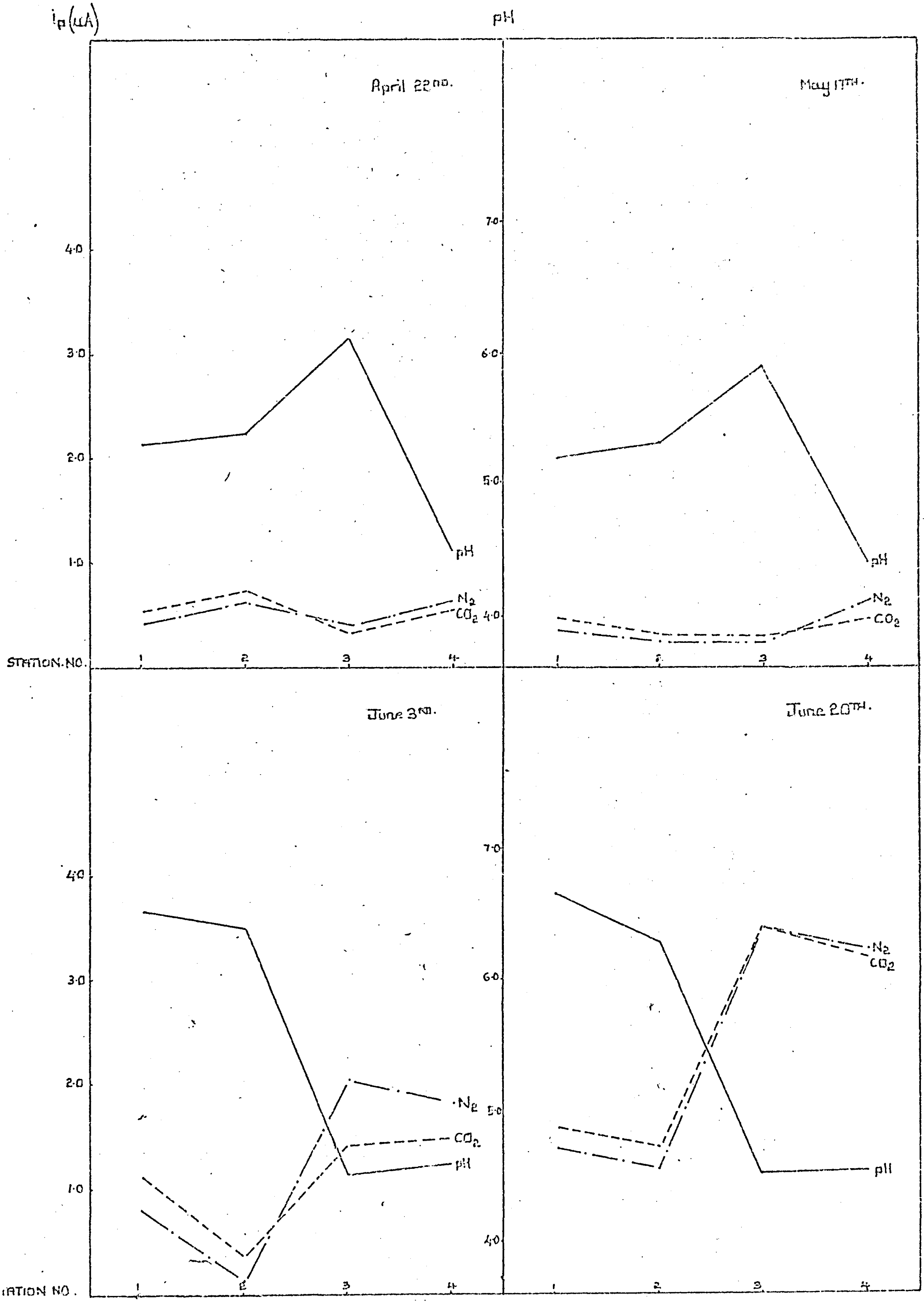

7.2.1. Zinc : Zn. There was no clear correlation between Zn peak currents and pH in the April and May samples. No significant concentration gradient was apparent in these samples and Zn concentrations were low at all stations.

In measurements made on June 3rd., higher concentrations of Zn were found in upstream water of low pH (4.51 to 4.59) at station 3 and 4.

In the final sampling on June 20th. all the Zn concentrations at individual stations had risen compared to the previous analysis even at stations 1 and 2 which had relatively high pH water (6.64 and 6.30). Measurement made after degassing the sample with carbon dioxide showed increased peak currents at stations 1 and 2 but lower peak currents at stations 3 and 4; the exception being station 3 in May where as at the first two stations a higher peak current was recorded in the second stage of the analysis. The fact that the peak current profiles shown in figure 38 are not parallel to each other in consecutive stages of analysis at each station is an indication of different Zn release values or complexation in that particular water sample at the lower pH of 3.80 ± 0.01.

The Zn concentration in the stream varied between 10^{-8} mol dm^{-3} and 2.35×10^{-7} mol dm^{-3} throughout the sampling period.

Figure 39.

Peak Current profiles for Cd

over the sampling period.

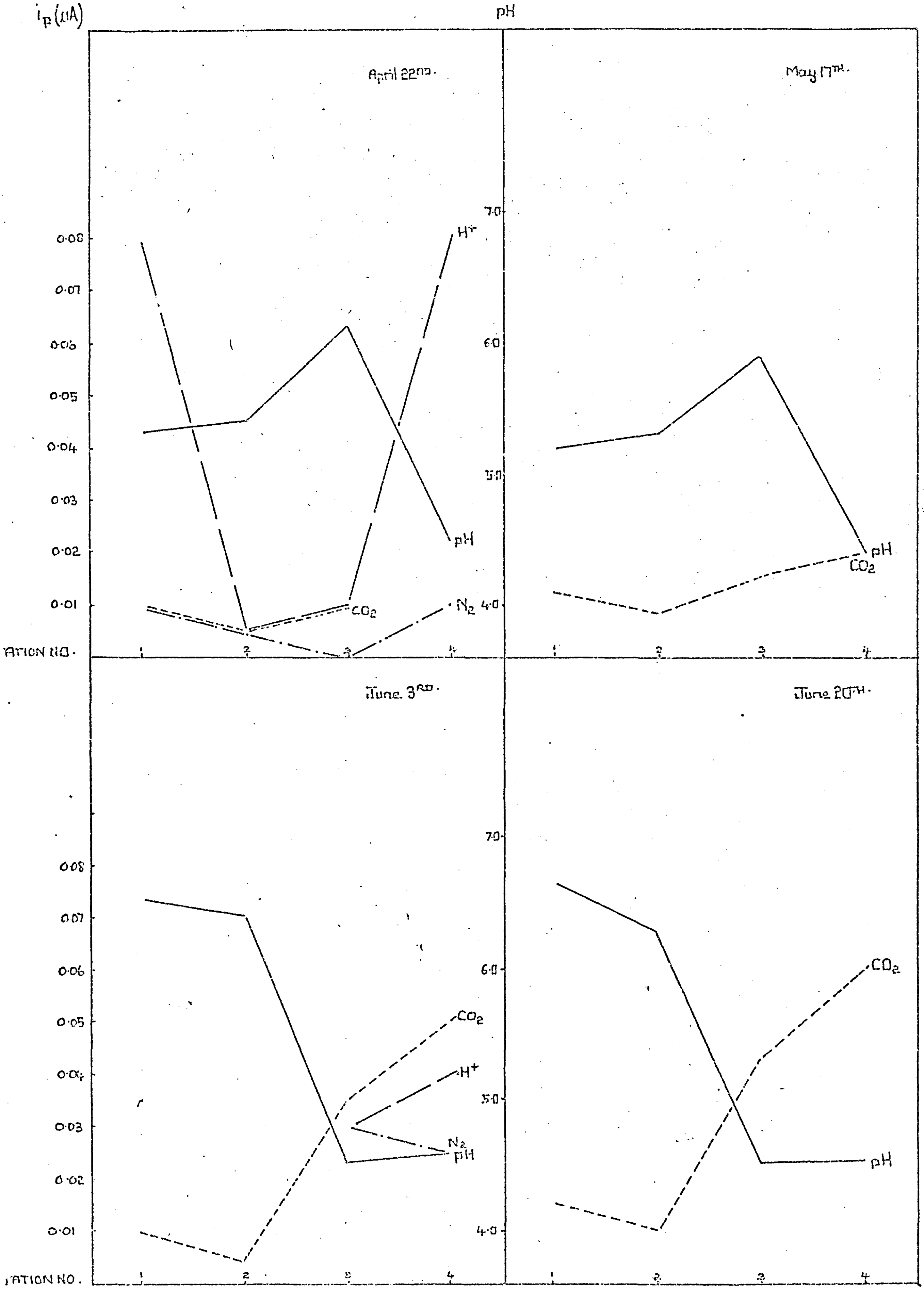

7.2.2. <u>Cadmium : Cd.</u> In April and May Cd concentrations measured in the stream water were very low at all stations and in the same order of magnitude as blank samples and possible leaching phenomena associated with the sample bottles. Higher peak currents were recorded after the addition of HNO_3 in samples taken from stations 1 and 4 in April. However contamination from the acid could not be ruled out.

In June 3rd. and 20th. samples although concentrations were still very low more Cd was found in the upstream water of low pH at stations 3 and 4. A concentration gradient with higher concentrations of Cd being found above station 2 was clear in the June samples.

In water of relatively high pH (> 6.0) few Cd anodic peaks were obtained after degassing with nitrogen.

The Cd peak was often lost in the increased background current after the addition of HNO_3 to the May and June samples. The peaks measured at pH 2 were smaller than those measured in carbonic acid at stations 3 and 4 in the June 3rd. samples.

Concentrations of Cd recorded from the stream water over the sampling period ranged from 0.35 to 5.23×10^{-9} mol dm^{-3}.

Peak Current profiles for Pb

over the sampling period.

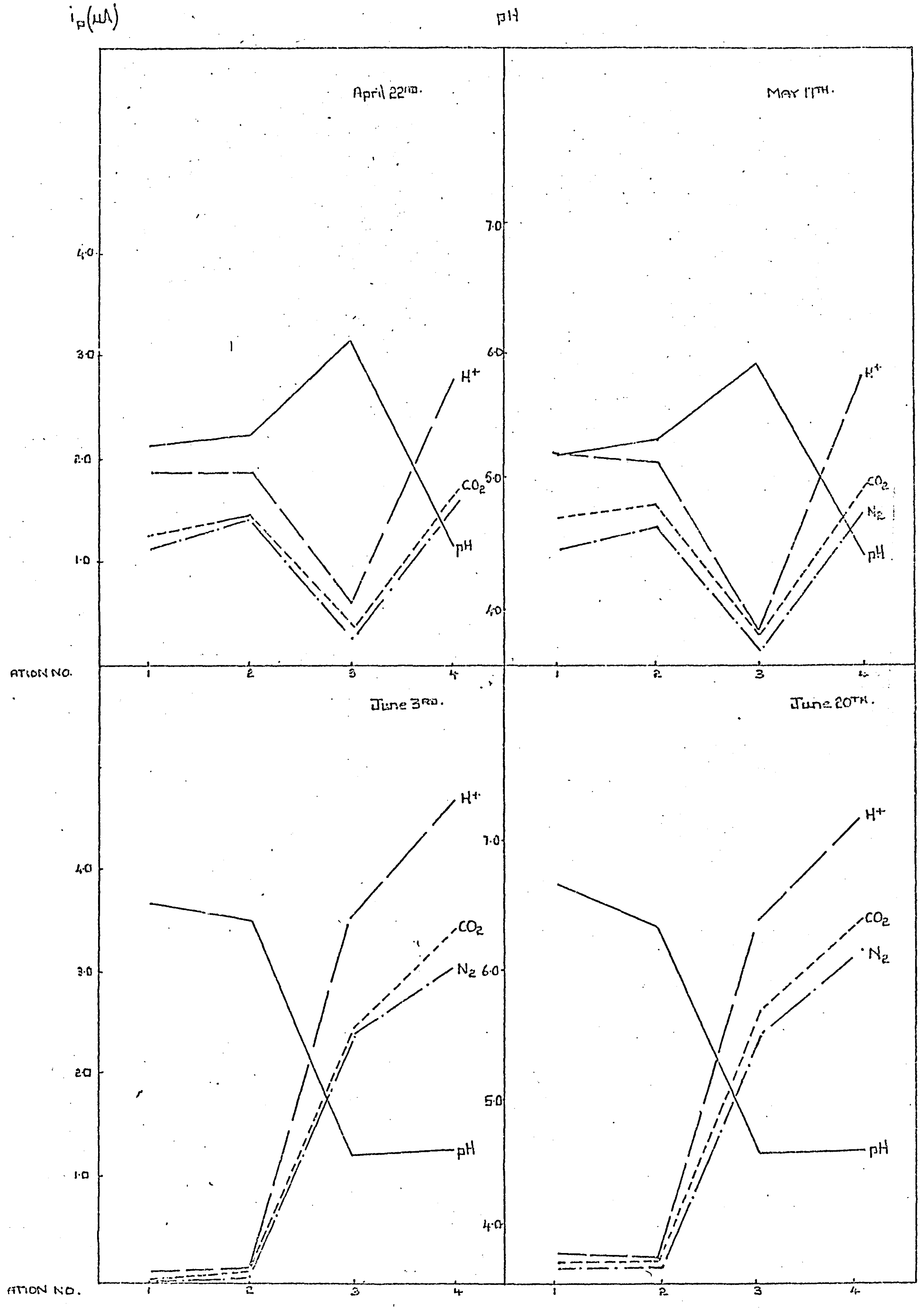

7.2.3. Lead : Pb. In April Pb concentrations were very similar at stations 1 and 2 but declined at station 3 where a slight pH increase (5.40 to 6.10) was observed. More Pb was found at station 4 than at the three lower stations; station 4 also had the lowest pH (4.20). In May a similar pH pattern and Pb concentration was observed as in April.

In June 3rd. and 20th. samples very little Pb was measured at stations 1 and 2 at pH's of between 6.30 and 6.64 . High Pb concentrations were found in the low pH water (4.50 to 4.59) upstream at stations 3 and 4.

From the peak current profile shown in Figure 40 it can be seen that the Pb anodic peak increased as the pH was lowered in each of three phases of the analysis. In April and May stations 1 and 2 (pH 5.20 to 5.40) showed increased release of Pb at pH 2. Station 4 (pH 4.40 to 4.50) followed a similar pattern however the increase in the Pb anodic peak at station 3 (pH 5.90 to 6.10) was minimal in comparison with the other 3 stations. Conversely in the June samples Pb release after the addition of acid at pH 2 was small at stations 1 and 2 (pH's 6.30 to 6.64) and increased upstream at station 3 (pH 4.50 to 4.51) and reached a maximum at station 4 (pH 4.40 to 4.50). Concentrations of Pb in the stream varied between 10^{-7} mol dm^{-3} to 10^{-9} mol dm^{-3} throughout the sampling period.

Peak Current profiles for Cu-1
over the sampling period.

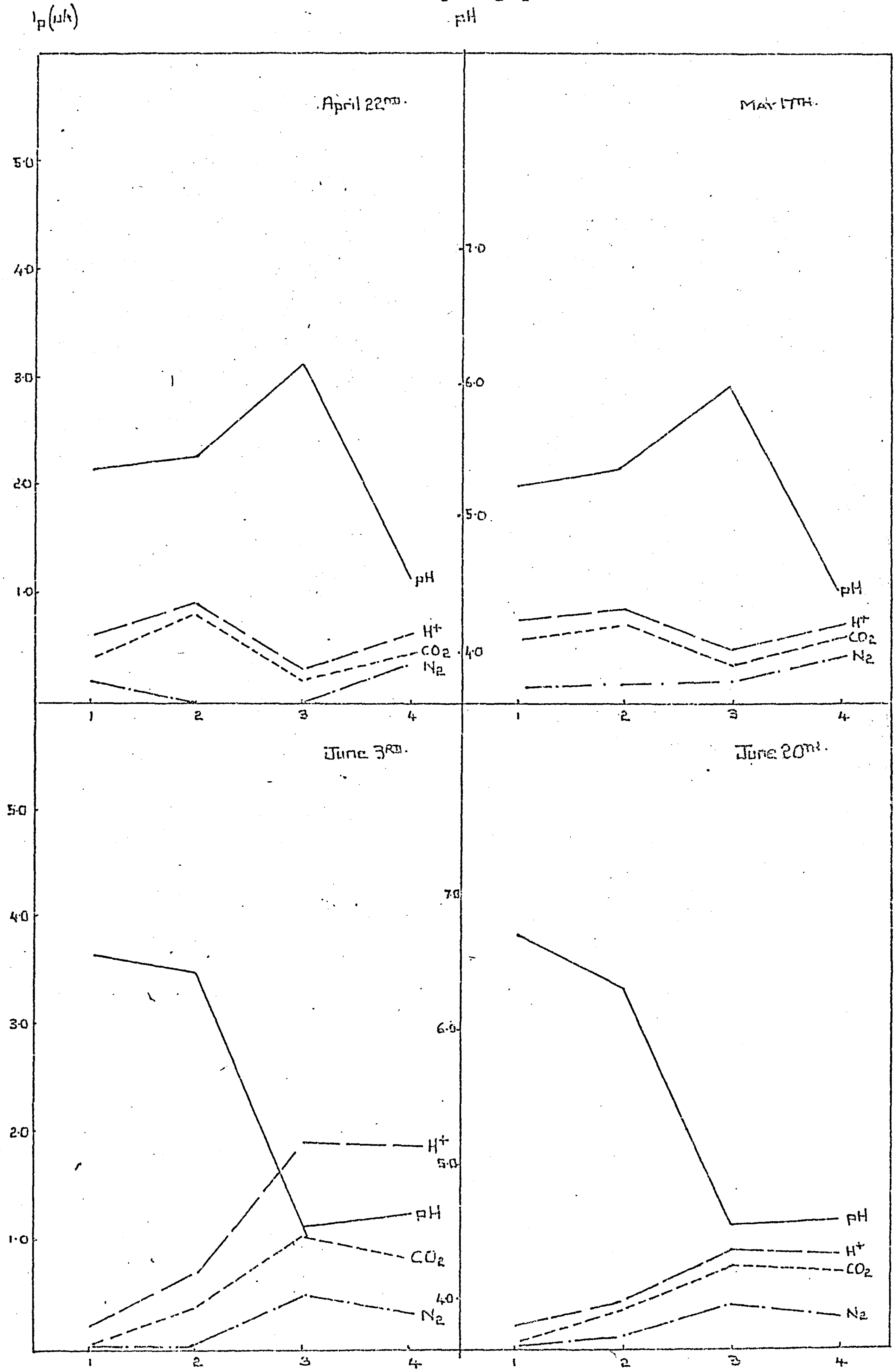

7.2.4. <u>Copper : Cu-1</u>. Cu-1 is considered to be the 'free' metal peak of a pair of closely associated peaks referred to earlier as the copper doublet.

The concentration of Cu-1, was low in April and May with no apparent concentration gradient. Station 3 with a high pH (6.1) water had the lowest concentration of the metal in the second and third stages of the analysis.

In June 3rd. samples, station 3 had low pH (4.50 to 4.51) water and the highest concentration of Cu metal; a similar but slightly lower concentration was found at station 4 with much lower concentrations being found at both lower stations downstream at higher pH values (6.30 to 6.64).

All the Cu concentrations had fallen in the June 20th. samples however the pattern where higher concentrations were found at upstream stations with lower pH values was repeated. The increased peak current measured from the sample at pH 2 was fairly consistent at all stations in April and May samples and led to a near parallel plot to the peak current measured in carbonic acid. Station 2 (pH = 5.30 to 5.40) samples produced the greatest increase in peak current at pH 3.80 on both sampling dates.

In June 3rd. samples more Cu was pH labile at the upstream stations 3 and 4 after successive lowering of pH in the sample. Much lower release at pH 2 was observed in the June 20th. samples and peak currents increased uniformly at all stations producing a near parallel plot to that measured in carbonic acid. The increase in metal concentration at pH 3.80 reflected the June 3rd. results where more metal was released from upstream, Peak Current profiles for Cu-2

over the sampling period.

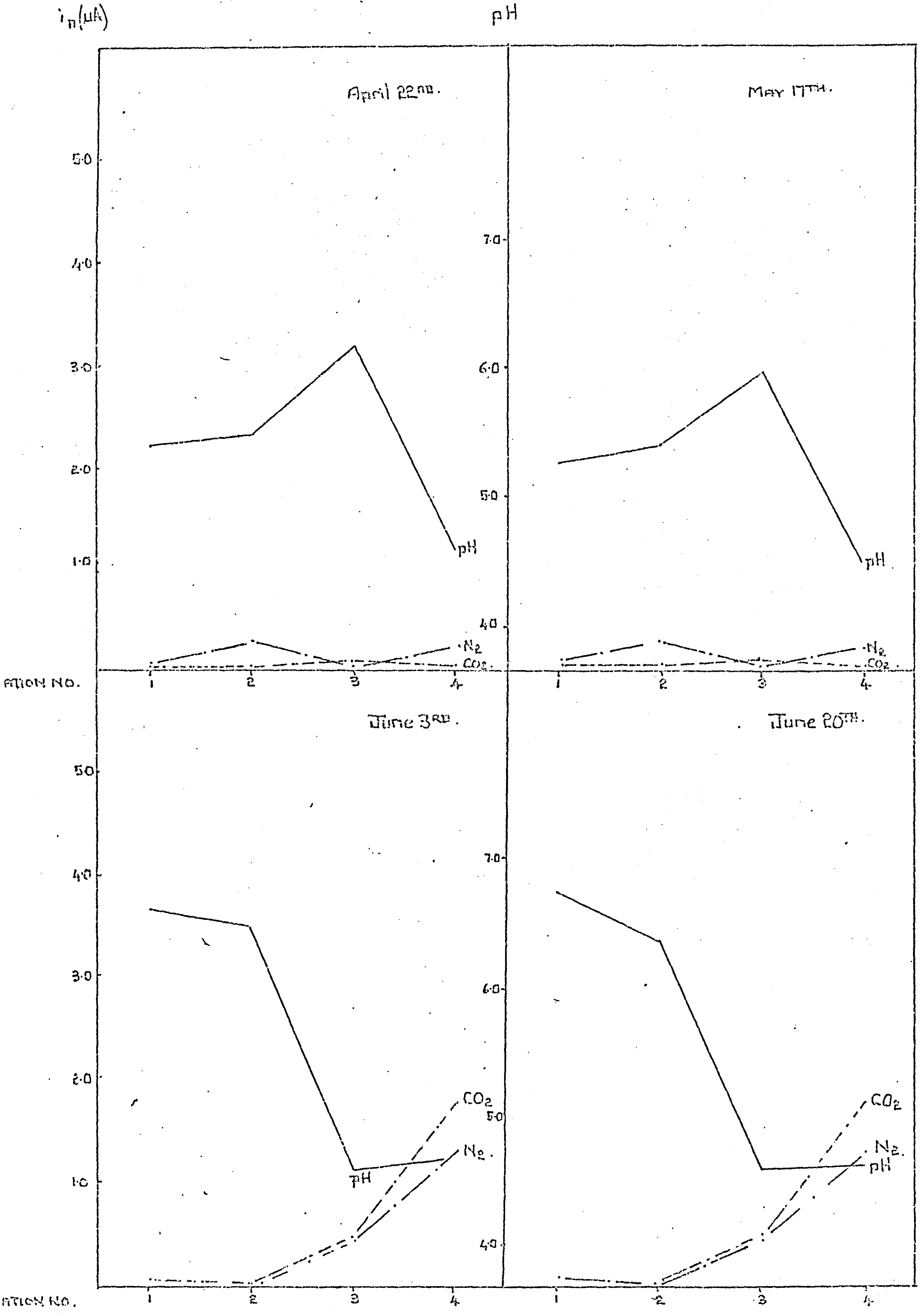

low pH water.

Cu-1 concentrations between 1.40×10^{-8} to 1.60×10^{-7} mol dm^{-3} were found in the stream water over the period of sampling. The highest value being measured at station 3.

7.2.5. Copper : Cu-2. Cu-2 is the second peak of the Cu doublet.

In April and May very low peak currents were measured at all stations and no trend was apparent. The June 3rd. and 20th. samples showed low Cu-2 concentrations in high pH waters at stations 1 and 2. Stations 3 and 4 at low pH values yielded progressively higher concentrations of Cu-2 on the two June sampling dates. Station 4 showed an increase release of Cu-2 at pH 3.80 when compared with station 3 over the same period.

Cu-2 disappeared in the final stage of the analysis at pH 2 in all samples. The anodic peak was not measured in all samples at the insitu pH or at pH 3.80 and was missing from both June samples taken from station 2.

7.3. % Release Values.

As the pH of the sample is lowered in each stage of the analysis procedure the increase (+ve % release) or decrease in peak height is recorded and the difference inequivalent concentration units expressed as a % of that found prior to lowering the pH.

Zinc : Zn . Negative release values were observed at stations 3 and 4 probably due to irreversible Zn adsorption onto particulate matter whilst degassing with nitrogen or formation of $ZnHCO_3^+$ species in carbonic acid. At station 1 and 2 release values ranged between 12.1% and 35%.

Cadmium : Cd . Very little information was gathered; all the values were negative between -4.8% and -7.1% under CO_2. After acidification -8.9% and -8.6% values were recorded at station 3 and 4. No information was available in May. In June, station 3 and 4 yielded -12% to -90.48% after degassing with CO_2 and this was further reduced on acidification to -21% and -21.2% at the respective stations. The peak currents were very near the limit of detection and bear little significance.

Lead : Pb . Under CO_2 alone between 1.06% and 104% release was observed. In acidic media values of between 29.8% to 65% were observed in April. In May, 9.8% to 40.35% was recorded with 13.92% at station 4.

In June 3rd. samples low release was observed in carbonic acid with 6.4% being the highest value at station 4. In acid between 26.6% and 63.3% was observed. On June 20th. no release was observed at stations 1 and 2. At station 3 and 4 between 4.8% and 4.6% was released in carbonic acid and this rose to 24.0% and 19.02% in acidic media.

Copper - 1 : Cu . Release values in carbonic acid media ranged from 2.54% to 15.3%. In May at station 2 as much as 33.1% increase in signal was observed. In acidic solution at pH 2 as much as 1175% and 1344% increase in signal was observed in June 3rd. samples. The corresponding values in June 20th. samples stabilised at 327% and 13.6% respectively.

Copper - 2 : Cu . Release values of between 126% and 927% were observed at stations 1 and 2; 0.81% was observed at station 4. In the June samples this increased to 32.6% and 641% in the final sample. No acid release was observed since the doublet peak disappeared at pH 2 in all cases.

Table 26.

% Release Values.

Station			(1)	(2)	(3)	(4)
April	Zinc	N_2/CO_2	20.43%	12.1%	-19.5%	-22.9%
May		"	30.92%	29.5%	- 5.1%	-44.3%
June 3rd		"	35.00%	14.2%	-49.3%	-27.1%
June 20th		"	12.30%	15.72%	0.79%	-2.7%
April	Cadmium	N_2/CO_2 CO_2/H^+	nil -	-7.1% -	nil -8.9%	-[illegible].8% -86%
May		N_2/CO_2 CO_2/H^+	nil -	- -	- -	- -
June 3rd		N_2/CO_2 CO_2/H^+	- -	- -	-12% -21%	-90.48% -21.20%
June 20th		N_2/CO_2 CO_2/H^+	- -	- -	- -	- -
April	Lead	N_2/CO_2 CO_2/H^+	1.06% 37.5%	1.2% 29.8%	32.9% 65.00%	2.08% 54.62%
May		N_2/CO_2 CO_2/H^+	12.2% 40.35%	10.6% 24.9%	104% 9.8%	13.5% 13.92%
June 3rd		N_2/CO_2 CO_2/H^+	nil 63.3%	1.6% nil	0.67% 33.3%	6.4% 26.6%
June 20th		N_2/CO_2 CO_2/H^+	nil nil	nil nil	4.8% 24.0%	4.6% 19.02%
April	Cu-1	N_2/CO_2	91.3% 92.0%	- 0.28%	- 34.5%	14.6% 26.6%
May		N_2/CO_2 CO_2/H^+	2.54% 16.6%	331% 6.75%	90.1% 22.1%	42.7% 3.9%
June 3rd		N_2/CO_2 CO_2/H^+	11.11% 1175%	22.22% 1344%	83.0% 119%	153% 94.6%
June 20th		N_2/CO_2	28.5% 327%	126% 13.6%	66.5% 6.6%	129% 7.2%

Table 26 (continued)

Station		(1)	(2)	(3)	(4)
April Cu-2	N_2/CO_2 CO_2/H^+	127% -	927% -	nil -	0.81% -
May	N_2/CO_2 CO_2/H^+	727% -	nil -	nil -	nil -
June 3rd	N_2/CO_2 CO_2/H^+	nil -	nil -	0.5% -	32.6% -
June 20th	N_2/CO_2 CO_2/H^+	62.9% -	nil -	0.9% -	641% -

Figure 43.

Station 1 peak current profiles for Zn, Pb, Cu-1 & Cu-2.

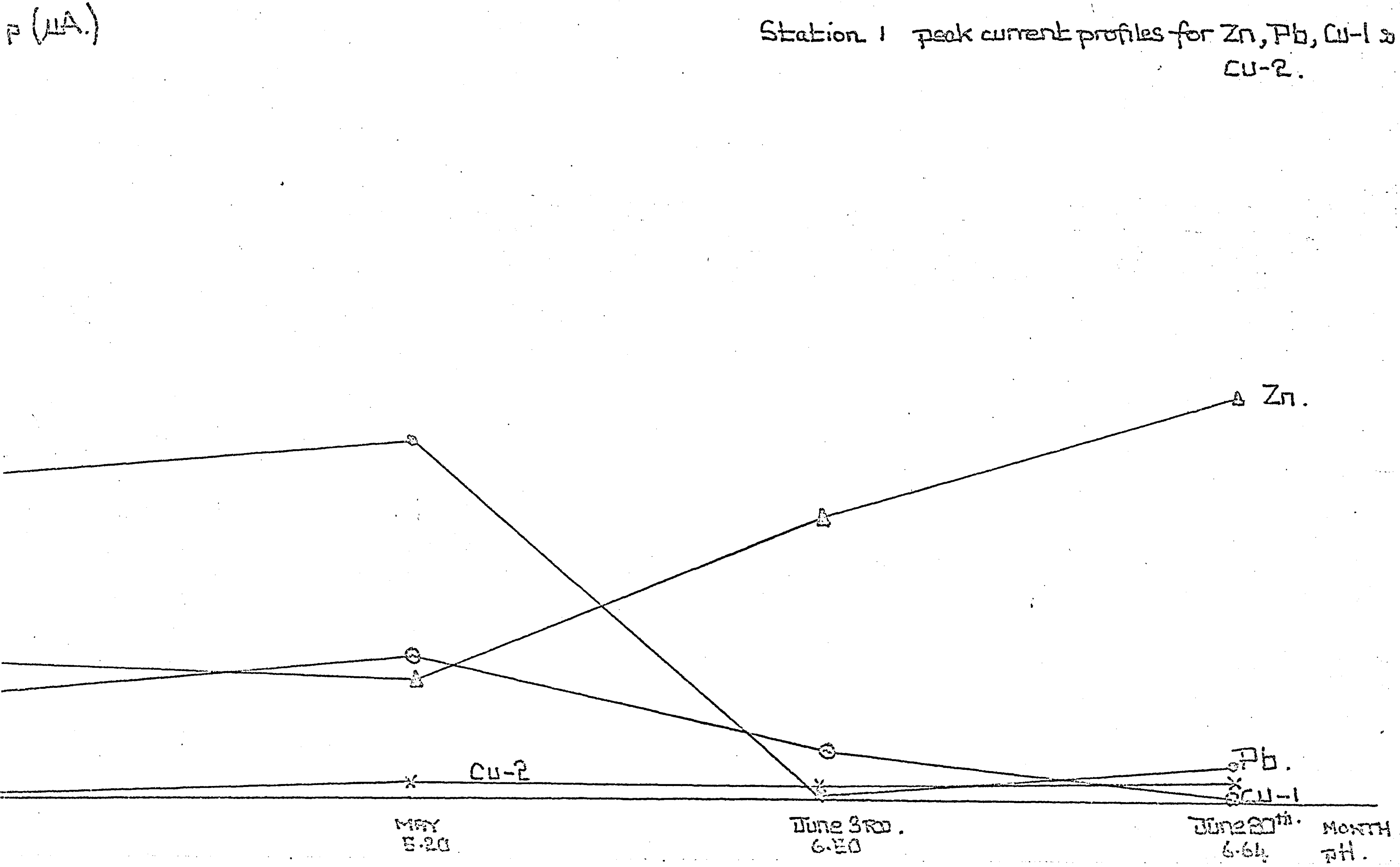

7.4. Station peak current profiles for Zn, Pb, Cu-1 and Cu-2 in H_2CO_3 throughout the sampling period.

7.4.1. Station 1. The pH increase from 5.30 to 6.64 over the period of sampling (Fig.43) was associated with the decline of Pb and Cu-1 anodic peak heights. Cu-2 remained unchanged and Zn increased in concentration in successive June samplings.

Figure 43.

Station 1 :

Individual peak current profiles throughout the sampling period.

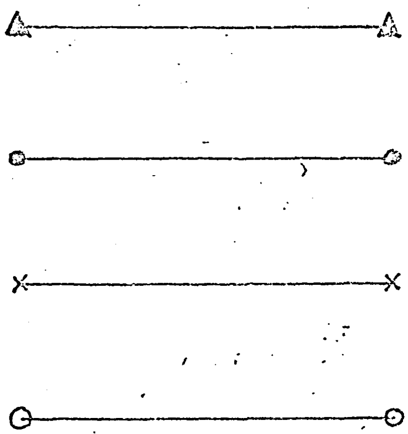

Zn $_{CO_2}$ i_p µA

Pb .. .. ..

Cu-2 .. ..

Cu-1 .. ..

Figure 44.

Station 2 : peak current profiles for Zn.,
Pb, Cu-1 , Cu-2 .

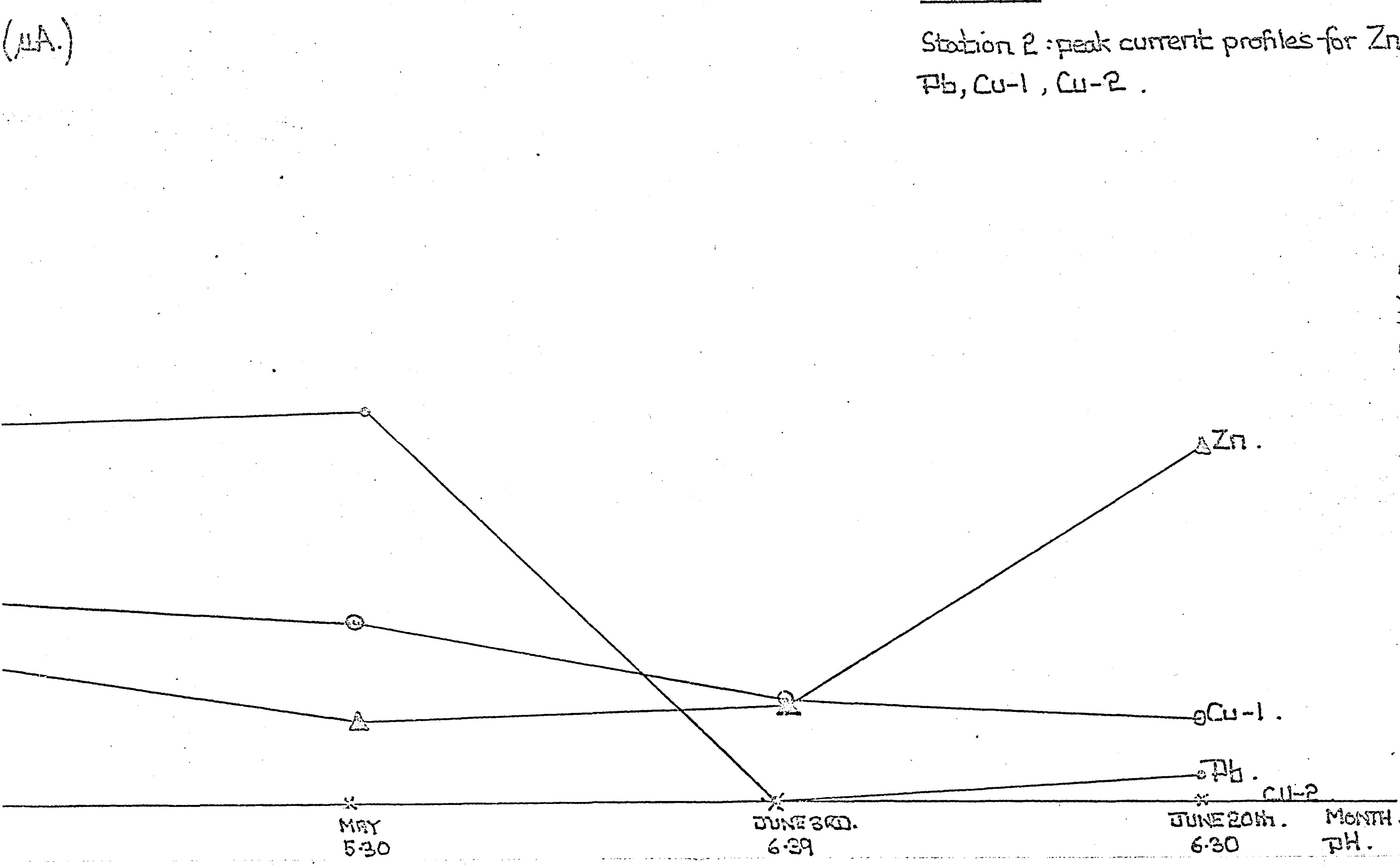

7.4.2. <u>Station 2</u>. This station follows a similar pattern to station 1. The pH increases from pH 5.40 on the first sampling date to 6.30 on June 20th. Pb once again declines together with Cu-1 anodic peak heights. Zn peak heights measured at station 2 in June 3rd. samples were lower than those at station 1 on the same date however, Zn does increase over the period of sampling as shown in (Fig.44).

Figure 44.

Station 2 :

Individual peak current profiles throughout the sampling period.

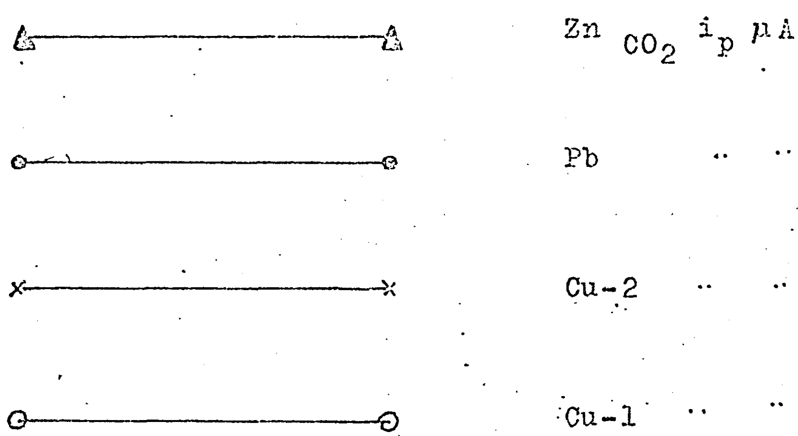

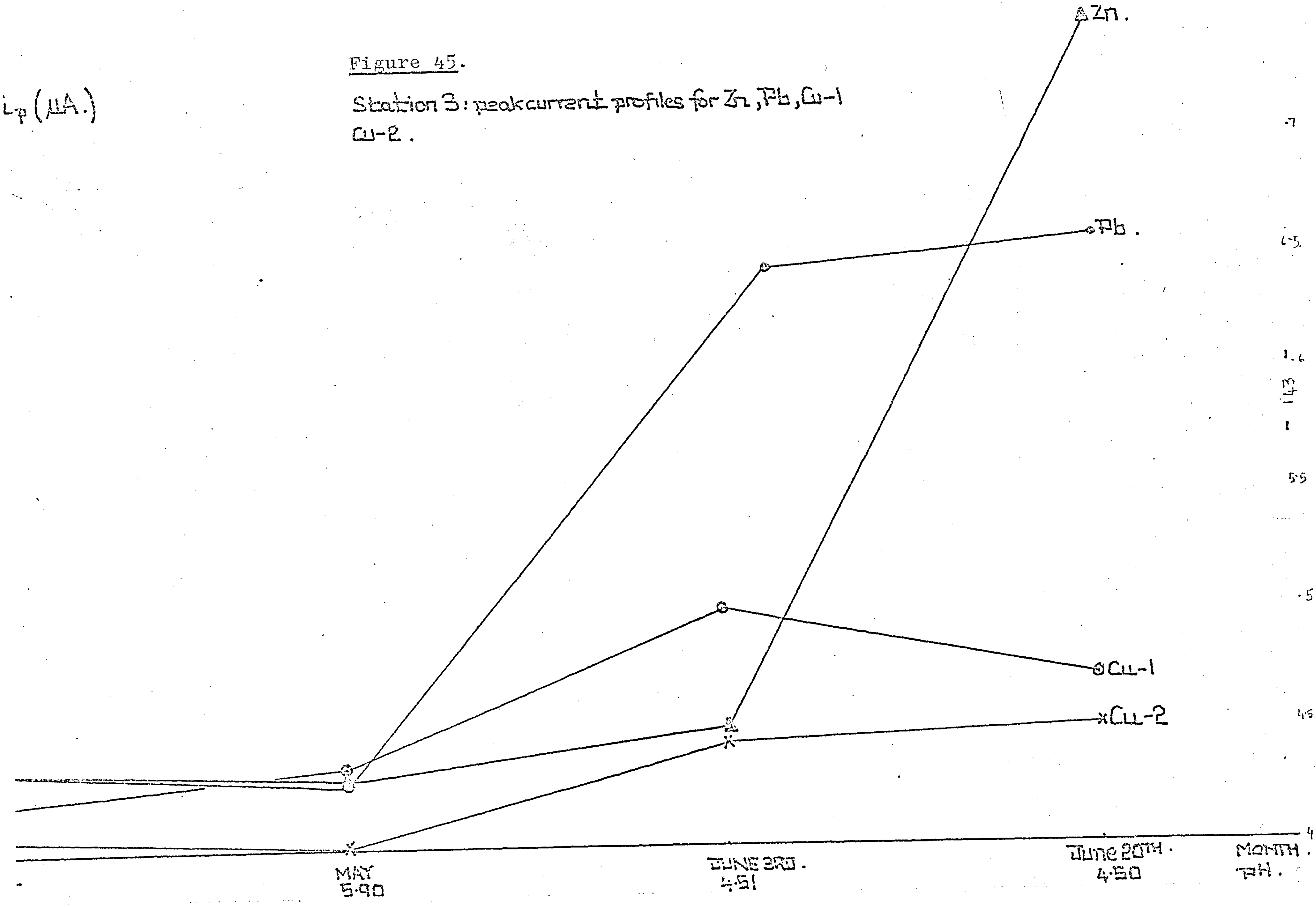

Figure 45.

Station 3: peak current profiles for Zn, Pb, Cu-1 Cu-2.

7.4.3. <u>Station 3</u>. At station 3 pH decreases over the sampling period from 6.10 in April to 4.50 on June 20th. Low peak currents were measured in April and May samples for all the metals plotted in Figure 45. In June Pb increased dramatically whereas Zn, Cu-1 and Cu-2 showed only a slight increase in peak height. In the final sampling at this station Zn also increased above the relatively high peak current of Pb. Cu-1, Cu-2 and Pb remained at similar levels to those measured on June 3rd. at pH 4.51.

Figure 45.

Station 3 :

Individual peak current profiles throughout the sampling period.

Zn CO_2 i_p µA

Pb .. .. ..

Cu-2 .. .. ..

Cu-1 .. .. ..

Figure 46.

Station 4: peak current profiles for Zn, Pb, Cu-1, Cu-2.

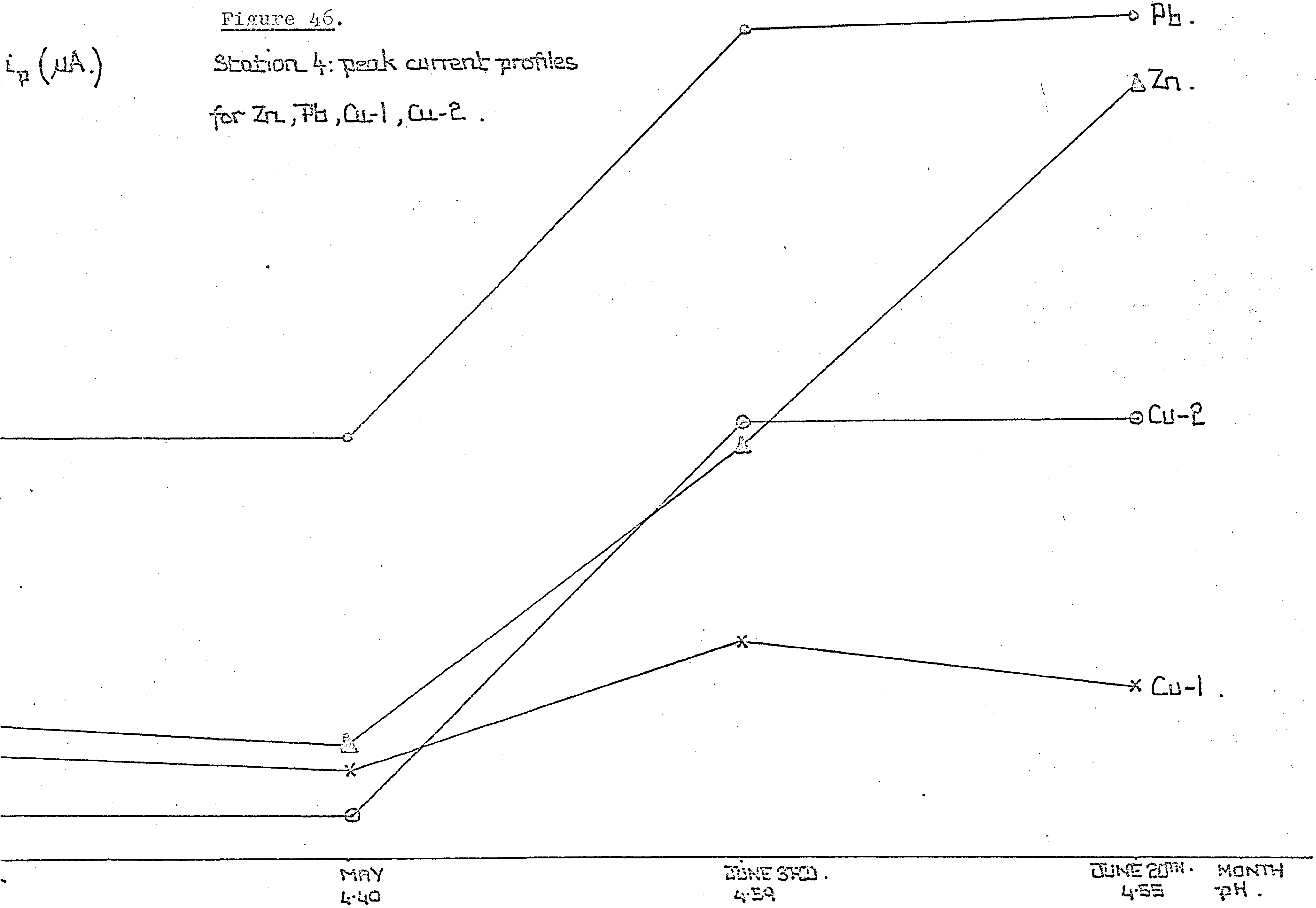

7.4.4. <u>Station 4</u>. Station 4 (Fig.46) has a water pH range of 4.20 in April rising to 4.59 in June. Pb is high initially but Cu-1, Cu-2 and Zn remain low in April and May. The concentration of all the metals as measured by the peak heights increases from May to June where they remain fairly constant on the last sampling date. The exception is Zn which goes on increasing in concentration in the month of June.

Figure 46.

Station 4 :
Individual peak current profiles throughout the sampling period.

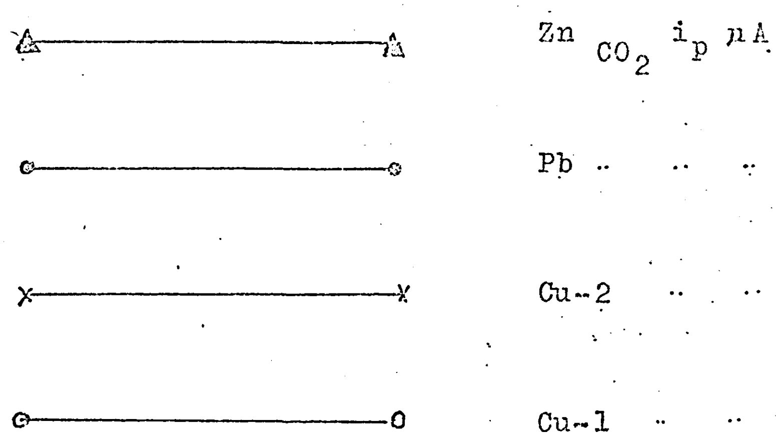

Figure 47.

Stream profile throughout the sampling period.

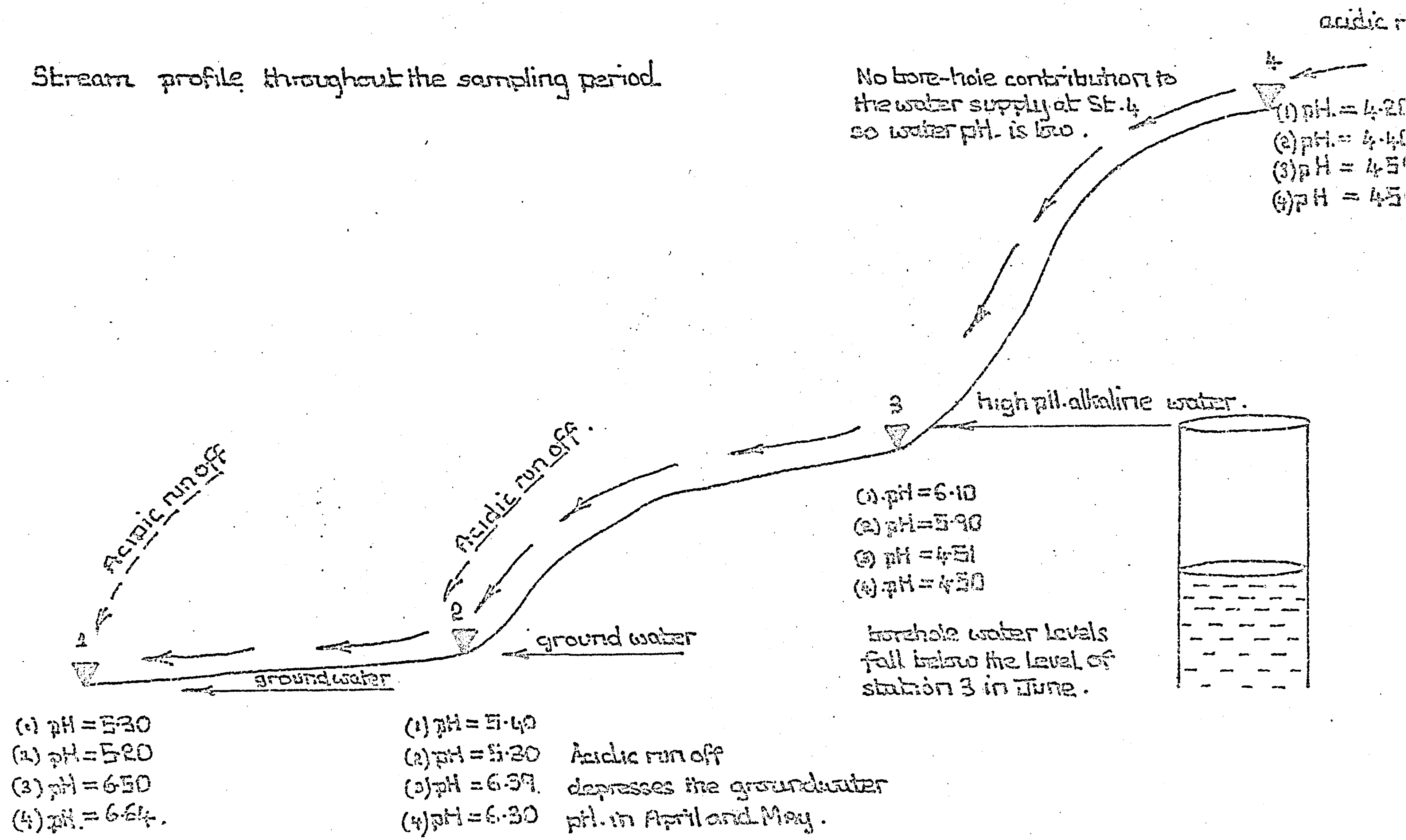

CHAPTER 8.

Discussion

8.1. General.

The stream supplying the Trout Hatchery is fed by two principal sources of water: alkaline ground water from boreholes and acidic run-off water from the peaty moorlands. The stream is just below the 4½ mile Rivelin water tunnel joining Ladybower Reservoir to Rivelin Dams which receives 500,000 gallons a day from the Kinderscout grit and from other lower grit beds. The stream itself is situated in an area where beds of sandstone interstratified with shales yield plentiful ground water. The best water-bearing beds of Chatsworth or Rivelin grit are of a thick coarse grained rock. Each bed of sandstone has its own water table which is generally sealed off from above and below by shales. The 'gritstones' or 'grits' are indeed a characteristic rock type on the surface and form conspicuous outcrops amoung the less obtrusive areas of shale. The sandstones are aggregates of quartz (SiO_2) feldspar and mica and it is from these deposits that the groundwater supplying the stream emanates (Eden et al 46).

In the diagram (Fig.47) of the sectional view of the stream it can be seen that in times of plentiful rainfall boreholes are full and supply the stream from station 3 downwards. Low pH values are thus encountered throughout the season at station 4 since only acidic run-off water is present. Trace metal concentrations tend to be high at station 4 and show a marked increase in June. The pH remains low at between 4.20 and 4.59 over the sampling period and thus any increase in metal concentration at station 4 may be attributed to a lower dilution factor in the dry month of June. The water at station 4 is rich in organic matter from the peaty soil. However, very little aquatic biological activity was observed here or at station 3; there was no algal growth even in June.

At station 3 groundwater dominates the supply providing the boreholes are full therefore relatively high pH (6.10 and 5.90) water was encountered in April and May and trace metal concentrations were low. In the drier month of June the bore-hole water levels fell such that they could no longer supply station 3. The supply of water to this station is now primarily acidic run-off water and as a result pH values dropped to between 4.51 and 4.50 in the June samplings. Low rainfall and low pH are contributory factors in producing much higher concentrations of trace metals at station 3 in June.

At stations 1 and 2 borehole groundwater levels never appear to fall below the level of these stations and thus can supply relatively high pH water throughout the sampling period. When there is abundant rainfall as in April and May small rivulets discharge acidic water directly from the moorland into stations 1 and 2 and thus depress the pH of the predominant groundwater to between 5.2 and 5.3. More Pb and Cu, was measured at stations 1 and 2 at these pH values than in June when little rain fell and no direct acidic run-off water cont-ributed to the supply. The pH rose to between 6.30 and 6.64 in June at station 1 and 2 and both Pb and Cu, concentrations declined even though the dilution factor had been reduced by the lack of rainfall.

In extreme flooding conditions borehole groundwater contributions to stream flow could reach a maximum and then be subject to a rate determining process with regard to rate of flow through the underground fissures supplying the stream. Acidic run-off from the moorland is not subject to a restriction of this nature since it is surface water. Temporary rivulets form and discharge acidic water from the moorland into all the stations such that the stream throughout its length could well take on the characteristics of station 4 (pH = 4.20 to 4.59). Higher trace metal concentrations may result at this low pH and contribute to the observed increase in fish mortality at the trout hatchery.

Discussion of individual metal concentrations will follow in the order in which the metals appear on a typical anodic scan in an ASV analysis i.e. Zn, Cd, Pb and Cu.

8.2. <u>Zinc : Zn</u>.

Zn concentrations were low in April and May and were between 0.99 and 3.06 ppb, the lower values being measured in relatively high pH water. The stream was swollen and inevitably rich in particulate matter which could scavenge Zn in solution by adsorption, this together with high dilution factors could account for the low levels of Zn encountered.

In June 3rd. samples slow flow rates were associated with high Zn concentrations being measured at station 3 and 4 which had 8.97 and 7.93 ppb Zn respectively. The pH at these stations was low and between 4.5 and 4.6. The pH pattern remained the same in the final sampling on June 20th., concentrations had risen to 15.40 ppb at station 3 and 14.43 ppb at station 4.

Figure 48.

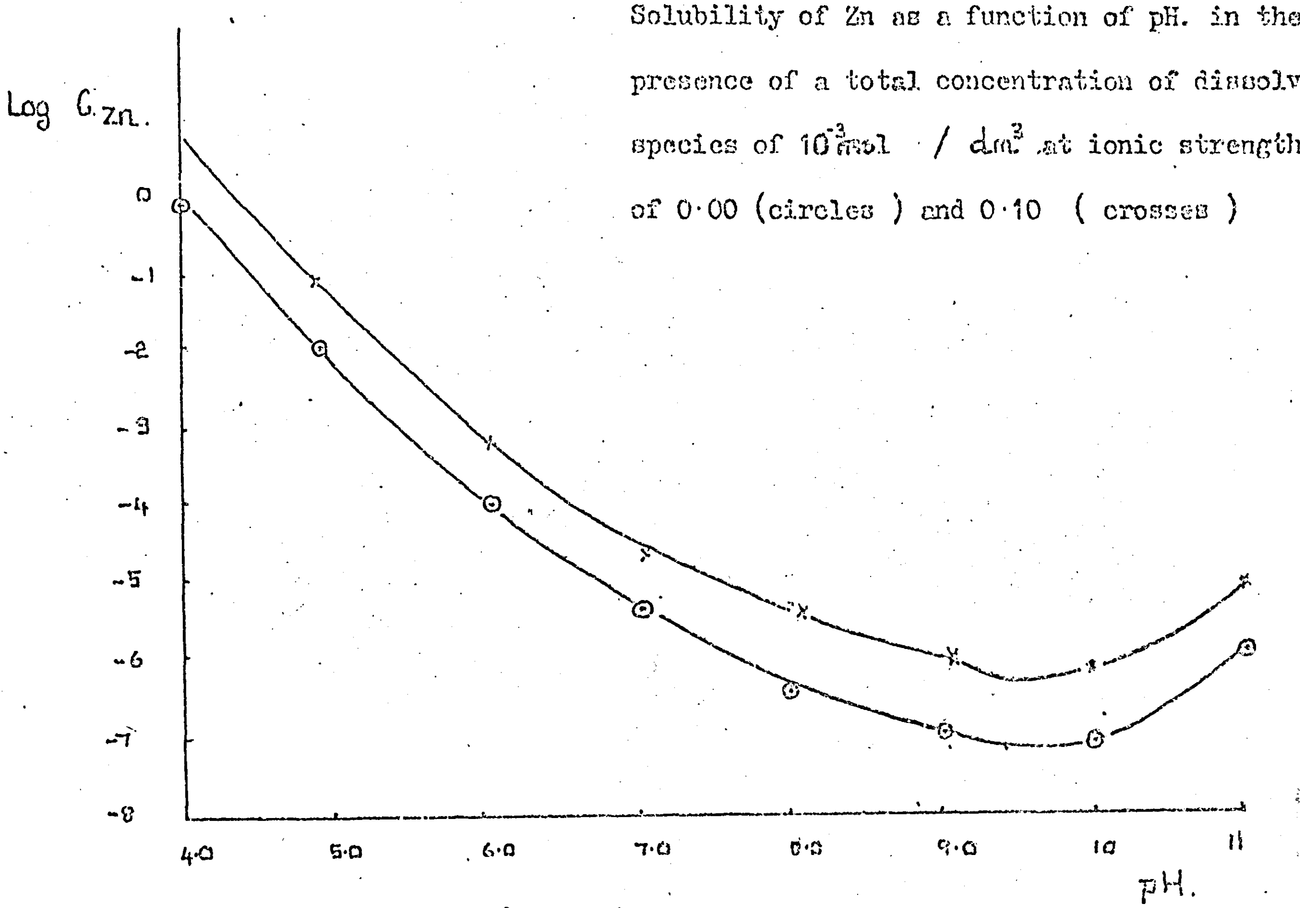

Solubility of Zn as a function of pH. in the presence of a total concentration of dissolved species of 10^{-3} mol / dm^3 at ionic strength of 0·00 (circles) and 0·10 (crosses)

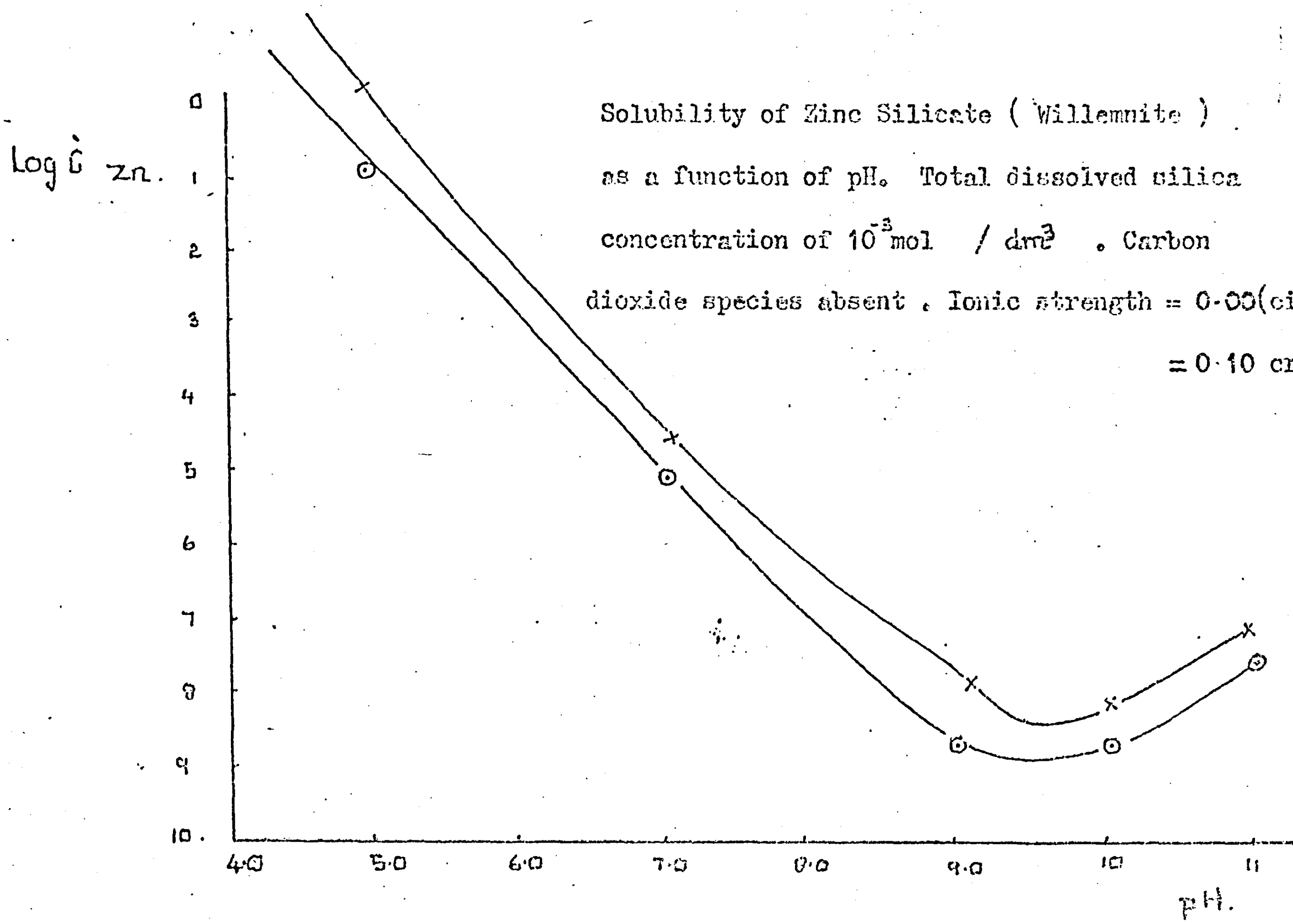

Solubility of Zinc Silicate (Willemnite) as a function of pH. Total dissolved silica concentration of 10^{-3} mol / dm^3 . Carbon dioxide species absent . Ionic strength = 0·00(circles)

= 0·10 crosses

Concentrations at stations 1 and 2 had also risen to 6.96 ppb and 6.11 ppb at comparatively high pH values of 6.64 and 6.30.

In both June samples a concentration gradient existed from station 2 upstream where the higher values for Zn were measured.

Zn concentrations did however increase at station 1 from 1.99 ppb in May to 6.96 ppb in the June 20th. samplings with an increase of water pH from 5.20 to 6.64.

The station characteristics of station 3 and 4 were very similar in June; the water was slow flowing and rich in organic matter from the peat banks of the stream; this together with the low pH and increased water temperature contributed to high Zn concentrations at this station.

Zn is a fairly abundant metal and small amounts are essential in plant and animal metabolism. Average soil concentrations range from 50 ppm with shale containing 95 ppm, sandstone 16 ppm and limestone 20 ppm. Cannon (47) found that peat concentrates Zn, this could well account for the higher concentrations found at station 4 which is rich in peat. Although Zn is known to be extracted by biota, productivity is limited at the low pH stations so that removal of Zn by this route may be ignored, this would help to build up Zn concentrations in the water at stations 3 and 4. Much of the groundwater in the stream is from sandstone grits which must be rich in silica. Hem (49) has shown that zinc silicate species may be the most effective control of Zn concentrations in groundwater since these species are less soluble than zinc carbonate at pH's in excess of pH 6.5 (Fig.48). Zinc silicate species may become important in

Speciation diagrams for Cu, Zn, Cd and Pb

in natural water.

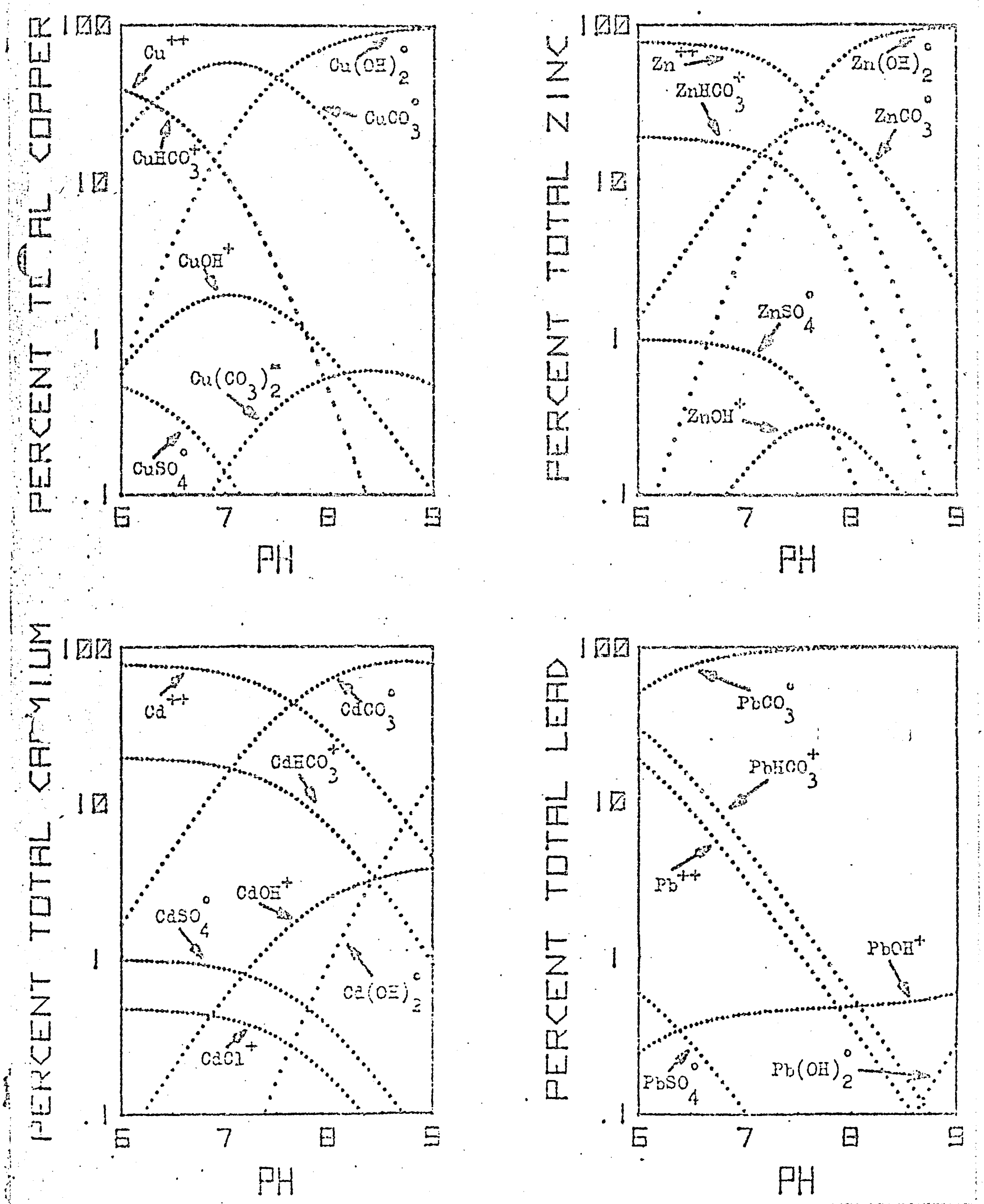

Zn removal mechanisms at the high pH stations on the stream studied.

Inorganic and to a limited extent organic complexation could determine Zn concentrations in the stream water. Low pH values of between 4 and 5 allow the free zinc ion to exist in solution at stations 3 and 4 together with possible associations with humic and fulvic compounds in colloidal form or in true solution. At higher pH values (6.50 - 6.64) at stations 1 and 2 in June hydroxide complexes are associated with Zn. However at pH's < 6.0 the Zn^{++} ion is the dominant species. The disappearance of Zn at high pH's was observed earlier in this work on stream water. The Zn ASV signal decreased whilst degassing the sample with nitrogen when pH values rose above 8.01, the signal declined on successive ASV analyses and became minimal at pH 8.5. Baudoin and Scoppa (48) have reported that association of Zn with hydroxide ions occurs until at pH 8.0 about 90% of the total Zn is present as $Zn(OH)_2^0$; thus speciation would account for the depletion of the anodic current. In subsequent analyses on stream water the anodic current measured under nitrogen exceeded that measured under CO_2 at stations 3 and 4 which is surprising since these are both low pH stations with the Zn ion being the dominant ionic species. The water however is rich in organic matter and degassing with nitrogen might together with a slight pH rise lead to the formation of colloidal material which could then adsorb a fraction of the Zn in solution. On analysing the sample under CO_2 the Zn may still be associated with the colloidal material and not be pH labile thus lowering the concentration in solution with the result that a lower anodic current was recorded in this stage of the analysis. An alternative explanation is that $ZnHCO_3^+$ forms to a significant degree in carbonic acid and this lowers the anodic peak current.

In this work Zn concentrations did not exceed 15.40 ppb ($\mu g\ dm^{-3}$) which is similar to the average value of $10 \mu g\ dm^{-3}$ (10 ppb) quoted by Hem (49) for river water. Much higher concentrations of $107 \mu g\ dm^{-3}$ (107 ppb) of Zn were reported by Lazarus et al (50) as an average for Zn in rainfall. In this work low values for Zn concentration were recorded in the wetter months of April and May and do not substantiate these findings. Dry fallout has been found to be a major source of particulate Zn at the land surface by other workers. Here it is available for transport by run-off into stream water. Zn concentrations could then build up from sedimentary and mineral deposits from the stream bed under slow-flow conditions as seen in the June samplings.

Equilibria between Zn in solution and mineral deposits in the stream may be altered through organic complexation, stream flow rate, temperature, ionic composition and speciation together with the pH of the water. Adsorption of high molecular organic material similar to humus occurs at inorganic surfaces in soil and stream sediments and metal ions may become strongly bound to this material. Such effects are difficult to quantify since they are often linked to growth and decay cycles of biota. A knowledge of these effects does however help to explain the Zn concentration found in the stream throughout the sampling period.

8.3. Cadmium : Cd

Cd concentrations in the stream water were consistently low being less than 1 ppb (1μg dm^{-3}) in any one sample throughout the sampling period. The values have little significance since they are below or near the limit of detection.*

In April and May no trend was apparent; all concentrations were very low. After the addition of acid between 0.36 and 0.73 ppb was recorded in the samples. However since the samples had as little as 0.08 ppb before acid addition the possibility of Cd contamination could not be ruled out. In June Cd levels were still low but showed some increase at the low pH stations 1 and 2.

In consideration of Cd concentration profiles for individual stations; station 4 shows a slight increase from 0.08 and 0.16 ppb in April and May to 0.40 and 0.48 ppb in the June samplings.

Cd anodic peaks were very small and were often not present under nitrogen. The element appears to be more sensitive to traces of oxygen being present. The mechanism of this interference is not known; reactions like:

$$2Cd(Hg) + O_2 + 2H_2O \rightarrow 2Cd^{2+} + 4OH^- \quad \text{after (Barendrecht, 51)}$$

may be important if the nitrogen purge of the sample is incomplete. The signal was often lost in the final stage of the analysis at pH 2 where background current increased slightly and swamped the small Cd signal. Only in the April samples did 'acid release' values exceed those values in the previous stages of the analysis.

Cd is a rarer element and not known to be essential for

* 2×10^{-9} mol dm^{-3} Cd.

life but is highly toxic to animals. Soil has an average concentration of 0.06 ppm and sandstone was reported by Bower (52) to have 0.05 ppm. Cd tends to be present in Zn minerals which would account for higher concentrations of the two metals being found together at stations 3 and 4. It has been pointed out by Baudoin and Scoppa (48) that the free Cd^{++} ion is the dominant species and that Cd undergoes less complexation than the other metals. Mancy (54) has shown that Cd organic complexes which are formed are labile and that the Cd is easily displaced by competitive reactions with calcium ions.

Cd in soils however, is tightly held and not readily removed by leaching. The metal may be complexed to a limited extent by organic material of low solubility or absorbed on manganese or iron oxide and hydroxide (53), this could account for the fact that few signals were recorded in analyses under nitrogen in some of the samples especially in the higher pH samples of the lower stations where this type of removal mechanism would be accentuated. The drop in pH provided by carbonic acid in the second stage of the analysis could allow partial desorption with the result that Cd was measured in nearly all samples at this pH (3.8).

8.4. <u>Lead : Pb</u>

Pb concentrations were much higher than the other metals in the stream and ranged between 0.49 ppb at station 1 in June 3rd. samples to 52.20 ppb on the same date at station 4, the values were found after the addition of nitric acid. It is unusual to find the extremes of concentration throughout the sampling period on one date and also that the lower value should be obtained under slow flow conditions with a comparatively low dilution factor in the dry month of June. The example serves to illustrate the enhancing effect that pH and possibly organic matter has on plumbo-solvency. Station 4 has water richin organic matter and has low pH values of 4.40. At station 1 at a pH of 6.50 very little Pb was in solution and likewise at station 2. Acid release of Pb in the final stage of the analysis yielded 0.31 ppb at station 1 and 10.97 ppb at station 4. This suggests that organo-lead complexes or association of Pb with organic matter does take place at station 4. At station 1 the adsorption of Pb onto particulate matter or the formation of hydroxo or carbonato species at the natural water pH could contribute to the free Pb ion after acidification of the sample at pH 2. Even though the value of Pb release at station 1 is much lower than that at station 4 the percentage release of 63.26% is higher when compared to 26.61% at station 4.

It is interesting to observe station 3 Pb concentrations as the pH of the water changes from 5.9 in May (10^{-8}mol dm^{-3} Pb) to 4.50 in June 3rd. samples (10^{-7}mol dm^{-3} Pb). Only 0.15 ppb Pb was released in May on acidification as opposed to 9.94 ppb in the June sample. This may be explained by the fact that calcium and magnesium are shown by Mancy (54) to complex with humic and fulvic compounds in solution in preference to certain trace elements providing the former concentration is sufficiently high. If this happens at station 3 in May then very little Pb will be complexed at pH 5.9. As acidic run-off water replaces alkaline groundwater in June the concentration of calcium and magnesium could fall to the point where Pb complexes with the fulvic and humic compounds in solution. On addition of acid the ligands may undergo protonation and thus release the Pb ion to be measured in the final stage ASV analysis at pH 2.

On examination of the Pb concentration profiles for individual stations Pb at station 3 and 4 was shown to increase in concentration throughout the sampling period and this may be attributed to lower dilution factors and fall in pH or alternatively maintenance of low pH values as at station 4. At stations 1 and 2 Pb concentrations decline from May to June with an increase in pH from 5.2 to 6.50; this is against the trend of higher Pb concentrations being found at other stations over the same period. pH appears to override the trend of lower dilution factors leading to higher Pb concentrations in June. Pb speciation is clearly important at pH's greater than 6.5 in explaining the low peak heights measured in these samples.

In natural waters Stum and Bilinski (25) have proposed that the following species can occur:

Pb^{2+} , $PbCO_3$, $Pb(CO_3)_2^{2-}$, $Pb(OH)^+$, $Pb(OH)_2$

and that carbonato lead complexes ($PbCO_3$) will be the most prevalent species but free Pb ions will predominate at pH values below 6.5. This is in agreement with the findings at stations 1 and 2. Most of the available Pb is, according to these workers associated with suspended material. Among the Pb(II) species the $Pb(OH)_2$ and $Pb(CO_3)$ species are very strongly adsorbed at interphases which could explain the removal of Pb as the water flows downstream in the June sampling at the high pH stations 1 and 2.

The lower stations have a higher water pH value and are more fertile with respect to algal and plant growth. The interface between rocks, sediment and water becomes covered in algal growth; this could modify leaching phenomena and provide fresh organic material with which Pb could associate. Although low values for Pb concentration could involve biotic factors, they are difficult to quantify.

Pb is found as the natural ore galena (PbS) in the Peak district and groundwater could well be associated with such ores. Acidic run-off water plays an important role in increasing plumbo-solvency within the stream and produced concentrations in the 10^{-7} to 10^{-9} mol dm^{-3} which compare favourably with Pb concentrations determined by Matson (17) for N. American freshwater lakes.

8.5. <u>Copper : Cu</u>

The highest concentration of Cu in the stream reached 10.1 ppb in acidic media in June 3rd. samples. 5.49 ppb was released on acidification at station 3. The stream was flowing slowly on this date and stations 3 and 4 were particularly rich in organic matter onto which Cu appears to associate. Cu concentrations increased at upstream stations in June; however, in the final sampling with increased flow conditions no such release of Cu on acidification was observed. Cu doublet peaks were most pronounced in both June samplings at station 4. Since the second Cu peak on an anodic scan was only partially electro-active no calibration was possible but using Cu-1 calibration figures these peaks were equivalent to between 5.89 and 7.81 ppb in June 3rd. samples. On acidification the Cu-2 peaks disappeared but did not add quantitatively to the Cu-1 signal. Organic compounds in solution probably interfere with the electrode at high concentrations as was found by Carter and Hume. These workers observed that electrodes showing doublet phenomena in humic acid solutions continued to do so even in clean solutions and they concluded that humic acid can adsorb on to the electrode surface and that it is this effect rather than reaction in solution which causes the doublet phenomena. In this work doublet phenomena were observed in clean solutions after medium exchange from stream water and in some blanks, Carter and Hume's results were re-inforced. Some doubt must be cast on interpretations of doublet waves in terms of organic complexation as proposed by Matson et al in view of these findings.

Cu does however undergo reactions with humic material as shown by Singer (53).

Figure 50.

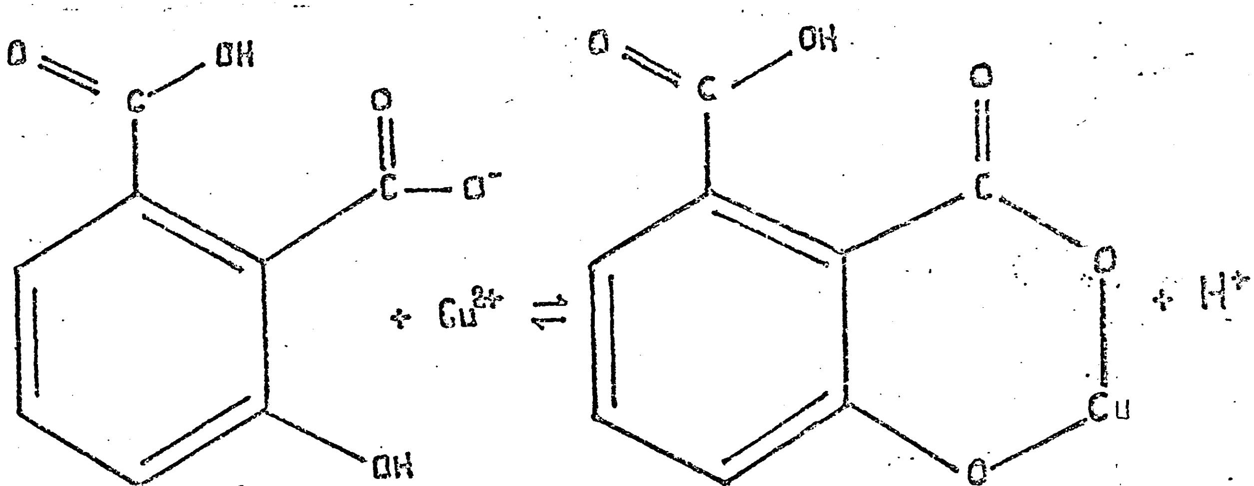

In acidic solutions the right to left reaction would be favoured thus releasing Cu from particulate or colloidal matter in suspension. This would account for higher 'acid release' values for Cu at upstream stations 3 and 4 at slow flow rates in June. Mancy has shown that Cu tends to form non-labile humic acid complexes and that Cu competes favourably with calcium for this complexation. In the June samples lower concentrations, 1.02 and 2.6 ppb were observed at the high pH stations 1 and 2. This may be explained by the fact that at natural water pH values higher than 6.0 considerable inorganic complexation of Cu with hydroxide and carbonate ions occurs. Only a small fraction of the total metal remains as free Cu ion (Fig.49). In April and May copper concentrations were low at all stations being less than 3.56 ppb. The lowest concentrations were observed at the high pH station 3 in the first two samplings. An 'acid release' value of 34% was observed at station 3 in April and yet no signal at all was obtained under nitrogen where the sample is near the natural pH of the stream (pH 6.5). In May more Cu was released at station 3 when the pH dropped to 3.8 in carbonic acid and a 90% increase in free copper ion concentration was observed. At the final pH of 2, a further 22% increase over the concentration observed in carbonic acid was obtained to give a total of 1.88 ppb Cu at this station. The speciation of Cu at pH 6.5 could thus explain the low signal obtained under nitrogen since the majority of the Cu is 'tied up' at the natural water pH at station 3 in the early samplings and at the lower stations 1 and 2 throughout the period of investigation.

Copper sulphate has been used to control algal blooms and concentrations as low as 1 to 2 ppb have been reported to be toxic to the algae Chlorella and diatom Nitzschia. The toxicity of Cu has been shown to be decreased by synthetic and natural organic chelators, colloidal adsorption or precipitation; all processes which may occur in natural water. Kolle et al (55) recorded 8.6 ppb of Cu in water from the river Rhine with soil concentrations of 50 ppm, Matson found between 3.16 and 36 ppb in unpolluted North American rivers. Maienthal et al (56) found similar values of between 20 and 90 ppb. The highest value found in the trout stream was 10.1 ppb which is comparable with the range of concentrations measured by Matson in river water.

CHAPTER 9.

CONCLUSION.

The analytical technique of ASV has been found to be aptly suited to trace metal analysis of Zn, Cd, Pb and Cu in natural water. The sensitivity of the technique (10^{-9} to 10^{-10} mol dm^{-3}) has allowed fluctuations in trace metal concentrations to be correlated with pH and changing water flow conditions over a period of three months.

Low pH waters associated with organic rich sediments and low dilution factors were seen to have increased trace metal concentrations particularly those for Zn, Pb and Cu (Figs. 38 to 42). It was apparent however from the station peak current profiles (Figs. 43 and 44) that at pH's 6.0, Pb and Cu concentrations declined whereas that of Zn did not. The increased pH appears to control the Pb and Cu concentrations either through speciation or the enhancement of a trace-metal removal mechanism.

The use of ASV as a tool for investigating speciation through the formation of doublet phenomena is doubtful since it appears to be a characteristic associated with the electrode structure itself.

The three stages of the analysis have allowed trace metals to be analysed at the nearly natural pH of stream water; a pH of 3.8 and finally at pH 2. Pb and Cu were seen to be pH labile. The phenomena was most apparent in water of pH 4 to 5 associated with organic matter where a low dilution factor was operative. The final pH (2) was the most effective at releasing the trace metals concerned. The fact that six analyses were performed on each ASV cell sample allowed the reproducibility of the technique to be verified for each individual sample.

The peak current calibration factor of the GCE for Zn, Cd, Pb and Cu in aged stream water in the 3 stages of the analysis remained constant to within $\pm$ 5% over a period of three months. The rotation of the electrode varied within $\pm$ 0.3%.

The ASV technique was convenient, highly sensitive and required only small samples. The lack of the necessity to preconcentrate the sample which is both time consuming and may lead to contamination, together with the provision of supporting electrolyte via the purge gas has helped to make the results more meaningful.

ASV however lacks versatility; there is always a need to calibrate the electrode in the medium to be analysed or in a model system. The ability to determine Zn, Cd, Pb and Cu from one voltammogram made ASV a particularly appropriate analytical technique to investigate the four trace metals in stream water whilst preserving a realistic analysis time for the procedure.

Bibliography

1. Zbinden C., Electrogravimetric Determination of Copper. Bulletin of the Society of Chemistry and Biology. Volume 13, page 35 to 38. (1931).
2. Rogers L.B. and Gardiner K.W., Coulometric Determination of Submicrogram Amounts of Cadmium and Zinc. Analytical Chemistry. Volume 25, page 1393. (1953).
3. Barker G.C. and Jenkins I.L., Use of Mercury Drop Electrodes in Anodic Stripping Voltammetry. The 'Analyst' Volume 77, page 685. (1952).
4. DeMars R.D. and Shain I., Anodic Stripping Voltammetry Using the Hanging Mercury Drop Electrode. Analytical Chemistry. Volume 29, page 1825. (1957).
5. Kemula W. and Kublik Z., "Use of the Hg drop Electrode for the Evaluation of Minute Amounts of Pb in Urine" Nature, Volume 189, page 57. (1961).
6. Matson W.R., Roe D.K. and Carritt D., "Composite Graphite-Mercury Electrode for Anodic Stripping Voltammetry". Analytical Chemistry, Volume 37, page 1594. (1965).
7. Nikelly J.E. and Cooke W.D., "Anodic Stripping Polarography". Analytical Chemistry, Volume 29, page 933. (1957).
8. Eisner V. and Mark H.B., Anodic Stripping Voltammetry of Trace Silver Solutions Employing Graphite Electrodes: Application to Silver Analysis of Rain and Snow Samples from Silver Iodide seeded Clouds. Journal of Electroanalytical Chemistry, Volume 24, pages 345-355. (1970).

9. Jacobs E.S., Anodic Stripping Voltammetry of Gold and Silver with Carbon Paste Electrodes.
Analytical Chemistry, Volume 35, Number 3, page 2112. (1963).

10. Marple T.L. and Rogers L.B., Polarographic Studies with a Stationary Mercury-Plated Platinum Electrode.
Analytical Chemistry, Volume 24, page 1351. (1953).

11. Florence T.M., Anodic Stripping Voltammetry with a Glassy Carbon Electrode Mercury Plated Insitu.
Journal of Electroanalytical and Interfacial Chemistry, Volume 27, pages 273 to 281. (1970).

12. Allen H.E., Matson W.R. and Mancy K.H., Trace Metal Characterization in Aquatic Environments by Anodic Stripping Voltammetry.
Journal of the Water Pollution Control Federation, April, page 573. (1970).

13. Ariel M., Eisner U. and Gottesfield S., Trace Analysis by Anodic Stripping Voltammetry: II. The Method of Medium Exchange.
Journal of Electroanalytical Chemistry, Volume 7, pages 307-314. (1964).

14. Whitnack G.C. and Sasselli R., Application of Anodic Stripping Voltammetry to the Determination of Some Trace Elements in Seawater.
Analytica Chimica Acta, Volume 47, pages 267-274. (1969).

15. Smith J.D. and Redmond J.D., Anodic Stripping Voltammetry Applied to Trace Metals in Seawater.
Journal of Electroanalytical and Interfacial Chemistry, Volume 33, pages 169-175. (1971).

16. Sinko I. and Dolezal J., Simultaneous Determination of Copper, Cadmium, Lead and Zinc in water by Anodic Stripping Polarography.
Journal of Electroanalytical Chemistry, Volume 25, pages 299-306. (1970).

17. Matson W.R., Allen H.E. and Rekshan P., Trace Metal Organic Complexes in the Great Lakes. Paper presented to the Division of Water, Air and Waste Chemistry.
American Chemistry Society, April (1969).

18. Hume D.N. and Carter J.N., Characteristics of the Mercury Coated Graphite Electrode in Anodic Stripping Voltammetry. Application to the study of Trace Metals in Environmental Water Systems.
Chemia Analityczna, Volume 17, page 747. (1972).

19. Stulikova M., The Deposition and Stripping of Mercury on a Glassy Carbon Rotating Disc Electrode.
Journal of Electroanalytical and Interfacial Electrochemistry, Volume 48, pages 33-45. (1973).

20. Fitzgerald W., Metal-Organic Interactions in the Marine Environment.
Chapter 12, pages 278-279. (1971) by A. Siegel. Published by Marcel Dekker.

21. Zirino A. and Healey M., pH Controlled Differential Voltammetry of certain Trace Transition Elements in Natural Waters.
Environmental Science and Technology, Volume 6, Number 3, page 243. (1972).

22. Zirino A. and Healey M., Inorganic Zinc Complexes in Seawater.
Limnology and Oceanography, Volume 10, pages 956-958. (1970).

23. Florence T.M., Determination of Trace Metals in Marine Samples by Anodic Stripping Voltammetry.
Journal of Electroanalytical Chemistry, Volume 35, page 237. (1972).

24. Gachter R., Lum-Shue-Chan K. and Chau Y.K., Complexing Capacity of the Nutrient Medium and its Relation to Inhibition of Algal Photosynthesis by Copper.
Schweizerische Zeitschrift Fur Hydrologie, Volume 35, page 252.(1973).

25. Stumm H. and Bilinski W., Pb(II) in Natural Waters.
Swiss Federal Institute of Technology. Federation Institute of Water Research and Water Pollution Control.
E.A.W.E. News 1. January. (1973).

26. Chau Y.K. and Lum-Shue-Chan K., Determination of Labile and Strongly Bound Metals in Lake Water.
Water Research, Volume 8, pages 383-388. (1974).

27. Roe D.K. and Toni J.E.A., An Equation for Anodic Stripping Curves of Thin Mercury Film Electrodes.
Analytical Chemistry, Volume 37, Number 12, page 1503. (1965).

28. Meites L., Polarographic Techniques.
(Second Edition Published by Interscience). (1964).

29. Vydra F. and Kopanica M., Voltammetry with Disc Electrodes and its Analytical Application.
Journal of Electroanalytical Chemistry, Volume 31, pages 175-181. (1971).

30. Frumkin A.N. and Tedoradze G.A.,
Zh Electrokhim, Volume 62, page 251. (1958).

31. Levich V.E., Physico-Chemical Hydrodynamics. State Publishing House of Physico-Mathematical Literature. Moscow. (1959).

32. Meites L., Purification of Supporting Electrolytes for Polarographic Trace Analysis by Controlled Potential Electrolysis at a Mercury Cathode.
Analytical Chemistry, Volume 27, Number 3. (1955).

33. Matson W.R., PhD Thesis, Massachusetts.
Institute of Technology, Cambridge, Mass. (1968).

34. Clem R.G., Personal Communication at a Conference on 'Anodic Stripping Voltammetry' Imperial College, London. April (1974).

35. Matson W.R., New Instruments and Techniques for Measuring Trace Metals in People and the Environment.
Environmental Science Associates Inc., Cambridge, Mass. (1974).

36. Clem R.G., Litton G. and Ornelas L.D., New Cell for Rapid Anodic Stripping Analysis.
Analytical Chemistry, Volume 45, Number 8, July. (1973).

37. Metters I.M., Lecture on 'Stripping Voltammetry' at a Symposium on Trace Metal Analysis.
Sheffield Branch of the Royal Institute of Chemistry, March. (1973).

38. Perone S.P. and Kretlow W.J., Anodic Stripping Voltammetry of Mercury(II) at the Graphite Electrode.
Analytical Chemistry, Volume 37, Number 8, page 968. (1962).

39. Van Dalen E. and De Vries, 'Voltammetry with a Plane Thin Mercury Film Electrode.
Journal of Electroanalytical Chemistry, Volume 8, pages 366-377. (1964).

40. Griffin Dr., 'Environmental Science Associates'. Demonstration of ASV Equipment. Manchester Airport, February (1974).

41. Clem R.G., Electroanalytical Rotated Cell for Anodic Stripping Analysis.
Application Notes, Volume 8, Number 1, McKee Pederson Instruments. (1973).

42. Clem R.G., Cause of Loss of Hydrogen. Overvoltage on Graphite Electrodes Used for Anodic Stripping Voltammetry.
Analytical Chemistry, Volume 47, Number 11, page 1779. (1975).

43. Fraser I., Electroanalytical Group Meeting of 'The Royal Institute of Chemistry'. Chelsea College, London Univ. March (1973).

44. Hume D.N., 'Analysis of Water for Trace Metals'. Chapter 2. Advances in Chemistry Series. Published by Wiley. Interscience 33-44. (1967).

45. Struempler A.W., Adsorption Characteristics of Silver, Lead, Cadmium, Zinc and Nickel on Borosilicate Glass, Polyethylene and Polypropylene Container Surfaces.
Analytical Chemistry, Volume 45, Number 13, page 2251. (1973).

46. Eden R.A., Stevenson I.P. and Edwards W., 'Geology of the Country around Sheffield'.
Published by Her Majesty's Stationery Office. (1967).

47. Cannon H.L., Geochemical relations of Zinc-bearing peat to the Lockport dolomite, Orleans County, New York.
U.S. Geological Survey, Bulletin 1000-D, 118-181. (1955).

48. Baudoin M.F. and Scoppa P., Calculated Distribution of the Chemical Species of Copper, Zinc, Cadmium and Lead in 16 Lakes of Northern Italy. Commission of the European Communities. EUR. 5052E; Joint Nuclear Research Centre. (1974).

49. Hem J.D., Chemistry and Occurrence of Cadmium and Zinc in Surface Water and Groundwater. Water Resources Research, Volume 8, Number 3, pages 661-679, June. (1972).

50. Lazarus A.L., Lorange E. and Lodge J.P., Lead and other metal ions in United States Precipitation. Environmental Science and Technology, Volume 4, pages 55-68. (1970).

51. Barendrect E., 'Stripping Voltammetry'. Electroanalytical Chemistry, Volume 2, Edited by J. Bard. pages 53-109. (1967).

52. Bowen H.J.M., Trace Metals in Biochemistry. pp 164, 179, 209, Academic, New York. (1966).

53. Singer P.C., Trace Metals and Metal-Organic Interactions in Natural Water. Published Ann Arbor. New York. (1973).

54. Mancy K.H., Trace Metal Characterisation by Anodic Stripping. Analytical Chemistry, Volume 10, pages 63-72.(1968).

55. Kolle W., Dorth K., Smiricz G. and Sontheimer H., Jahrbruch Vom Wasser, Volume 38, pages 183-196. (1971).

56. Maienthal E.J. and Taylor J.K., Polarographic Methods in Determination of Trace Inorganics in Water. Chapter 10 of Polarographic Methods. Published by Wiley. (1968).

Courses attended in conjunction with this work:

(1) A Symposium on Trace Metal Analysis organised by the Sheffield Branch of 'The Royal Institute of Chemistry' at Sheffield University. March 1973.

(2) Electroanalytical Group Meeting: (Royal Institute of Chemistry): Modern Electroanalytical Techniques. Chelsea College, London S.W.7. March 1973.

(3) Environmental Chemistry. A post-graduate course of 13 lectures organised by Sheffield University Chemistry Department. March 1974.

(4) 'Environmental Science Associates'. Demonstration of Anodic Stripping Voltammetry Equipment. February 1974.

(5) A Conference on 'Anodic Stripping Voltammetry' (ASV) held at Imperial College, London. April 1974.